

https://dspace.org/

Targeted inactivation of hepatitis B virus genome using enhanced transcription activator-like effector nucleases containing a sharkey fokI nuclease domain

Singh, Prashika

2018

https://hdl.handle.net/10539/25431

Downloaded from a DSpace repository. https://dspace.org/

Targeted inactivation of hepatitis B virus genome using enhanced Transcription Activator-Like Effector Nucleases containing a Sharkey *Fok*I nuclease domain

Prashika Singh

A dissertation submitted to the Faculty of Health Sciences, University of the Witwatersrand, in fulfilment of the requirements for the degree of

Master of Science in Medicine

Johannesburg, 2018

Declaration

I, Prashika Singh (student number: 671465) declare that this dissertation is my own work. It is being submitted for the degree of Master of Science in Medicine at the University of the Witwatersrand, Johannesburg. It has not been submitted before for any degree or examination at this or any other University.

……....……

……day of ……., 2018

Dedication

To my Family

Publications and presentations

Conference Proceedings

Poster Presentation

Singh. P, Ely. A, and Arbuthnot. P., (2016), Generation and characterisation of HBV transgenes for the establishment of stable virus producing cell lines, DST-NRF Nanotechnology symposium, 27-28 June, Pretoria, South Africa

Singh. P, Ely. A, and Arbuthnot. P., (2016), Characterisation of a replication-competent HBV sequence for the generation of a stable virus-producing cell line, 25th SASBMB Congress, 10-14 July, East London, South Africa

Singh. P, Ely. A, and Arbuthnot. P., (2016), Generation and characterisation of HBV transgenes for the establishment of stable virus producing cell lines, University of Witwatersrand, Faculty of Health Science Research Day, 31-32 August, Parktown, South Africa

Singh. P, Ely. A, and Arbuthnot. P., (2017), Inactivation of hepatitis B viral replication using Sharkey TALENs, Molecular Biosciences Research Thrust, Postgraduate Research Day, 30th of November, Johannesburg, South Africa

Oral Presentation

Singh. P, Smith. T, Ely. A, and Arbuthnot. P., (2017), Using Obligate Heterodimeric TALENs to Mutate Hepatitis B Virus DNA, African Centre for Gene Technologies (ACTG) Genome Editing Forum, 7 July, Pretoria, South Africa

Abstract

Despite the availability of an effective vaccine, hepatitis B virus (HBV) infections are a major public health problem with approximately two thirds of the world's population having been exposed to this virus. This DNA virus infects hepatocytes causing inflammation and is the causative agent of hepatitis B. Upon infection the viral genome is transported to the nucleus and repaired to covalently closed circular DNA (cccDNA). The cccDNA intermediate is responsible for the persistence of HBV in chronically infected individuals and acts as a viral reservoir. Current treatments are not able to target the stable cccDNA and highlight the need for the development of new therapies. This project focused on the development of anti-HBV transcription activator-like effector nucleases (TALENs) with improved efficiency and safety. TALENs are designer nucleases that induce double-stranded breaks (DSBs) within DNA. This stimulates host repair pathways that results in insertions or deletions (indels) that cause frame-shift mutations and disrupt targeted genes. TALENs are highly promising as they are able to target cccDNA and could lead to a functional cure for HBV. Existing anti-HBV TALENs have been designed to target conserved sites in the *S* and *C* open reading frames of the HBV genome. The third generation obligate heterodimeric Sharkey variants are enhanced *Fok*I nuclease domains that were generated by altering certain amino acid residues in the wild-type *Fok*I nuclease domain. Sharkey TALENs were produced by substituting the wild-type *Fok*I domain of existing anti-HBV TALENs with Sharkey variants. In vitro analysis of the anti-HBV Sharkey TALENs demonstrated expression of the nucleases in liver-derived cells. However, the wild-type anti-HBV TALENs exhibited superior inhibitory effects as compared to the Sharkey TALENs. Sequence-specific cleavage was achieved by both surface (S) and core (C) Sharkey TALENs however the latter achieved greater targeted cleavage. Mutagenesis analysis of HBV DNA from extracted HepG2.2.15 cells revealed the Sharkey C TALEN achieved 12.1% targeted cleavage greater compared to the Sharkey S TALEN. Efficacy was assessed in vivo in the mouse hydrodynamic injection model of HBV replication. In vivo viral markers of HBV replication were assessed and the Sharkey anti-HBV S and C TALENs were able to reduce viral surface antigen secretion by 57% and 78% respectively, whereas both Sharkey TALENs achieved a 96% reduction of circulating viral particle equivalents. The Sharkey TALENs were able to reduce viral mRNA production by 35% and 45% and pregenomic RNA levels by 73% and 80%. Minimal toxicity in vitro and in vivo was observed using the Sharkey TALENs indicating that reduction of markers of HBV replication were as a consequence of the action of the Sharkey anti-HBV TALENs. Results for the Sharkey C TALEN were comparable to the wild-type TALENs in vitro and in vivo.

Abstract

Despite the inhibition of HBV replication achieved with third generation Sharkey TALENs, a more comprehensive analysis of anti-HBV Sharkey TALEN activity in different in vitro and in vivo models of HBV replication is necessary. In addition, in depth analysis of potential off-target effects is required to comprehensively examine the safety of these variants. Nonetheless, in this study the Sharkey TALENs are able to inhibit HBV replication cccDNA and transcription, thereby further validating the use of TALENs as a potential therapy for chronic HBV infection.

Acknowledgments

1. Firstly, I would like to express my heartfelt appreciation to my supervisors Prof. Abdullah Ely and Prof. Patrick Arbuthnot for the endless support, patience, guidance and encouragement throughout my postgraduate studies and dissertation write up.
2. I would like to thank Prof Toni Cathomen for supplying the RM101-3rd generation Sharkey KKR and pUC57 Sharkey ELD plasmids and Dr Kristie Bloom for supplying the TALEN plasmids and assistance with the CelI assay.
3. I am thankful to Dr Wolfgang Prinz for extracting and supplying CelI single-stranded nuclease.
4. I would like to thank Tiffany Smith for her assistance and support.
5. I would truly like to thank all the members of the Antiviral Gene Therapy Research Unit (AGTRU), past and present for their assistance and support.
6. I would like to thank my family for their support and encouragement.
7. Finally, I would like to extend my gratitude to the National Research Foundation (NRF) of South Africa and Poliomyelitis Research Foundation (PRF) for financial assistance.

Table of Contents

Declaration....ii

Dedication....iii

Publications and presentations....iv

Abstract....v

Acknowledgments....vii

Table of Contents....viii

List of Figures....xii

List of Tables....xiv

List of Abbreviations....xv

Chapter 1....1

1 Introduction....1

1.1 Epidemiology of the hepatitis B virus....1

1.2 HBV infection and genome structure....2

1.3 Current HBV treatments....8

1.4 Targeting cccDNA of HBV....9

1.5 Sequence-specific designer nucleases....10

1.6 Transcription activator-like effector nucleases (TALENs)....11

1.7 Mechanisms of mutation of sequence-specific designer nucleases....14

1.8 Improvements to the sequence-specific designer nuclease scaffold....16

1.9 The FokI nuclease domain....16

*1.9.1 Modification of the Fok*I *nuclease domain*....17

1.10 Targeting HBV using sequence-specific designer nucleases....20

1.11 Aims....21

Chapter 2....22

Materials and Methods....22

2.1 Plasmids....22

Table of Contents

2.1.1 HBV target plasmid 22
2.1.2 Reporter plasmids 22
2.1.3 Wild-type TALENs 22
2.2 Generation of third generation obligate heterodimeric Sharkey TALENs 23
2.2.1 Transformation of wild-type TALEN and Sharkey-encoding plasmids 23
2.2.2 Construction of the Sharkey anti-HBV TALENs 23
2.3 Characterisation of the enhanced TALENs in cultured mammalian cells 26
2.3.1 Large Scale Plasmid preparation 26
2.3.2 Immunofluorescence staining of anti-HBV TALENs 26
2.3.3 Transfection of Huh 7 cells to evaluate HBsAg knockdown 27
2.3.4 Transfection of HepG2.2.15 cells and knockdown analysis 28
2.3.4.1 DNA extraction from HepG2.2.15 cells 29
2.3.4.2 Amplification of DNA for CelI assay 29
2.3.4.3 CelI assay 30
2.3.5 Assessment of Sharkey TALEN toxicity in cultured cells 30
2.4 Assessment and evaluation of Sharkey TALENs in vivo 31
2.4.1 Large-Scale Endotoxin-Free plasmid preparation 31
2.4.2 Hydrodynamic injection of mice 31
2.4.3 Bioluminescence imaging 32
2.4.4 Blood collection and processing 32
2.4.4.1 Quantification of HBV viral particle equivalents 32
2.4.4.2 In vivo assessment of Sharkey TALEN-mediated toxicity 33
2.5.5 Liver collection and processing 33
2.5.5.1 RNA extraction 33
2.5.5.2 Reverse transcription of RNA to cDNA 33
2.5.5.3 DNA extraction from Liver 35
Chapter 3 36
3 Results 36

Table of Contents

3.1 Construction of anti-HBV Sharkey TALENs 36
3.2 Anti-HBV Sharkey TALENs efficiently express in liver-derived cells 40
3.3 Anti-HBV Sharkey TALEN knockdown HBsAg in liver-derived cells 42
3.4 Sharkey TALENs mediated inhibition of HBsAg and targeted disruption of HBV DNA in vitro 44
3.4.1 Sharkey TALENs mediate efficient HBsAg reduction in HepG2.2.15 cells 44
3.4.2 Anti-HBV Sharkey TALENs mediate on-target cleavage in vitro 46
3.5 Lack of anti-HBV Sharkey TALEN-mediated toxicity in vitro 50
3.6 In vivo Sharkey TALEN-mediated silencing 52
3.7 Sharkey TALEN-mediated reduction of VPEs in vivo 55
3.8 In vivo Sharkey TALEN-mediated reduction of HBV transcription 57
3.9 In vivo Sharkey TALEN-mediated on-target cleavage 60
3.10 Lack of Sharkey TALEN-mediated toxicity in vivo. 63
Chapter 4 65
4 Discussion 65
4.1 Targeting cccDNA of HBV by Sharkey TALENs 65
4.2 Efficiency of Sharkey TALENs 66
4.3 Safety of Sharkey TALENs 69
4.4 Future Work 70
4.4.1 Off-target analysis 70
4.4.2 Delivery of anti-HBV Sharkey TALENs 71
4.5 Conclusion 72
Chapter 5 73
Appendix 73
5.1 Preparation and transformation of chemically competent E. coli 73
5.2 Large-scale plasmid preparation 75
5.3 Digestion of the Sharkey encoding plasmids 76
5.4 BglI digestion of the wild-type TALEN plasmids 77

Table of Contents

5.5 Agarose Gel Electrophoresis....78
5.6 Extraction of DNA fragments from agarose gel (Gel extraction)....79
5.7 Small scale plasmid preparation....80
5.8 Sequence analysis of the anti-HBV TALENs....81
5.8.1 Confirmation of Sharkey mutations in the FokI nuclease domain of the Sharkey TALEN monomers....81
5.8.2 Chromatograms of the anti-HBV TALEN plasmids....83
5.9 Cell Culture....98
5.9.1 Culturing and growth of mammalian cells....98
5.9.2 General procedure used for seeding or passaging cells....99
5.10 Large-scale plasmid preparation (Endotoxin-free)....100
5.11 Digestion of endotoxin-free plasmids....101
5.12 Ethics Certificate....103
5.13 Simulated agarose gel showing double digestion of Sharkey encoding plasmids....104
5.14 Transfection efficiency of anti-HBV TALENs in Huh 7 cells....105
5.15 Transfection efficiency of anti-HBV TALENs in HepG2.2.15 cells....106
5.16 PCR amplification of sequences for the CelI assay....107
5.17 Transfection efficiency of anti-HBV TALENs in HEK293 cells....109
5.18 Detection of anti-HBV TALENs in vivo lack....110
5.19 PCR amplification of in vivo sequences for the CelI assay....111
Chapter 6....113
6. References....113

List of Figures

Figure 1.1: Schematic diagram of HBV replication cycle. 6
Figure 1.2: Schematic representation of the genomic organisation of HBV. 7
Figure 1. 3: Schematic of the structure of TALENs. 13
Figure 1. 4: Models of mammalian cell DNA repair 15
Figure 1. 5: Alignment of the different *Fok*I nuclease domain variants 19
Figure 2.1: Cloning strategy for the generation anti-HBV Sharkey TALEN-encoding plasmids. 25
Figure 3.1: Enzymatic digestion of the wild-type TALEN plasmids. 37
Figure 3.2: Enzymatic digestion of the Sharkey encoding plasmids. 38
Figure 3.3: Screening of the third generation obligate heterodimeric Sharkey S and C TALEN plasmids by enzymatic digestion. 39
Figure 3.4: Detection of expressed Sharkey and wild-type S and C TALENs in cultured Huh7 cells using immunofluorescence. 41
Figure 3.5: Assessment of Sharkey TALEN-mediated knockdown of HBsAg in Huh 7 cells. 43
Figure 3.6: Sharkey and wild-type TALEN-mediated HBsAg reduction in HepG2.2.15 cells. 45
Figure 3.7: CelI-mediated cleavage of heteroduplexes. 48
Figure 3.8: Sharkey S and C TALEN-mediated cleavage of HepG2.2.15 DNA. 49
Figure 3.9: In vitro assessment of TALEN mediated cytotoxicity. 51
Figure 3.10: Bioluminescence imaging of mice treated with Sharkey TALEN, wild-type TALEN and mock plasmids in vivo. 53
Figure 3.11: Assessment of Sharkey TALEN-mediated knockdown of HBsAg in vivo. 54
Figure 3.12: Sharkey TALEN-mediated inhibition of HBV viral replication in vivo. 56
Figure 3.13: Sharkey TALEN-mediated knockdown of HBV mRNA expression in vivo. 59
Figure 3.14: Wild-type and Sharkey S TALEN-mediated in vivo on-target cleavage 61
Figure 3.15: Wild-type and Sharkey C TALEN-mediated in vivo on-target cleavage. 62
Figure 3.16: Assessment of Sharkey TALEN-associated liver toxicity. 64

Figure 5.1: Restriction enzyme digestion of the plasmids encoding the Sharkey variants (KKR and ELD). 76
Figure 5.2: Enzymatic digestion of wild-type TALEN plasmids. 77

List of Figures

Figure 5.3: Multiple sequence alignment of S and C Sharkey nuclease domains. 82
Figure 5.4: A chromatogram of the wild-type S TALEN sequence. 85
Figure 5.5: A chromatogram of the right Sharkey S TALEN sequence. 88
Figure 5.6: A chromatogram of the left Sharkey S TALEN sequence. 91
Figure 5.7: A chromatogram of the right Sharkey C TALEN sequence. 94
Figure 5.8: A chromatogram of the left Sharkey C TALEN sequence. 97
Figure 5.9: Restriction enzyme digestion of the marker and control endotoxin-free plasmids. 101
Figure 5.10: Screening of endotoxin-free wild-type and Sharkey TALEN plasmids. 102
Figure 5.11: Simulated double digestion of Sharkey encoding plasmids. 104
Figure 5. 12: Transfection efficiency of Sharkey and wild-type TALENs in Huh 7 cells. 105
Figure 5. 13: Transfection efficiency of Sharkey and wild-type TALENs in HepG2.2.15 cells. 106
Figure 5.14: PCR amplification of the *HBx* positive control and target sites for S and C TALENs. 107
Figure 5.15: PCR amplification of S and C TALEN target site from experimental transfections. 108
Figure 5.16: Transfection efficiency of Sharkey and wild-type TALENs in HEK 293 cells. 109
Figure 5.17: Delivery of anti-HBV TALENs in vivo. 110
Figure 5.18: PCR amplification of the *HBx and pUC118* region in vitro. 111
Figure 5.19: PCR amplification of S and C TALEN target site from experimental mice. 112

List of Tables

Table 1.1: Nucleotide binding specificity of TALE RVDs 12

Table 2.1: Anti-HBV TALENs plasmids and their nuclease encoding domains…….. 26

Table 2.2: Primer sequences used to amplify TALEN target sequences for CelI assay…….. 30

Table 2.3: Sequences of the primers used in qPCR to quantify HBV mRNA 34

List of Abbreviations

1. AAV	- Adeno-associated virus
2. ALT	- Alanine aminotransferase
3. BCP	- basic core promoter
4. bp	- Base pair
5. BSA	- Bovine serum albumin
6. cccDNA	- Covalently closed circular DNA
7. ChIP	-Cross-linking chromatin immunoprecipitation
8. CMV	- Cytomegalovirus
9. CRISPR/Cas9	- Clustered Regularly Interspaced Short Palindromic Repeat (CRISPR)/CRISPR-associated 9 (Cas9)
10. crRNAs	- CRISPR RNAs
11. DSB	-Double-stranded breaks
12. ddH2O	- Double distilled water
13. DAPI	- 4',6-diamidino-2-phenylindole
14. DMEM	- Dulbecco's Modified Eagle's Medium
15. DMSO	- Dimethyl sulphoxide
16. dsODNs	- Double-stranded oligonucleotides
17. *E. coli*	- *Escherichia coli*
18. EDTA	- Ethylene diamine tetra-acetic acid
19. eGFP	- Enhanced green fluorescent protein
20. ELISA	- Enzyme Linked Immunosorbent assay
21. FBS	- Foetal bovine serum
22. FITC	- Fluorescein isothiocyanate

23. FLuc	- Firefly luciferase
24. FDA	-Food and Drug Administration
25. GAPDH	- Glyceraldehyde-3-phosphate dehydrogenase
26. gRNA	- Guide RNA
27. GUIDE-seq	- Genome-wide unbiased identification of DSBs evaluated by sequencing
28. HA	- Haemagglutinin epitope
29. HE	- Homing endonuclease
30. HEK	- Human embryonic kidney
31. Huh7	- Human hepatoma 7
32. HBcAg	- Hepatitis B core antigen
33. HBeAg	- Hepatitis B e antigen
34. HBsAg	- Hepatitis B surface antigen
35. HBV	- Hepatitis B virus
36. HBx	- Hepatitis B virus X protein
37. HCC	- Hepatocellular carcinoma
38. HDI	- Hydrodynamic injection
39. HDR	-Homology-directed repair
40. Indel	-Insertion and deletion
41. IDLV	- integrase-deficient lentivirus
42. IFN-α	- Interferon alpha42. Indel
43. mRNA	- messenger RNA
44. MTT	- 3-(4,5-Dimethylthiazol-2-yl)-2,5-diphenytetrazolium bromide
45. NAs	- Nucleos(t)ide analogues
46. NHEJ	- non-homologous end joining

47. NLS - Nuclear localisation signal
48. nm - Nanometres
49. NMRI - Naval Medical Research Institute
50. NTCP - Sodium taurocholate co-transporting polypeptide
51. OD - Optical density
52. ORF - Open Reading Frame
53. PAM - Protospacer Adjacent Motif
54. PBS - Phosphate buffered saline
55. PCR - Polymerase chain reaction
56. PEG-IFN-α - PEGylated IFN-α
57. PEI - Polyethylenimine
58. PFA - Paraformaldehyde
59. pgRNA - Pregenomic RNA
60. qPCR - Quantitative PCR
61. rcDNA - Relaxed circular DNA
62. SELEX - Systematic evolution of ligands by exponential enrichment
63. sgRNA - Single guide RNA
64. S TALEN - Surface TALEN
65. RT-qPCR - Reverse transcriptase quantitative PCR
66. RVD - Repeat variable di-residue
67. VPE - Viral particle equivalent
68. TALE - Transcription activator-like effector
69. TALEN - Transcription activator-like effector nuclease
70. tracrRNA - Transactivating crRNA
71. WGS - Whole genome sequencing

72. WT - Wild-type

73. ZF - Zinc Finger

74. ZFN - Zinc Finger Nuclease

75. ZFP - Zinc Finger Protein

Chapter 1

1 Introduction

1.1 Epidemiology of the hepatitis B virus

Hepatitis B virus (HBV) infections are a major public health problem with approximately two thirds of the world's population having been exposed to this virus. Of these it is estimated that 250-400 million people have progressed to chronicity (WHO, 2015). HBV is a small enveloped virus and is the prototype virus of the *Hepadnaviridae* family of viruses (Liang, 2009). As the name suggests members of this family are DNA viruses that infect the liver (Marion and Robinson, 1983). HBV infects hepatocytes causing inflammation and is the causative agent of hepatitis B. It is estimated that 780 000 people die from hepatitis B-related complications (Lozano et al., 2013). The majority of hepatitis B-related deaths, estimated at 650 000-780 000 per year, are caused by cirrhosis and hepatocellular carcinoma (HCC). HBV infection in South Africa is a critical problem with an estimated 2.5 million people chronically infected (Spearman and Sonderup, 2014).

HBV causes both acute and chronic infections. Acute infections are characterised by mild or no symptoms and the immune system usually clears the infected hepatocytes. Individuals who are not able to clear the virus after six months are diagnosed as having a chronic infection (Viola et al., 1981, De Franchis et al., 1993). Unfortunately it is chronic carriers that are at an increased risk of developing HCC and cirrhosis. Chronic HBV infection is a significant risk factor for HCC, accounting for 60% of HCC cases worldwide and an estimated 80% within developing countries (McGlynn et al., 2001). Progression from acute to chronic infections is dependent on a number of factors such as age, HBV immunisation and current immune status. Approximately 90% of infants exposed at birth, 30-50% of children exposed before they turn 6 and 5% of adults exposed to HBV will develop chronic infection (WHO, 2017). Chronically infected individuals have a 15–25% risk of dying from HBV-related complications such as HCC and cirrhosis if they were infected during childhood (WHO, 2017). HBV is transmitted parenterally (Pourkarim et al., 2014) and in low endemic countries the most common mode of transmission is through sexual transmission and the use of contaminated needles and blood products. In Africa and Asia, both regions of high endemicity, transmission is mainly horizontal (between children) and from mother-to-child respectively (WHO, 2017). HBV

prevalence varies from 1% to 10% depending on the geographic region, with the highest prevalence in sub-Saharan Africa and Southeast Asia (Lago et al., 2014). In Africa, specifically sub-Saharan Africa, the prevalence of HBV infections is large with up to 8% of the population being chronic carriers. HBV is divided into eight well-characterised genotypes (A-H) and genotypes I and J have recently been identified (Huy et al., 2008, Tatematsu et al., 2009). This is a result of the high nucleotide substitution rate of the virus which has led to a relatively high degree heterogeneity and sequence diversity between viruses (Zhang et al., 2016).

1.2 HBV infection and genome structure

The HBV genome is approximately 3.2 kilobase pairs in size making it one of the smallest DNA viruses (Summers et al., 1975). HBV uses reverse transcription during its replication cycle however, unlike retroviruses, it does not integrate its genome into that of its host. Instead the viral genome is maintained episomally as covalently closed circular DNA (cccDNA) in the nucleus (Miller and Robinson, 1984). HBV consists of an outer lipid bilayer, with embedded viral surface proteins (large, middle and small), that surrounds the nucleocapsid. The nucleocapsid in turn comprises viral core proteins, arranged in an icosahedron, that encapsidates the viral genome which exists as a partially double-stranded relaxed circular DNA (rcDNA).

Early steps in the viral replication cycle have remained relatively obscure and it was only recently that the sodium taurocholate co-transporting polypeptide (NTCP) was identified as the receptor that HBV uses for entry (Yan et al., 2012). This receptor is expressed on hepatocytes and has been shown to be responsible for viral entry by interacting with the large surface protein of HBV (Yan et al., 2012) (Figure 1.1). HBV likely interacts with heparan sulphate proteoglycans (Schulze et al., 2007) followed by binding to NTCP and enters the cell through cell-mediated endocytosis (Glebe and Urban, 2007). Once inside the cell the nucleocapsid is transported to the nucleus where it is disassembled and the rcDNA is released. The rcDNA is composed of a complete minus (-) strand with the viral polymerase covalently attached to its 5’ end and an incomplete plus (+) strand that contains an RNA oligonucleotide attached to its 5’ end. The RNA oligonucleotide functions as a primer for the synthesis of the plus strand. The viral polymerase and RNA sequence are removed, plus strand synthesis is completed and the gaps in the two strands are ligated resulting in conversion of rcDNA to cccDNA (Beck and Nassal, 2007). This replicative intermediate serves as a template for viral transcription and is crucial for the establishment of persistent infection (Guo et al., 2012). The

cccDNA is transcribed into several RNAs including three subgenomic RNAs (*pre-S1*, *pre-S2* and *HBx* mRNAs) and two greater-than-genome-length RNAs (pregenomic RNA (pgRNA) and *precore* RNA) (Revill and Locarnini, 2016) (Figure 1.1). The nuclear episomal cccDNA is compact and comprises four overlapping open reading frames (ORFs) namely *precore*/*core* (*C*), *surface* or *envelope* (*S*), *polymerase* (*P*), and *X* (Elizalde et al., 2018) (Figure 1.2). Gene expression is regulated by four promoters and includes the pre-S1, pre-S2 and X promoters and the basic core promoter (BCP). The *C* ORF encodes the core and precore proteins. Whereas the core protein or HBV c antigen (HBcAg) is translated from the pgRNA and makes up the viral capsid precore is translated from the *precore* RNA and is processed to ultimately yield HBV e antigen (HBeAg). The *P* ORF is located on the pgRNA as well as the precore RNA and is translated from pgRNA. The *P* ORF encodes the polymerase protein which is responsible for the reverse transcription of pgRNA (Liang, 2009). The *S* ORF, which can be divided into the *pre-S1*, *pre-S2* and *S* regions, codes for the 3 surface envelope proteins or HBV surface antigens (HBsAgs). While the *pre-S1* mRNA serves as template for translation of the large HBsAg, the *pre-S2* mRNA serves as template for translation of the middle and small HBsAgs. Finally, the *X* ORF codes for the HBV X (HBx) protein, which is translated from the *HBx* mRNA (Liang, 2009).

Viral replication is initiated when the viral polymerase binds to the pgRNA, from which it is translated, signalling encapsidation of the pgRNA (Dandri and Petersen, 2016). Viral core proteins or HBcAgs, which are also translated from the pgRNA, form the capsid around the pgRNA. Within the capsid the pgRNA is reverse transcribed by viral polymerase to the minus strand. As the pgRNA is reverse transcribed, the RNaseH activity of the viral polymerase also degrades it. A small RNA oligonucleotide is left behind which translocated from the 3'-end of the minus strand to its 5'-end (Ko et al., 2014**).** The RNA oligonucleotide now functions as a primer for synthesis of the plus strand. The minus strand circularises such that its 5'- and 3'-ends are in close proximity allowing the plus strand to be synthesised across the gap between these two ends (Blum et al., 1989). Plus strand synthesis does not go to completion resulting in the rcDNA genome within the viral capsid (i.e. the nucleocapsid) (Seeger and Mason, 2015). Translation of the HBsAgs occurs at the endoplasmic reticulum which subsequently embeds themselves within its membrane. The nucleocapsid buds into the endoplasmic reticulum, acquires an envelope, embedded with surface proteins (Seeger and Mason, 2015) and is subsequently secreted out of the cell by exocytosis (Tuttleman et al., 1986, Wu et al.,

1990). Alternatively, the nucleocapsid can enter the nucleus and replenish the pool of cccDNA.

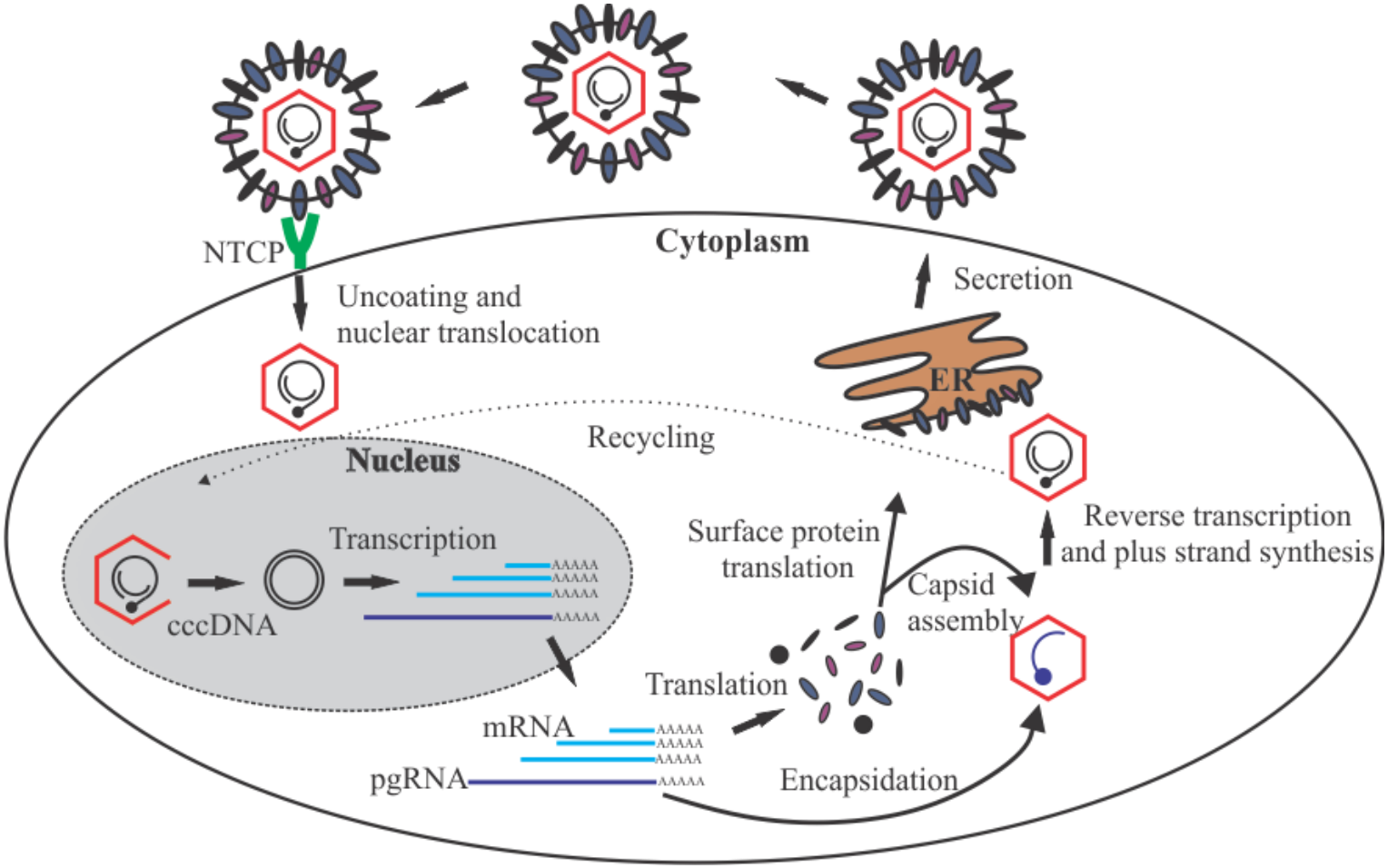
NTCP
Cytoplasm
Uncoating and
nuclear translocation
Secretion
ER
Recycling
Nucleus
Transcription
cccDNA
AAAAA
Surface protein
translation
Reverse transcription
and plus strand synthesis
Capsid
assembly
Translation
mRNA
pgRNA
Encapsidation

Figure 1.1: **Schematic diagram of HBV replication cycle.**

Attachment of the HBV virion to the NTCP receptor on hepatocytes initiates the infection event and gains cell entry through endocytosis. After entry into the cell, the nucleocapsid is translocated to the nucleus. In the nucleus rcDNA is released and repaired by viral and host proteins to form cccDNA. The cccDNA is the viral template responsible for transcription of pgRNA and subgenomic RNAs which are subsequently transported to the cytoplasm. Viral RNAs are translated into polymerase, HBV e antigen, HBx, surface and core proteins. The polymerase, once translated, binds to the pgRNA initiating encapsidation. Encapsidation of the pgRNA initiates its reverse transcription of the minus strand which in turn serves as template for synthesis of the plus strand. This produces the mature nucleocapsid containing the rcDNA genome. The nucleocapsid buds into the endoplasmic reticulum and acquires an envelope, embedded with surface proteins. The progeny virion is subsequently secreted out of the cell by exocytosis. Alternatively, the nucleocapsid can be transported to the nucleus to replenish the pool of cccDNA.

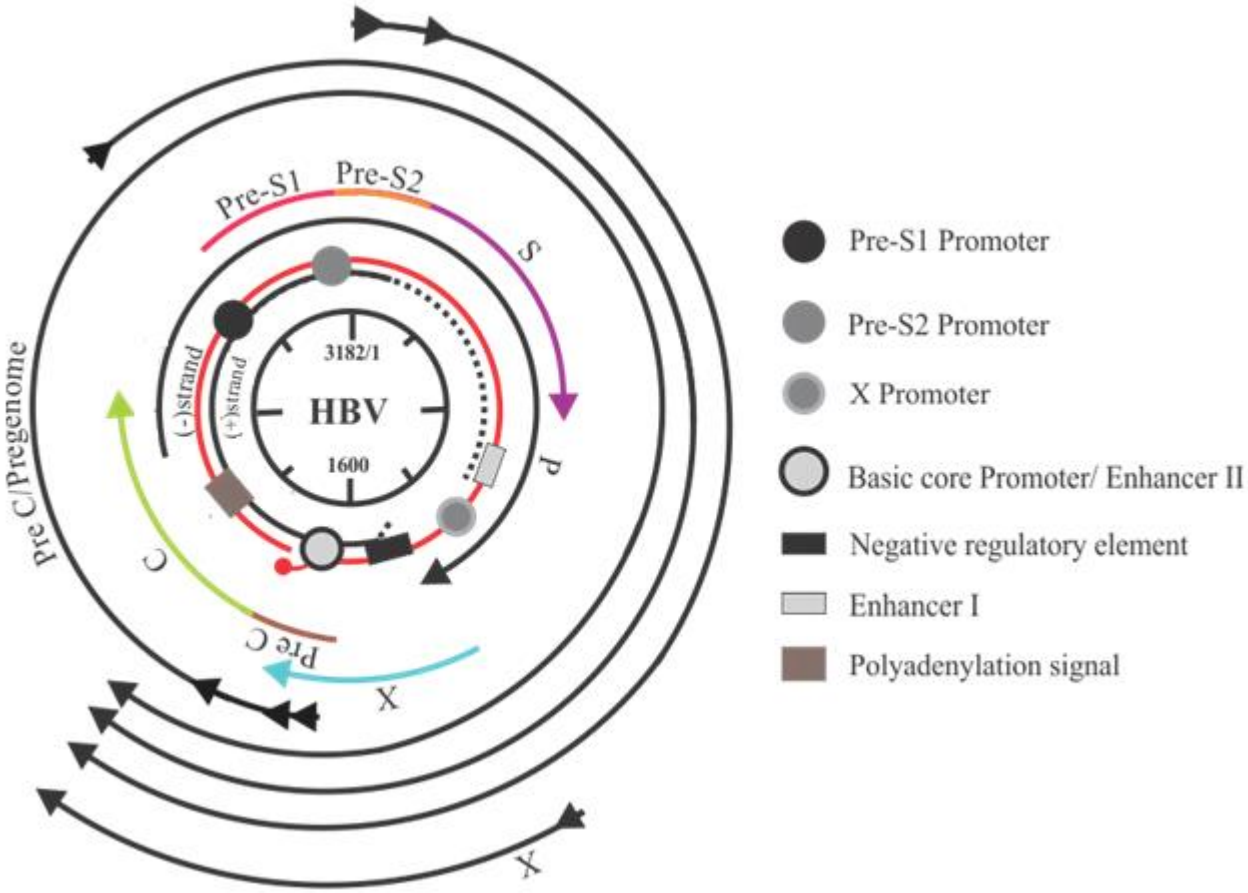

Figure 1.2: Schematic representation of the genomic organisation of HBV.

The centre of the figure represents the partially double-stranded rcDNA that is composed of plus (+) and minus (-) strands. The HBV genome is compact consisting of four overlapping ORFs. The *polymerase*, *surface*, *precore*/*core* and *X* ORFs are represented by the arrows surrounding the genome. These ORFs encode for polymerase, three surface proteins, core, e antigen as well as the X protein. The four outer arrows surrounding the genome represent the viral transcripts. The arrowheads at the 5' ends of the transcripts represent transcription start sites and that transcripts with multiple arrowheads at their 5' ends exist as multiple species. (Adapted from (Moolla et al., 2002)).

1.3 Current HBV treatments

Effective vaccines are available and have been shown to reduce the occurrence of new HBV infections. Vaccination however offers little therapeutic benefit to the estimated 250-400 million chronically infected individuals (Lemoine et al., 2013). The current conventional treatment for HBV includes several drugs approved by the Food and Drug Administration. These include immunomodulating agents (interferon-α (IFN-α) and PEGylated-IFN-α) and nucleos(t)ide analogues (NAs) (Zoulim and Locarnini, 2013). These therapies are able to reduce viraemia and viral replication which leads to improvements in the clinical outcome (Wilson et al., 2016) but do not affect the cccDNA. IFN-α and PEGylated-IFN-α function as immunomodulators and stimulate the host's immune system to clear the virus. A major shortcoming of interferon-based therapies is that only a small number of individuals, approximately 40% of treated patients, exhibit long-term clinical benefits (van Zonneveld et al., 2004), with less than 10% of treated patients showing a sustained virological response (elimination of serum HBsAg) (Trépo et al., 2014). Furthermore, the utility of interferon therapy is hampered by severe side effects.

NAs are very potent drugs and are better tolerated than interferon-based therapies (Zoulim and Locarnini, 2009). NAs function by inhibiting the reverse transcription step of the viral life cycle thereby suppressing viral replication (Zoulim and Perrillo, 2008). NAs approved for management of chronic hepatitis B include lamivudine, adefovir, entecavir, telbivudine and tenofovir. Advantages of using NAs include ease of administration and tolerance of the drug. However adverse side effects associated with long-term use have been reported. Furthermore, NAs have been shown to select for viral mutants resulting in the emergence of drug resistant virus (Cheng et al., 2015). Lamivudine, commonly the first line treatment for chronic hepatitis within developing countries, has been associated with high mutation rates, approximately 70% (Cheng et al., 2015). More importantly, however, NAs often produce a limited therapeutic benefit and require lifelong treatment which is costly and increases the risk of toxicity. Disruption of NA treatment results in resurgence of viral replication (Bessesen et al., 1999) and viral reactivation (Lai et al., 2014, Wong et al., 2006). While NA and IFN-α treatments are effective at inhibiting the replication of viral DNA within the cytoplasm they do not impact nor completely remove cccDNA reservoir.

The goal of HBV therapy is to eliminate or permanently disable cccDNA and gene therapy approaches have been evaluated as a strategy to achieve this goal. HBV has been targeted in cell culture and animal models using various gene therapy approaches. Numerous studies have targeted viral gene expression using RNA interference (Shlomai and Shaul, 2003), ribozymes (von Weizsäcker et al., 1992) and external guide sequences (Zhang et al., 2013). At the protein level, capsid-targeted viral inactivation (Beterams and Nassal, 2001) as well as dominant negative HBV mutants (Scaglioni et al., 1994) have been used. While there have been some successes, to varying degrees, none of these strategies has been able to successfully eliminate or disable cccDNA permanently. Engineered sequence-specific nucleases have been used to target HBV genome at the DNA level and more specifically are capable of permanently disabling cccDNA. As a consequence research efforts have focused on improvement and delivery of these nucleases for the management of chronic hepatitis B.

1.4 Targeting cccDNA of HBV

Extensive research has shown that cccDNA acts as a viral reservoir and is responsible for the persistence of HBV in chronically infected individuals (Königer et al., 2014). This replication intermediate resides within the nucleus as an episomal minichromosome and is thought to persist for years (Nassal, 2008). Therefore eliminating this DNA will potentially lead to a cure for chronic hepatitis B. HBV exist in hepatocytes in different forms as the virus goes through the replication cycle, however the cccDNA intermediate has been shown to be maintained within hepatocytes for months to years (Lai et al., 2014). This cccDNA is not eliminated by the licensed antiviral therapy. The use of genome engineering has been gaining popularity as a curative approach to target latent and persistent viral infection. Gene editing tools have proven successful over the past decades in molecular biology and has allowed for manipulation of genes. Currently available genome editing tools include homing endonucleases (HEs) (Terasaki, 1996), the clustered regularly-interspaced short palindromic repeats (CRISPR) and CRISPR-associated proteins (Cas) (CRISPR/Cas) system (Hille and Charpentier, 2016), zinc finger nucleases (ZFNs) (Beerli and Barbas, 2002) and transcription activator-like effector nucleases (TALENs) (Boch et al., 2009). These gene editing technologies function by inducing double-stranded breaks (DSBs) within DNA and this stimulates two cellular DNA repair mechanisms namely homology-directed repair (HDR) or the error-prone non-homologous end joining (NHEJ) process (Gaj et al., 2013, Wyman and Kanaar, 2006). Gene editing technologies take advantage of these pathways to induce targeted disruption of genes.

1.5 Sequence-specific designer nucleases

HEs are a class of DNA-cleaving enzymes and are found in introns, in certain microbial organisms, phages, and viruses (Terasaki, 1996). With HEs the DNA-binding domain has DNA-cleaving activity making these nucleases much smaller than others. Their small size facilitates vectorisation and delivery. HEs have been shown to have high specificity for their DNA targets and have very little toxicity due to the reduced off-target cleavage (Aubert et al., 2011). HEs are also known as meganucleases as they recognise relatively long sequences of approximately 14–40 bp (Belfort and Bonocora, 2014**).** HEs have been categorised into five families, namely LAGLIDADG, PD-(D/E)XK HE , HNH, GIY-YIG and His-Cys box (Stoddard, 2011, Belfort and Bonocora, 2014) and each family cleaves target DNA in different ways (Chevalier et al., 2001). The major challenge with the use HEs has been the difficulty associated with redirecting HE cleavage specificity (Schiffer et al., 2012). Association of cleavage activity and DNA-binding activity within the same protein domain significantly hampers the cleavage activity of HEs when altering DNA-binding activity (Schiffer et al., 2012).

Zinc-finger nucleases (ZFNs) are sequence-specific artificial nucleases engineered to bind and cleave target DNA specifically. ZFNs consist of two domains, the DNA-binding domain comprising His2-Cys2 zinc fingers (ZFs) and a DNA cleavage domain from the *Fok*I nuclease. Each ZF consists of approximately 30 amino acids bound by a single atom of zinc in a conserved ββα conformation (Beerli and Barbas, 2002). This structure is maintained by the chelation of a zinc ion and hydrophobic interactions (Klug, 2010)**.** Each α-helix of the ZF recognises a base triplet in the major groove of DNA (Kandavelou et al., 2005). ZFNs typically consist of three to six ZFs (Pabo et al., 2001) that are covalently tethered together generating the DNA-binding domain that recognises between 9 and 18 base pairs (Moscou and Bogdanove, 2009). The *Fok*I endonuclease is the non-specific DNA cleavage domain (Guo et al., 2010). As a type IIs restriction endonuclease the DNA-binding-domain of *Fok*I is separate from its nuclease domain (Pingoud and Jeltsch, 2001). Consequently, the nuclease domain of *Fok*I can be added to a ZF DNA-binding domain to create a new nuclease (Durai et al., 2005). ZFNs are engineered as two monomers which come together on the target sequence. When the two monomers come together the *Fok*I nuclease domains dimerise, become active and induce a DSB (Bitinaite et al., 1998). The major disadvantage of ZFNs is the difficulty associated with their construction as DNA binding is dependent on surrounding

ZFs. The affinity and specificity of the each finger is influenced by context, where each ZF in the array influences binding of its neighbouring ZF making construction of the array difficult (Fu and Voytas, 2012).

The discovery of the bacterial adaptive immune system known as the CRISPR/Cas system has led to development of a new gene editing tool (Hille and Charpentier, 2016). Naturally, the CRISPR/Cas system functions to protect bacteria from foreign DNA sequences. Upon infection by a bacteriophage the bacterium will incorporate pieces of the invading viral DNA into its own genome, specifically into the CRISPR/Cas locus (Amitai and Sorek, 2016, Heler et al., 2014). These sequences are transcribed and processed into CRISPR RNAs (crRNAs). Together with a transactivating crRNA (tracrRNA), crRNAs associate with the nucleases called Cas proteins. The Cas proteins is directed to DNA sequences homologous to the crRNA and digestion of the DNA thereby protecting the bacterium from infection (Hille and Charpentier, 2016). The CRISPR/Cas system has been exploited by producing a single small guide RNA (sgRNA) that mimics the crRNA and tracrRNA. sgRNAs can be produced against any target of interest and when complexed with a Cas protein direct the nuclease to the target to induce a DSB (Jinek et al., 2012). CRISPR/Cas systems have been used to induce mutagenesis in a number of organisms including bacteria (Jiang et al., 2013), zebrafish (Hwang et al., 2013), plants (Li et al., 2013) and numerous others. The specificity of the CRISPR/Cas system is dependent on RNA-DNA recognition unlike other sequence-specific nucleases. To date, the system from *Streptococcus pyogenes* (CRISPR/Cas9) has been the one most commonly used for gene editing (Hsu et al., 2014). CRISPR/Cas9 causes cleavage at the target site when the sgRNA hybridises with a ~20 nucleotide sequence next to the protospacer adjacent motif (PAM) sequence enabling the Cas9 endonuclease to cleavage target DNA (Cencic et al., 2014, Mekler et al., 2017). Genome editing tools have been generated from different Cas nucleases derived from various species of bacteria and each system differs in sgRNA and PAM sequences. As with other sequence-specific nucleases, the different CRISPR/Cas systems exhibit off-targets effects (Sander and Joung, 2014). In addition several studies have indicated the frequency of off-target indels mutations can sometimes be comparable to on-target mutation (Fu et al., 2013, Fu et al., 2014)

1.6 Transcription activator-like effector nucleases (TALENs)

TALENs have similar architecture to that of ZFNs in that they comprise a DNA-binding domain fused to a DNA cleavage domain. The DNA-binding domains of TALENs are based on transcription activator-like effectors (TALEs) from *Xanthomonas* bacteria (Boch et al.,

2009). TALE proteins consist of a nuclear localisation signal, a DNA-binding domain and a transcription activation domain (Jankele and Svoboda, 2014). The DNA-binding domain of TALEs consists of 33-35 amino acid repeats that vary at positions 12 and 13 (Figure 1.3). Amino acids 12 and 13 are known as the repeat variable di-residues (RVDs) and confer specific recognition of a single nucleotide to the DNA-binding domain (Schornack et al., 2006). The RVD recognition code has been deciphered and has allowed the design of artificial TALEs targeted against any sequence of interest (Boch, Scholze, Schornack *et al*., 2009, Moscou and Bogdanove, 2009). Over 20 unique RVD sequences have been identified and the seven that are commonly used includes NI (Asn and Ile), NN (Asn and Asn), NG (Asn and Gly), HD (His and Asp), IG (Ile and Gly), NH (Asn and His) and NK (Asn and Lys) (Table 1.1). The use of the different RVDs combinations provides the TALE with flexibility however the choice of RVDs affects the binding specificity and risk for potential off-target effects. Studies have shown that TALENs employing the NK RVD are less active compared to the NN RVD (Huang et al., 2011). The NH RVD has been shown to exhibit greater binding affinity for the G nucleotide than the NK RVD (Cong et al., 2012). The NH and NK RVDs have been shown to bind G more specifically and also reduced the risk of off-targets (Cong et al., 2012, Christian et al., 2012). Thus use of different RVDs allows for the targeting of any DNA sequence. More importantly the choice of RVD also determines efficiency and specificity of the designer nuclease. Much like ZFNs, TALENs are created by fusing the endonuclease domain of *Fok*I to a TALE DNA-binding domain. TALENs are designed as left and right monomers that bind their target DNA sequence allowing the *Fok*I nuclease domains to dimerise and create a DSB (Figure 1.3).

Table 1.1: Nucleotide binding specificity of TALE RVDs

Repeat variable di-residues (Amino acid)	DNA Nucleotide specificity
NI	A
NN	G or A
NG	T
HD	C
IG	T
NH	G
NK	G

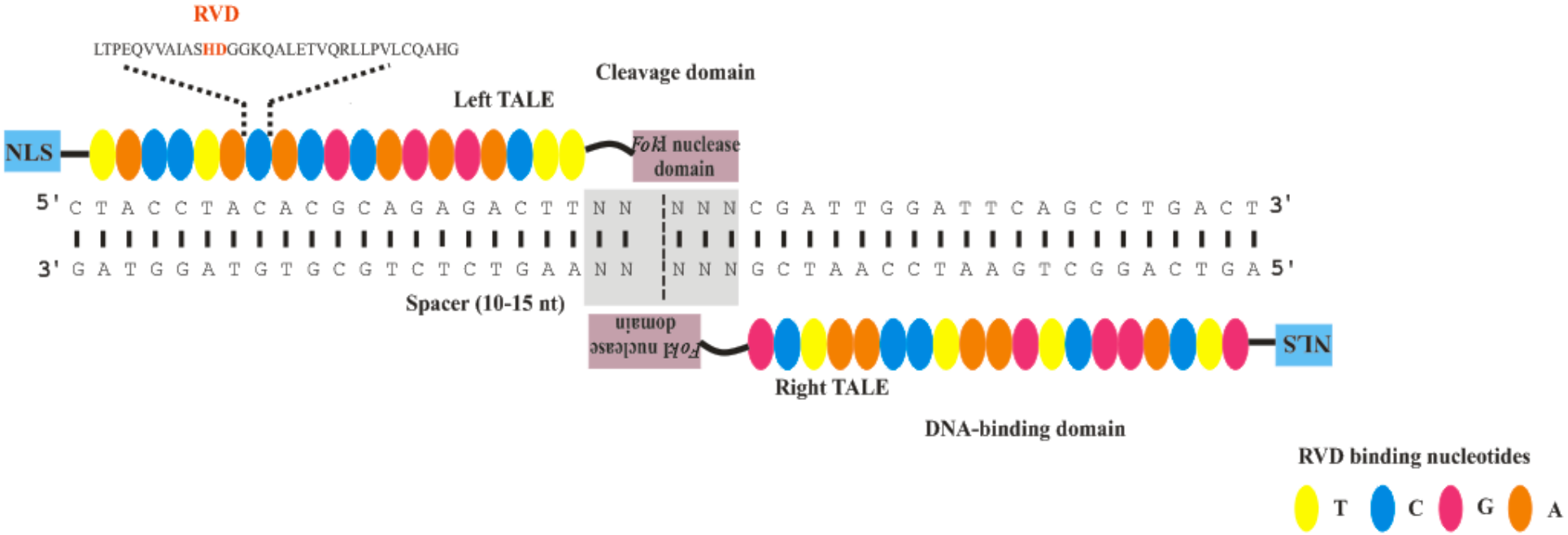

Figure 1. 3: Schematic of the structure of TALENs.

Diagrammatic representation of a TALEN which comprise of a DNA-binding domain (TALE) fused to a DNA cleavage domain (*Fok*I nuclease domain) and a nuclear location signal attached on the 5′ ends_The diagram illustrates the left and right TALEN monomers bound to target DNA. The diagram depicts the spacer region required for dimerisation of the *Fok*I nuclease domains as well as the RVDs required to bind to DNA. Refer to the dash line in context of the spacer region (approximately15bp).Adapted from (Kim and Kim, 2014).

1.7 Mechanisms of mutation of sequence-specific designer nucleases

DSBs are lesions formed in both strands of DNA causing a break in DNA duplex. These DSBs are hazardous and highly toxic to the cells and if left un-repaired can lead to apoptosis (Jackson and Bartek, 2009). Repair of DNA damage is crucial for maintaining genome integrity (Khanna and Jackson, 2001) and cell survival (van Gent et al., 2001). Organisms have, therefore, evolved a number of DNA repair mechanisms, which include HDR and NHEJ. While DSBs induce both pathways, mammalian cells predominantly use NHEJ to repair these types of lesions (Lieber et al., 2003, Orii et al., 2006).

HDR repairs DSBs with high fidelity as it uses undamaged homologous DNA to repair the lesion. The undamaged homologous DNA functions as template for synthesis of new DNA thereby allowing for accurate repair (Jasin and Rothstein, 2013). NHEJ like HDR is one of the pathways activated when DSBs occur. NHEJ uses microhomologies which are short homologous DNA sequences that are generally present as single-stranded overhangs on the ends of DSBs. If overhangs generated are compatible, DNA can be restored to its original state as the DSBs ends are re-ligated and in most cases the repair is precise (Schiffer et al., 2012). However if the overhangs are not compatible, imprecise repair occurs and can even result in the loss of nucleotides. Repeated cleavage by the nuclease and repair by NHEJ will eventually result in indels (Schiffer et al., 2012). This makes the use of designer nucleases, such as TALENs, an attractive and valuable strategy for antiviral gene therapy as the virus can be disabled through target cleavage and mutation.

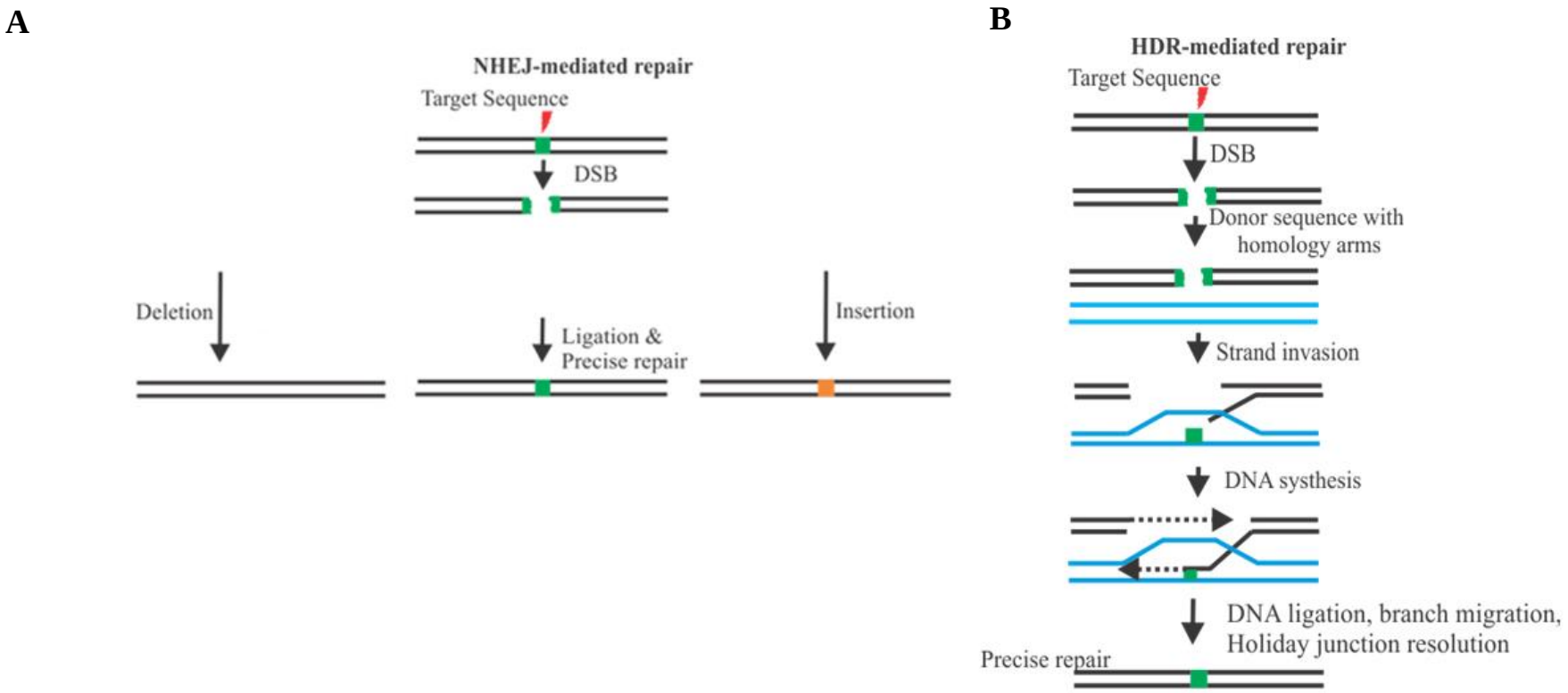

Figure 1. 4: Models of mammalian cell DNA repair

(**A**) The NHEJ repair pathway joins DSBs with blunt or complementary ends together. If the DSBs have overhangs that are not complementary, these overhangs are either filled in or resected and this has the potential to cause indels. Repeated cleavage by engineered nucleases and repair by NHEJ greatly increases the chances of indels. The solid black lines represent the double-stranded DNA, the green box represents the breakpoint and the orange box represents inserted DNA. (**B**) During HDR, nucleotides are resected from each end of the DSB to produce 3' overhangs. One of the free 3' ends invades the donor DNA at the point of homology and is extended in a template-dependent manner. The extended strand may now hybridise to the other 3' overhang, which in turn is extended. Finally ligation of the two strands completes the repair process. The solid black lines represent the double-stranded DNA, solid blue lines represent donor sequences, the green box represents repaired DNA. Adapted from (Dudáš and Chovanec, 2004).

1.8 Improvements to the sequence-specific designer nuclease scaffold

Multiple strategies have been used to improve the efficiency, specificity and sensitivity of designer nucleases such as TALENs and include modification of the TALE scaffold (DNA-binding domain) and the *Fok*I nuclease (DNA cleavage domain). The architecture of the TALEN protein is determined by its scaffold and improvements of the scaffolds includes the length of N- and C-terminal domains as well as amino acid substitution within the RVD monomers. Varying the length of the C-terminus and N-terminus of the TALE protein has yielded second-generation nucleases known as Goldy, Sunny and Platinum TALENs (Cermak et al., 2011). Varying the lengths of TALE constructs has been shown to confer improved DNA cleavage efficiency. Optimisation of the DNA-binding domain improves specificity (Chandrasegaran and Carroll, 2016) while modifications to the *Fok*I nuclease domain improve efficiency, and as a result safety, of these designer nucleases as a shorter period of time is required for these designer nuclease to carry out the same function and this ultimately reduces the probability that it will cause off-target effects (i.e safety increases).The residues responsible for the dimerisation of the *Fok*I nuclease domain are critical for nuclease function and can be altered to improve designer nuclease architectures.

*1.9 The Fok***I** *nuclease domain*

Nucleases are enzymes that are capable of cleaving the phosphodiester bonds in nucleic acid sequences (Rittié and Perbal, 2008). Endonucleases and exonucleases are two classes of nucleases that differ in their mode of action; endonucleases cleave DNA internally while exonucleases cleave nucleic acids from the ends (Rittié and Perbal, 2008). *Fok*I is a type IIs restriction endonuclease and was isolated from *Flavobacterium okeanokoites* (Durai et al., 2005). It has been well-characterised as a fusion domain (Pingoud and Silva, 2007) and endonuclease (Silva et al., 2011). This *Fok*I nuclease domain has been used in ZFNs and TALENs (Lippow et al., 2009). As a result of the bipartite structure of type IIs restriction endonucleases, *Fok*I cleaves the target sequences at a distance from the recognition sequence (Wah et al., 1997). The *Fok*I endonuclease normally exists as a monomer with a single catalytic domain and needs to dimerise with a second *Fok*I monomer to generate DSBs (Wah et al., 1998).

New active derivatives of the *Fok*I nuclease domain such as heterodimeric and Sharkey domains have been generated. ZFNs and TALENs are designed to function through dimerisation of left and right (L/R) monomers to form heterodimers. However, due to the inherent symmetry of the *Fok*I nuclease domain, it is also possible for homodimerisation to occur between two left (L/L) or two right (R/R) monomers (Szczepek et al., 2007). Through the use of mutagenesis (Guo et al., 2010), structure-guided design (Miller et al., 2007, Szczepek et al., 2007) and DNA shuffling (Doyon et al., 2011) enhanced heterodimeric versions of *Fok*I have been generated. Studies have reported obligate heterodimeric nucleases have improved safety profiles (Miller et al., 2007).

*1.9.1 Modification of the Fok***I** *nuclease domain*

The use of TALENs has been shown to have reduced cytotoxicity compared to other designer nucleases, presumably owing to increased specificity and reduced off-target effects. Improvements to ZFN and TALEN architecture design have been extensively evaluated to reduce or eliminate homodimer formation and increase their catalytic efficiency (Miller et al., 2007). To achieve this numerous strategies have been employed to improve efficiency and prevent homodimer formation.

While the first generation of engineered nucleases utilise the wild-type *Fok*I nuclease domain, second generation ZFNs and TALENs utilise variants containing mutations that favour heterodimerisation over homodimerisation (Miller et al., 2007). The left monomer (EL) variant contains the Q486E and the I499L mutations, whereas the right monomer (KK) variant contains the E490K and I538K mutations (Figure 1.5). This was shown to improve activity of ZFNs, however later studies demonstrated that the second generation ZFNs dimerise weakly (Szczepek et al., 2007). This is as a result of disruption of the hydrophobic pocket at the *FokI* dimerisation interface. Mutations that stabilises dimerisation between the left and right monomers were added to produce third generation nucleases (Kumar and Nussinov, 2002). This entailed substituting the asparagine at position 496 with the negatively charged aspartic acid (N496D) in the left monomer (variant ELD) and substituting histidine at position 537 with the positively charged arginine (H537R) in the right monomer (variant KKR). Introduction of these oppositely charged amino acids favours formation of salt bridges between left and right monomers thereby stabilising heterodimers.

Although the ZFN architectures are suitable for endogenous gene targeting, they would often result in fewer mutations (Perez et al., 2008) which could be a result of reduced binding affinities between the specialised cleavage domains (Miller et al., 2007). To further improve cleavage efficiency Guo et al. used directed evolution to optimise the catalytic activity of the *Fok*I nuclease domain and generated the Sharkey variant (Guo et al., 2010). These variants differ at two amino acids to the wild-type *Fok*I nuclease domain with S418P and K441E substitutions (Figure 1.5). Third generation obligate heterodimeric Sharkey nuclease domains were generated by incorporation of the Sharkey variants (S418P and K441E) into the third generation obligate heterodimeric (ELD and KKR) nuclease architecture (Doyon et al., 2011).

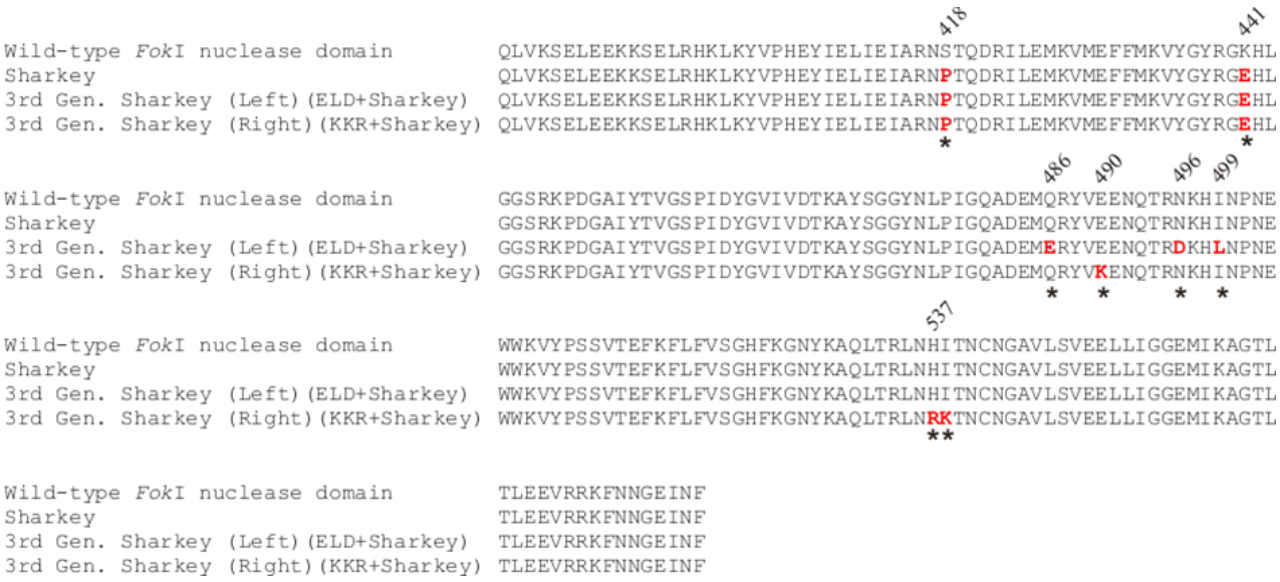

Figure 1. 5: Alignment of the different *Fok*I nuclease domain variants.

Amino acid sequence alignment of the wild-type *Fok*I nuclease domain with the different Sharkey *Fok*I nuclease domain variants produced by the mutation of particular amino acids (indicated by an asterisk). The top sequence represents the wild-type *Fok*I nuclease domain, the second sequence represents the Sharkey *Fok*I nuclease variant and the third and fourth sequences represent the obligate heterodimeric third generation Sharkey *Fok*I nuclease variants.

1.10 Targeting HBV using sequence-specific designer nucleases

Several studies have been conducted to evaluate the efficacy of designer nucleases targeting the HBV genome. Zinc finger proteins (ZFPs) were generated that targeted the enhancer region of duck hepatitis B virus. This study was able to demonstrate significant reduction of viral protein expression; however the effect was not maintained over time as ZFPs did not mutate the viral DNA (Zimmerman et al., 2008). Cradick and colleagues engineered ZFNs to target and inhibit HBV viral replication. Targeted inhibition of viral DNA was achieved, however the study failed to demonstrate modification of cccDNA by the ZFNs (Cradick et al., 2010). ZFNs were further improved by introduction of heterodimeric nuclease domains and were delivered using self-complementary adeno-associated viral (AAV) vectors in vivo. Targeted mutagenesis as well as inhibition of HBV replication, over a period of 14 days, was observed and was associated with few off-target effects (Weber et al., 2014). Several studies using the CRISPR/Cas system in vitro and in vivo indicated targeted inhibition of HBV replication. Lin and colleagues were the first to use the CRISPR/Cas system to target HBV and while demonstrating degradation of HBV genomes they did not observe disruption of viral cccDNA (Lin et al., 2014). A similar study by Seeger and Sohn, in contrast, was able to demonstrate targeted disruption of cccDNA (Seeger and Sohn, 2014).

Although there are limited studies using TALENs against HBV, these nucleases have been used with great success. Bloom and colleagues were the first to demonstrate the use of anti-HBV TALENs in cultured liver-derived cells and in vivo (Bloom et al., 2013). Dimeric anti-HBV TALENs were designed to target four conserved sites within the *S, C* and *P* ORFs of HBV. The S and C TALENs were designed against the *S* and *C* ORFs respectively, while the P1 and P2 TALENs were designed against transcriptional regulatory elements within the *P* ORF. In vitro analysis of the anti-HBV TALENs demonstrated that the S and C TALENs were effective and demonstrated targeted mutagenesis of viral DNA in an HBV producing cell line, HepG2.2.15. T7E1 assays demonstrated targeted mutagenesis of approximately 35% and 12% by the S and C TALENs respectively. In vivo assessment was carried out in the mouse hydrodynamic injection (HDI) model of HBV replication. The S and C TALENs were able to reduce HBsAg levels by 90% and viral particle equivalents (VPEs) by 70%. Deep sequencing demonstrated on-target mutagenesis of 58% by the S TALEN and 87% by the C TALEN. A subsequent study by Chen *et al.* demonstrated successful inactivation of HBV replication through the use of dimeric TALENs (Chen et al., 2014). The TALENs were

designed to target conserved regions within the *C* and *P* ORFs. L1/R1 and L2/R2 TALENs were designed to target the *C* region while the L3/R3 TALEN was designed to target the *P* region of the HBV genome. In vitro and in vivo assessment demonstrated that the all three TALENs were able to cause reduction in markers of viral replication. In the mouse HDI model anti-HBV TALENs were able to reduce levels of HBV pgRNA, VPEs and HBsAg. In addition Chen and colleagues combined the TALENs with interferon-α and observed a synergistic antiviral effect. These engineered nucleases are capable of inhibiting HBV replication, demonstrating the effectiveness of these tool however further improvements to these genome editing tools is critical for an effective HBV therapy.

1.11 Aims

The aim of the current project was the development of engineered nucleases with improved efficiency and safety through the incorporation of the third generation obligate heterodimeric Sharkey variants into existing anti-HBV TALENs. These variants were cloned into existing anti-HBV TALENs targeting the *S* and *C* ORFs of HBV. The anti-HBV S and C Sharkey TALENs was evaluated in liver-derived Huh7 cells for expression of the Sharkey TALENs. In vitro assessment of Sharkey TALENs was conducted through the transfection of liver-derived cells (Huh7 and HepG2.2.15). In vivo assessment of Sharkey TALENs was carried out in the mouse HDI model of HBV replication and markers of viral replication (HBsAg, viral RNA and viral DNA) were measured. CelI assays were conducted to measure targeted mutagenesis and assessment of Sharkey TALEN-mediated toxicity was evaluated in vitro (cell culture) by MTT assay and in vivo by ALT measurements from the livers mice.

Chapter 2

Materials and Methods

2.1 Plasmids

2.1.1 HBV target plasmid

The pCH-9/3091 plasmid is a replication-competent plasmid that was generated by Nassal and colleagues (Nassal et al., 1990). This plasmid was used as the target plasmid for in vitro and in vivo assessments, as it is able to model HBV replication. The pCH-9/3091 plasmid contains a greater-than-genome length HBV sequence under the control a cytomegalovirus (CMV) immediate early promoter-enhancer. Transcription of this greater-than-genome length sequence produces the pgRNA which establishes viral replication.

2.1.2 Reporter plasmids

The pCI-neo-eGFP reporter plasmid (Passman et al., 2000) containing the enhanced green fluorescent protein (eGFP) under the transcriptional control of a CMV promoter and was used for assessment of transfection efficiency in cultured cells. The pCI-neo-FLuc reporter plasmid (Ely and Arbuthnot, 2010) expresses Firefly luciferase under the transcriptional control of a CMV promoter and was used for the assessment of transfection efficiency in the HDI model.

2.1.3 Wild-type TALENs

TALENs generated by Bloom and colleagues were designed to target four conserved sites within the *S*, *C* and *P* ORFs of HBV (Bloom et al., 2013). The S and C TALENs were designed against the *S* and *C* ORFs respectively, while the P1 and P2 TALENs were designed against transcriptional regulatory elements within the *P* ORF. TALE monomers were generated from the TALE protein AvrBs4 scaffold (Mussolino et al., 2011). The right and left TALE arrays were cloned downstream of a haemagglutinin (HA) tag and nuclear localisation signal and upstream of a *Fok*I nuclease domain sequence. This entire sequence was under the transcriptional control of a CMV promoter/enhancer. For optimal cleavage, each monomer (right and left) was designed to target and bind 19 nucleotide sequences that started with a thymine at the 5’ end. In addition 13 base pair sequences, comprising the spacers, separated the binding sites of the left and right monomers.

2.2 Generation of third generation obligate heterodimeric Sharkey TALENs

2.2.1 Transformation of wild-type TALEN and Sharkey-encoding plasmids

Wild-type TALENs monomers (SR, SL, CR, CL), RM101-3rd generation Sharkey KKR and pUC57 Sharkey ELD (unpublished data) (KKR and ELD) plasmids were used to transform 100 µl of chemically competent *E. coli* (Appendix 5.1). Bacterial cells transformed with wild-type TALEN plasmids and KKR Sharkey-encoding plasmid were plated on Luria-Bertani agar plates containing kanamycin (100 µg/ml) whereas bacteria transformed with the ELD Sharkey-encoding plasmid were plated on an agar plate containing ampicillin (100 µg/ml) and incubated at 37 °C overnight. Colonies for the wild-type TALEN monomers and Sharkey plasmids were inoculated in 150 ml of Luria-Bertani medium supplemented with kanamycin (100 µg/ml) or ampicliin (100 µg/ml) and incubated overnight at 37 °C with shaking.

S and C TALEN monomer plasmids as well as the plasmids encoding the Sharkey variants (KKR and ELD) were purified using the Plasmid Maxi Kit (Qiagen, Hilden, Germany) according to the manufacturer's instructions (Appendix 5.2). The purified wild-type TALEN plasmids were screened with *Bgl*I and Sharkey plasmids (KKR and ELD) were digested with *AvaI*, *Sph*I, *Acc*I (Appendix 5.3, Figure 5.1**)** and *Bgl*I (Appendix 5.4, Figure 5.2) in a 20 µl reaction volume. The digestion reactions were set up as follows, 1 µg of each wild-type TALEN monomer (SR, SL, CR or CL) plasmid or each of the Sharkey plasmids (KKR or ELD), 2 µl of 10× Buffer, 1 U of the respective enzyme and ddH_2O to a final volume of 20 µl. The digestions were incubated at 37 °C for 2 hours and the restriction digests were resolved on a 1 % agarose gel containing ethidium bromide (0.5 µg/ml) (Appendix 5.5).

2.2.2 Construction of the Sharkey anti-HBV TALENs

To produce third generation anti-HBV Sharkey TALENs the sequence encoding the wild-type *Fok*I catalytic domain was replaced with the sequence encoding the Sharkey variants (Figure 2.1). The S and C TALEN monomers were double digested to excise the wild-type *Fok*I nuclease domain.The digestion reactions were carried out in two steps. The first digestion was carried out in a 20 µl reaction volume containing 1 µg of each wild-type TALEN monomer, 2 µl 10× Buffer, 1 U *Apa*I, and ddH_2O. The digestion reaction was incubated at 37 °C for 2 hours. The restriction digests were resolved on a 1 % agarose gel containing ethidium bromide (0.5 µg/ml) and imaged using a G:BOX UV transilluminator (Syngene, Cambridge,

UK). The single linearised band was excised from the gel and purified using the Qiagen MinElute Gel Extraction kit according to the manufacturer's instructions (Qiagen, Hilden, Germany) (Appendix 5.6). The purified *Apa*I digested plasmid was further digested with *Bam*HI to remove the wild-type *Fok*I nuclease domain-encoding sequence. The second digestion was carried out in a 20 µl reaction volume with the entire volume of purified linearised plasmid DNA, 2 µl of buffer, 1 U of *Bam*HI and ddH_2O. The digestion reaction was incubated at 37 °C for 2 hours. The restriction digests were resolved on a 1 % agarose gel containing ethidium bromide (0.5 µg/ml). The backbones of the S and C TALEN plasmids were excised from the gel and purified with the Qiagen MinElute Gel Extraction kit according to the manufacturer's instructions. The ELD and KKR plasmids were digested with the same enzymes (*Apa*I and *Bam*HI) to excise the enhanced Sharkey *Fok*I nuclease domain-encoding sequences.

The ELD and KKR variant sequences were ligated into the left and right monomers of the wild-type TALENs respectively. The KKR and ELD variant sequences were ligated at a 3:1 ratio to the S and C TALEN plasmid backbones in a 20 µl reaction volume that consisted of 2 µl of 10× Ligation buffer, 1 U of T4 DNA Ligase and ddH_2O to a final volume of 20 µl. Ligation mixes were incubated overnight at 14 °C. Thereafter the ligation mixes were used to transform 100 µl of chemically competent cells *E. coli*. The transformed cells were plated on Luria-Bertani agar plates containing kanamycin (100 µg/ml) and incubated at 37 °C overnight. Colonies were selected and inoculated in 10 ml of Luria-Bertani medium supplemented with kanamycin (100 µg/ml). This was incubated on a shaker overnight at 37 °C. Plasmid DNA was extracted using EconoSpin™ All-in-One Spin Columns according to manufacturer's instructions (Epoch Life Sciences, MO, USA) (Appendix 5.7). The plasmids were screened by enzyme digestion using *Dra*I and *Ava*II for the right S and C Sharkey TALEN monomer plasmids (SR+KKR and CR+KKR) and with *Dra*I and *Eco*RI for the left S and C Sharkey TALEN monomer plasmids (SL+ELD and CL+ELD). The digestion reactions were set up as follows, 1 µg of each Sharkey TALEN plasmid, 2 µl of 10× Buffer, 1 U of each enzyme and ddH_2O to a final volume of 20 µl. The digestion reactions were incubated at 37 °C for 2 hours and resolved on a 1% agarose gel containing ethidium bromide (0.5 µg/ml). Clones positive for the correct sized insert were sequenced to confirm that the left and right monomers included the correct variants (Inqaba Biotec, Pretoria, South Africa) (Appendix 5.8, Figure 5.3 to 5.8). The correct plasmids are hereafter referred to as anti-HBV Sharkey TALEN plasmids (Table 2.1).

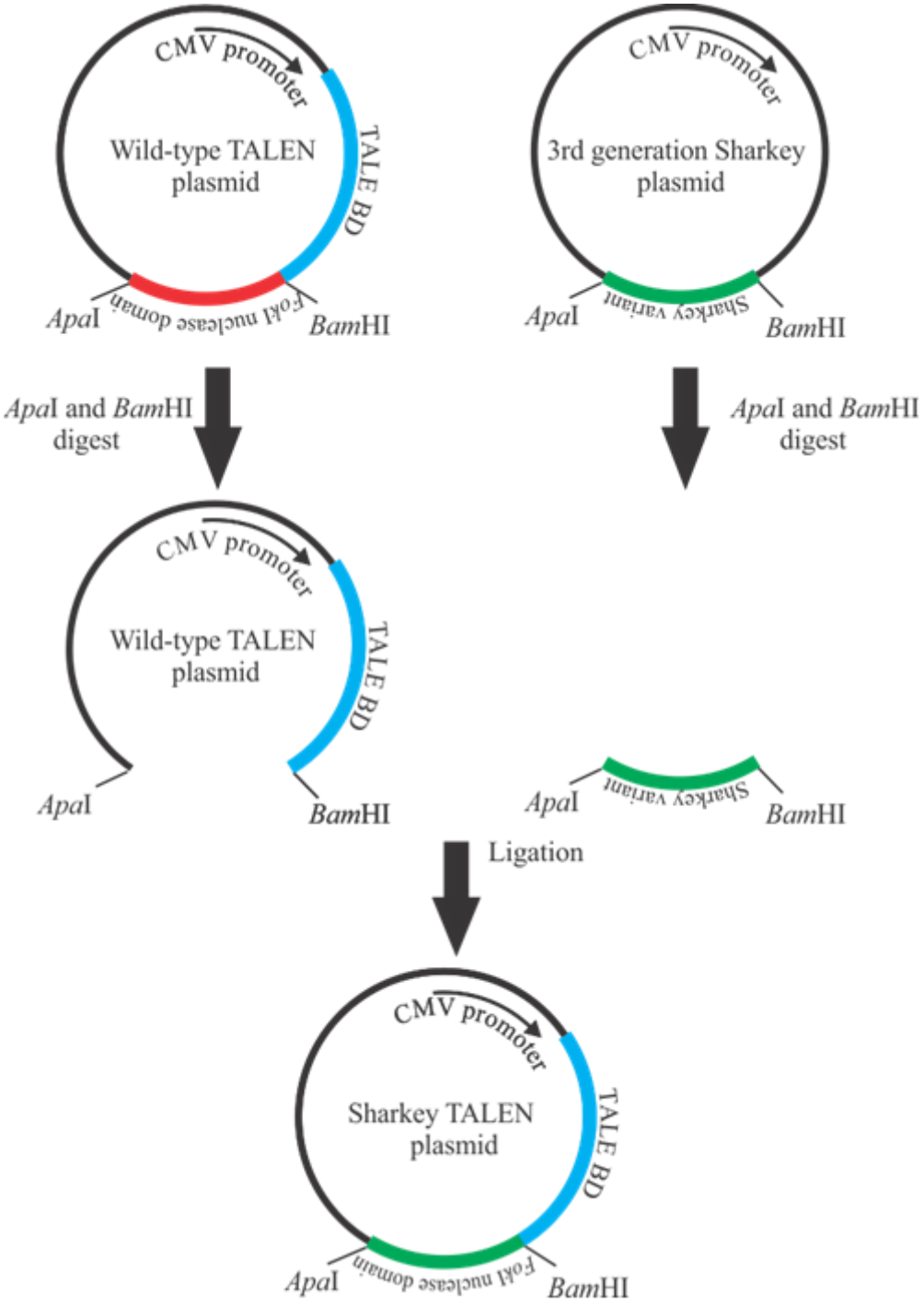

Figure 2.1: Cloning strategy for the generation anti-HBV Sharkey TALEN-encoding plasmids.

The Sharkey anti-HBV TALEN plasmids were generated by replacing the sequence encoding the wild-type *Fok*I catalytic domain with the sequence encoding the Sharkey variants (KKR or ELD). The wild-type *Fok*I nuclease domain and Sharkey variant sequences (KKR and ELD) were excised from their respective plasmids with *Apa*I and *Bam*HI.

Table 2.1: Anti-HBV TALENs plasmids and their nuclease encoding domains

Plasmid	TALEN generation	Viral target	Nuclease Domain
pCMV SR+WT	First generation	*S* ORF	Wild-type *Fok*I nuclease domain
pCMV SL+WT	First generation	*S* ORF	Wild-type *Fok*I nuclease domain
pCMV CR+WT	First generation	*C* ORF	Wild-type *Fok*I nuclease domain
pCMV CL+WT	First generation	*C* ORF	Wild-type *Fok*I nuclease domain
pCMV SR+KKR	Third generation	*S* ORF	Third generation Sharkey *Fok*I nuclease domain
pCMV SL+ELD	Third generation	*S* ORF	Third generation Sharkey *Fok*I nuclease domain
pCMV CR+KKR	Third generation	*C* ORF	Third generation Sharkey *Fok*I nuclease domain
pCMV CL+ELD	Third generation	*C* ORF	Third generation Sharkey *Fok*I nuclease domain

[1]

2.3 Characterisation of the enhanced TALENs in cultured mammalian cells

2.3.1 Large Scale Plasmid preparation

The Sharkey and wild-type S and C TALEN monomer plasmids, HBV replication competent plasmid (pCH-9/3091), mock plasmid (pUC118) and marker plasmid (pCI-neo-eGFP) were prepared using the QIAGEN Plasmid Maxi Kit (Qiagen, Hilden, Germany) according to the manufacturer's instructions (Appendix 5.2).

2.3.2 Immunofluorescence staining of anti-HBV TALENs

Twenty four hours prior to transfection, Huh 7 cells were seeded, in 48-well CellStar® plates (Greiner Bio-One, Frickenhausen, Germany) at 80 000 cells per well in 250 µl of complete DMEM (Appendix 5.9). Huh 7 cells were transfected with 200 ng of wild-type or Sharkey TALEN plasmids using 1:1 ratio Lipofectamine™ 3000 (Thermo Scientific, CA, USA) to

[1] The R denotes the right monomer and L denotes left monomer

plasmid DNA. The wild-type TALENs were used as positive controls and pUC118 was used as a negative control.

Transfection reactions were incubated at 37 °C and 5% CO_2 for the duration of the experiment. Cells separately transfected with pCI-neo-eGFP were used to assess the efficiency of transfection. All transfection reactions were performed in triplicate. Forty-eight hours after transfection immunofluorescence staining was conducted on the transfected cells.

To determine wild-type and Sharkey TALEN monomer expression, immunofluorescence was carried out on transfected cells. Transfection efficiency was assessed by analysis of GFP expression through a Fluorescein isothiocyanate (FITC) filter using a fluorescence microscope (Axiovert 100M, Zeiss, Oberkochen, Germany). The medium was removed and the cells were washed with 200 µl of 1× phosphate buffered saline (PBS) (Sigma-Aldrich, MO, USA). The Huh 7 cells were subsequently fixed in 200 µl of 4% paraformaldehyde (PFA) at room temperature for 15 minutes. The PFA was removed and the cells were washed twice with 200 µl of 1× PBS and incubated with 200 µl of 0.1% Triton-X (Sigma-Aldrich, MO, USA) in PBS for 10 minutes at room temperature. The cells were then washed twice with 200 µl of 1× PBS and blocked in 100 µl of 1% bovine serum albumin (BSA) (Roche Applied Science, Mannheim, Germany) in 1× PBS at room temperature for 1 hour in a humidity chamber. One hundred microlitres of mouse anti-HA primary antibody (Abcam, Cambridge, UK), diluted 1:200 in 1% BSA, was added to each well and incubated in a humidity chamber for 1 hour at room temperature. The cells were washed twice with 200 µl of 1× PBS. One hundred microlitres of fluorescently labelled (Alexa Fluor 488) secondary antibody (Thermo Scientific, CA, USA), diluted 1:200 in 1% BSA, was added to each well and incubated in the dark for 40 minutes at room temperature. The cells were washed twice with 200 µl of 1× PBS and stained with 100 µl of 1× 4, 6-diamidine-2-phenylindole chloride (DAPI) for 5 minutes at room temperature. Thereafter, DAPI was removed and the cells washed twice with 200 µl of 1× PBS. FITC and DAPI filters were used to detect signal from the cells and were imaged using a fluorescence microscope.

2.3.3 Transfection of Huh 7 cells to evaluate HBsAg knockdown

Twenty four hours prior to transfection, Huh 7 cells were seeded, in 6-well CellStar® plates (Greiner Bio-One, Frickenhausen, Germany) at 960 000 cells per well in 2 ml of complete low glucose DMEM (Appendix 5.9).Lipofectamine™ 3000 was used to co-transfect pCH-9/3091 and pCI-neo-eGFP with the wild-type TALEN, Sharkey TALEN or pUC118 (mock) plasmids. The transfection mix was prepared as follows: 200 ng of pCI-neo-eGFP, 300 ng of

pCH-9/3091 and 500 ng of left and 500 ng of right monomer or 1000 ng of pUC118. Transfection mixes were added to cells and incubated at 37 °C and 5% CO_2 for the duration of the experiment. An HBsAg ELISA was carried out 48 hours after transfection.

To determine HBsAg levels in the culture supernatant an ELISA was carried out 48 hours post transfection using the Monolisa™ HBs Ag ULTRA kit (Bio-Rad, CA, USA). One hundred microlitres of supernatant was removed from the transfected cells and added to a well of the microplate. Fifty microlitres of conjugate working solution was added to each well. The plate was covered with adhesive film and incubated at 37 °C for 1 hour and 30 minutes. After incubation the plate was washed using the Immuno Wash™ 1575 Microplate Washer (Bio-Rad, CA, USA). One hundred microlitres of the development solution was added to each well and incubated in the dark for 30 minutes at room temperature. After 30 minutes of incubation in the presence of substrate, the reaction was terminated using 100 µl of stopping solution and incubated at room temperature for 4 minutes. The optical densities of the samples were measured at 490/655 nm using the iMark™ Microplate Reader (Bio-Rad, CA, USA).

2.3.4 Transfection of HepG2.2.15 cells and knockdown analysis

A day prior to transfection HepG2.2.15 cells were seeded in 6-well CellStar® plates 960 000 cells per well in 2 ml of complete DMEM (Appendix 5.9). Two hours before transfection culture supernatant was harvested to determine baseline HBsAg expression levels. Lipofectamine™ 3000 was used to co-transfect HepG2.2.15 cells. Transfection mixes were prepared as follows; 4600 ng of pUC118 or 2300 ng of plasmid expressing the left wild-type or Sharkey TALEN monomers (SL, SL+ELD, CL and CL+ELD) and 2300 ng of plasmid expressing the corresponding right wild-type or Sharkey TALEN monomer (SR, SR+KKR, CR and CR+KKR) and 400 ng pCI-neo-eGFP. HepG2.2.15 cells were incubated at 32 °C and 5% CO_2. Co-transfection of HepG2.2.15 with pUC118 and wild-type TALENs functioned as negative and positive controls respectively.

Transfections were performed in triplicate. For the first (day 3), second (day 8) and third (day 14) transfection, 100 µl of medium was removed for ELISA (Section 2.3.3) forty eight hours post-transfection and growth medium was replaced. On day 5 growth medium was removed and cells washed with 500 µl of saline/EDTA. The saline/EDTA solution was removed and 500 µl of TrypLE Express (Gibco™, Thermo Scientific, CA, USA) was added to each well and incubated at 32 °C (5% CO_2) for 5 minutes. After the incubation period 500 µl of medium was added and the cells were re-suspended. The re-suspended cells were transferred into sterile 1.5 ml microcentrifuge tubes and centrifuged at 200 ×g for 3 minutes. The pellet was

re-suspended in 1000 µl of saline and 800 µl at stored at -70 °C. The remaining cells (~200 µl) were re-seeded into 6-well plates, 1800 µl of fresh medium was added and incubated at 32 °C (5% CO_2). This transfection procedure was repeated twice. The triple transfected HepG2.2.15 cells harvested and stored at-70 °C were used for CelI assays.

2.3.4.1 DNA extraction from HepG2.2.15 cells

To confirm targeted sequence disruption at the intended sites, total DNA was extracted from HepG2.2.15 cells using the QIAamp® DNA Blood Mini Kit as per manufacturer's instructions (Qiagen, Hilden, Germany). Two hundred microlitres of the HepG2.2.15 cells harvested from the transfections was used, 20 µl of proteinase K was added and the solution mixed vigorously by pulse vortexing for 15 seconds. To each sample 200 µl of AL buffer was added and mixed by pulse vortexing for 15 seconds. The samples were then incubated at 56 °C for 10 minutes. Thereafter the samples were briefly centrifuged, 200 µl of ethanol (98-100 %) was added to each sample and mixed by pulse vortexing for 15 seconds. The mixture was transferred to a spin column, centrifuged at 6000 ×g for 1 minute and the flow-through discarded. To each column 500 µl of AW1 buffer was added and centrifuged for 1 minute at 6000 ×g. The flow-through was discarded, 500 µl of AW2 buffer was added and centrifuged at 20 000 ×g for 3 minutes. The flow-through was discarded; the spin column was added into a new collection tube and centrifuged at 20 000×g for an additional minute. The column was placed in a clean 1.5 ml microcentrifuge tube and 200 µl of ddH_2O was added, incubated at room temperature for 5 minutes and centrifuged at 6000 ×g for 1 minute. The concentrations of the DNA samples were measured spectrophotometrically using the NanoDrop™ 1000 Spectrophotometer (Thermo Scientific, CA, USA).

2.3.4.2 Amplification of DNA for CelI assay

For the CelI assay, sequences flanking the Sharkey S and C TALEN sites were amplified from the DNA extracted from transfected cells using the KAPA HiFi HotStart ReadyMix (Kapa Biosystems, MA, USA). Primer sets used for PCR are listed in Table 2.2. The PCR reaction mix was prepared as follows: 12.5 µl of KAPA HiFi HotStart ReadyMix, 10 pmol each of forward and reverse primers, 5 µl template DNA and ddH_2O made up to a final volume of 25 µl. PCR conditions were as follows: initial denaturation at 95 °C for 2 min; 30 cycles of 95 °C for 15 s, 58 °C and 60 °C for 15 for C and S TALEN target sites respectively, and 72 °C for 15 seconds followed by a final elongation at 72 °C for 5 minutes and cooling to 4 °C. Successful PCR amplification was assessed by checking 3 µl of each reaction by agarose gel electrophoresis using Orange G loading dye. The remaining 22 µl of the reaction

was column-purified using the Qiagen MinElute Gel Extraction kit according to the manufacturer's instructions (Qiagen, Hilden, Germany) (Appendix 5.6). Purified amplicons were quantified by spectrophotometry.

Table 2.2: Primer sequences used to amplify TALEN target sequences for CelI assay

Target Sites	Forward Primer	Reverse Primer
***S* ORF**	5'-TGC ACC TGT ATT CCC ATC-3'	5'-CTG AAA GCC AAA CAG TGG-3'
***C* ORF**	5'-ACC ACC AAA TGC CCC TAT-3'	5'-TTC TGC GAG GCG GCG A-3'

2.3.4.3 CelI assay

To determine whether TALENs successfully introduced mutations at target sites CelI assays were set up as follows: 200 ng of PCR amplified DNA, 1× NEB Buffer 2 (New England Biolabs, NJ, USA) and ddH_2O to a final volume of 12 µl. The samples were denatured at 95 °C for 5 minutes, cooled to 35 °C at 0.1 °C/s and incubated at 35 °C for a further 2 minutes to allow for heteroduplex formation. Samples were cooled to 4 °C and incubated on ice for 5 minutes after which 1 µl of the CelI enzyme (extracted from celery by Dr Wolfgang Prinz) was added and incubated at 37 °C for 25 minutes. Samples were allowed to cool to 4 °C for an additional 10 minutes. Each sample received 4 µl of Orange G Loading dye and was resolved on a 2% agarose gel. Migration patterns of the DNA bands were visualised using UV transillumination and separated bands were quantified by densitometry using ImageJ (version 1.46)(Guschin et al., 2010, Abramoff et al., 2004). Percentage targeted disruption was calculated using the following equation:

$$\text{Targeted cleavage} = 100 \times \left[1 - \left(1 - \frac{Fraction\ cleaved}{Fraction\ uncleaved + Fraction\ cleaved}\right)^{\frac{1}{2}}\right]$$

2.3.5 Assessment of Sharkey TALEN toxicity in cultured cells

A methyl-thiazolyl-tetrazolium (MTT) assay was carried out to determine cell viability after treatment with Sharkey TALENs. HEK293T cells were seeded into 6-well CellStar® plates twenty four hours prior to polyethylenimine (PEI) transfection. HEK293T cells were used as

they transfect well and are more sensitive for cytotoxicity assessments. Cells were transfected in triplicate with wild-type TALEN, Sharkey TALEN and pUC118 plasmids as follows: 15 ng pCH-9/3091, 15 ng pCI-neo-eGFP and 85 ng each of left and right TALEN plasmids or 170 ng of pUC118. An untransfected control consisting of cells receiving no DNA as well as cells treated with 50% dimethyl sulphoxide (DMSO) (positive control) was included in separate wells. The cell viability was assessed forty eight hours post transfection by adding 20 µl of 3-(4, 5-Dimethylthiazol-2-yl)-2, 5 diphenyltetrazoliumbromide (MTT) solution (5 mg/ml) in 1× PBS to each well and incubating at 37 °C (5% CO_2) for 1 hour. Cell culture medium was gently aspirated and the purple formazan by-product was re-suspended in 200 µl of DMSO by aspirating up and down gently. Optical density of the samples was measured at 570 and 650 nm using the iMark™ Microplate Reader.

2.4 Assessment and evaluation of Sharkey TALENs in vivo

2.4.1 Large-Scale Endotoxin-Free plasmid preparation

The wild-type and Sharkey TALEN plasmids, HBV replication competent plasmid (pCH-9/3091), pUC118 and pCI-neo-FLuc were prepared for the in vivo assessment using the EndoFree® Plasmid Maxi Kit (Qiagen, Hilden, Germany) according to the manufacturer's instructions and DNA pellets were re-suspended in 100 µl of sterile H_2O (Appendix 5.10). The purified endotoxin-free plasmids were screened by enzymatic digestion (Appendix 5.11, Figure 5.9 and Figure 5.10).

2.4.2 Hydrodynamic injection of mice

In vivo assessment of anti-HBV Sharkey TALENs was carried out in the mouse HDI model of HBV replication. All experiments on animals were conducted in accordance with protocols approved by the University of the Witwatersrand Animal Ethics Screening Committee (Appendix 5.12). Three to five week old female Naval Medical Research Institute (NMRI) mice were divided into five groups (mock (pUC118), wild-type S TALEN, wild-type C TALEN, Sharkey S TALEN and Sharkey C TALEN). The injectate comprised of a plasmid DNA-containing saline solution equal to 10% of the body weight of each individual mouse (final volume of 2-3 ml). The DNA/saline solutions contained 5 µg HBV target DNA (pCH-9/3091), 5 µg pCI-neo-FLuc and either 20 µg of pUC118 or 10 µg of each corresponding right and left TALEN-expressing plasmids.

2.4.3 Bioluminescence imaging

Using the IVIS Kinetic In Vivo Optical Imaging System (PerkinElmer, MA, USA,) bioluminescence imaging was conducted to assess liver transfection by the plasmids. Mice were injected intraperitoneally with 150 mg/kg of luciferin (PerkinElmer, MA, USA), anaesthetised using isoflurane and imaged. Mice in which bioluminescence was not detected were excluded from the study.

2.4.4 Blood collection and processing

Anti-HBV-mediated Sharkey TALEN knockdown analysis was conducted on the blood samples collected on days 3 and 5. Mice were anaesthetised with isoflurane and blood was collected by retro-orbital bleeding.

The blood samples were incubated at 4 °C for 1 hour to allow for coagulation. After the incubation period, samples were centrifuged at 6000 ×g for 10 minutes at 4 °C. The serum was carefully removed and placed in clean microcentrifuge tubes. For ELISAs 25 µl of the serum was adjusted to 100 µl with saline. Surface antigen expression was assessed using the Monolisa™ HBs Ag ULTRA kit according to the manufacturer's instructions (Section 2.4.2.1). To quantify VPEs 25 µl was made up to 200 µl with saline and total DNA was extracted using QIAamp® DNA Mini Kit according to the manufacturer's instructions (Section 2.4.3.1).

2.4.4.1 Quantification of HBV viral particle equivalents

Circulating VPEs from experimental and control mice were determined by qPCR using the CFX96 Touch™ Real-Time PCR Detection System (Bio-Rad, CA, USA). The Acrometrix HBV Panel (Thermo Scientific, CA, USA) was used as a standard to quantify real-time qPCR data. The qPCR reactions were prepared as follows, 10 pmol each of the respective surface reverse and forward primers (Table 2.2), 10 µl of 2× FastStart Essential DNA Green Master (Roche Applied Science, Mannheim, Germany) and 5 µl of template DNA made up to a final volume of 20 µl with nuclease-free water. The thermal cycling conditions were as follows: initial denaturation at 95 °C for 10 minutes followed by 40 cycles of denaturation at 95 °C for 20 seconds, annealing at 57 °C for 20 seconds and final extension at 72 °C for 20 seconds. Directly after qPCR a melting curve analysis was conducted, the cycling conditions were as follows: denaturation at 95 °C for 10 seconds followed by cooling at 65 °C for 1 minute and heating to 95 °C at a ramp rate of 0.1 °C/s with continuous signal acquisition.

2.4.4.2 In vivo assessment of Sharkey TALEN-mediated toxicity

One hundred microlitres of serum from the day 5 bleeds was diluted with an equal volume of saline and used to assess liver toxicity. Liver ALT levels were quantified by the National Health Laboratory Service (NHLS) in the Charlotte Maxeke Johannesburg Academic Hospital using a kinetic assay with an automated photometric analyser (Roche Diagnostics, Rotkreuz, Switzerland). All serological results were adjusted to account for the initial serum dilution.

2.5.5 Liver collection and processing

Mock and anti-HBV TALEN-treated mice were sacrificed by CO_2 exposure 5 days post-injection and their livers harvested. The liver samples were sectioned for DNA and RNA extraction.

2.5.5.1 RNA extraction

One millilitre of TRIzol® Reagent (Thermo Scientific, CA, USA) was added to approximately 100 mg of liver and homogenised. The homogenate was centrifuged for 10 minutes at 7 500 ×g and the supernatant transferred to a clean 1.5 ml microcentrifuge tube. Two hundred microlitres of chloroform was added to the supernatant and mixed vigorously. The samples were incubated at room temperature for 5 minutes and centrifuged at 12 000 ×g for 15 minutes at 4 °C. Approximately 500 µl of the upper aqueous phase was transferred to a clean 1.5 ml microcentrifuge tube. To the aqueous phase 500 µl of absolute isopropanol was added, mixed by inverting the microcentrifuge tube and incubated at room temperature for 5 minutes. Following incubation the samples were centrifuged at 12 000 ×g for 15 minutes. The supernatant was discarded and the pellet was washed in 1 ml of 75% ethanol followed by centrifugation at 7 500 ×g for 5 minutes. The supernatant was removed and the pellet briefly centrifuged to collect residual ethanol for removal. The pellet was left to air dry and re-suspended in 100 µl of RNase-free water. The concentration and purify of the RNA samples were measured by spectrophotometry using the NanoDrop™ 1000 Spectrophotometer.

2.5.5.2 Reverse transcription of RNA to cDNA

The QuantiTect reverse transcription kit (Qiagen, Hilden, Germany) was used to reserve transcribe 1 µg of extracted RNA from the liver. Briefly, 1 µg of RNA and 2 µl of gDNA were made up to a final volume of 14 µl using RNase-free water and incubated at 42 °C for 8 minutes. Thereafter, 4 µl of 5× QuantiTect reverse transcription (RT) buffer, 1 µl of RT primer mix and 1 µl of QuantiTect reverse transcriptase was added, incubated at 42 °C for 30

minutes and followed by heat inactivation at 95 °C for 3 minutes. The expression of *surface* RNA and pregenomic RNA was quantified by qPCR and relativised to mouse *glyceraldehyde-3-phosphate dehydrogenase* (m*GAPDH*) mRNA levels. The qPCR reaction mix was prepared as follows, 10 pmol each of the respective reverse and forward primers (Table 2.4), 10 µl of 2× FastStart Essential DNA Green Master, 5 µl of template DNA and was made up to a final volume of 20 µl using RNase-free water. The Bio-Rad CFX96™ Real Time System was used for the qPCR and the thermal cycling conditions were as follows, initial denaturation at 95 °C for 10 minutes, 40 cycles of denaturation at 95 °C for 20 seconds, followed by annealing at 57 °C for 20 seconds, extension at 72 °C for 20 seconds. Directly after qPCR a melting curve analysis was conducted, the cycling conditions were as follows: denaturation at 95 °C for 10 seconds followed by cooling at 65 °C for 1 minute and heating 95 °C at a ramp rate of 0.1 °C/s with continuous signal acquisition.

Table 2.3: Sequences of the primers used in qPCR to quantify HBV mRNA

Target Sites	Forward Primer	Reverse Primer
Surface (HBS)	5'-TGC ACC TGT ATT CCC ATC-3'	5-’CTG AAA GCC AAA CAG TGG-3'
Core (BCP)	5-'ACC ACC AAA TGC CCC TAT-3'	5'-TTC TGC GAG GCG GCG A-3'
mGAPDH	5'-TTC ACC ACC ATG GAG AAG GC-3'	5'-GGC ATG GAC TGT GGT CAT GA-3'

2.5.5.3 DNA extraction from Liver

For DNA extraction from liver tissue, each sample was weighed, an equal volume of saline added and the samples mechanically homogenised. DNA was extracted from homogenised tissue samples using the QIAamp® DNA Blood Mini Kit as per the manufacturer's instructions (Qiagen, Hilden, Germany). Briefly, 50 µl of homogenate (a volume equivalent to 25 mg of liver) was added to a clean microcentrifuge tube and the volume adjusted to 100 µl with saline. To this mixture 100 µl Buffer ATL was added, followed by 20 µl of proteinase K and the samples mixed by pulse vortexing for 15 seconds. The samples were incubated at 56 °C in a shaking water bath for approximately 3 hours to allow for complete lysis of the liver tissue. After incubation the samples were briefly centrifuged, 4 µl RNase A (100 mg/ml) added, the samples vortexed for 25 seconds and subsequently incubated at room temperature for 2 minutes. The samples were briefly centrifuged before adding 200 µl Buffer AL, pulse-vortexed for 15 seconds and incubated at 70 °C for 10 minutes. After the incubation, 200 µl of ethanol (98-100%) was added to each sample and mixed by pulse-vortexing for 15 seconds. The mixture was transferred to a spin column and centrifuged at 6000 ×g for 1 minute. The flow-through was discarded, 500 µl of AW1 was added and the tube was centrifuged for 1 minute at 6000 ×g. The flow-through was discarded, 500 µl of AW2 was added and the tube was centrifuged at 20 000×g for 3 minutes. The spin column was transferred to a new collection tube and centrifuged at 20 000×g for 1 minute to remove residual wash buffer. The column was subsequently placed in a clean 1.5 ml microcentrifuge tube, 100 µl of ddH_2O was added and centrifuged at 6000 ×g for 1 minute to elute the DNA. The concentration of the DNA samples were measured spectrophotometrically using a NanoDrop™ 1000 Spectrophotometer. The extracted DNA was used for CelI assay as described in Sections 2.3.4.2 and 2.3.4.3.

Chapter 3

3 Results

3.1 Construction of anti-HBV Sharkey TALENs

Anti-HBV Sharkey TALENs were generated by incorporating of the third generation obligate heterodimeric Sharkey variants into existing wild-type anti-HBV TALENs. The Sharkey TALENs consist of a TALE domain, which is a DNA-binding domain engineered to target the HBV genome, and a Sharkey nuclease domain, which has been proven to have increased catalytic activity (Guo et al., 2010). These Sharkey TALENs have been designed against the *S* and *C* ORFs and cause targeted disruption at these sites. To increase and improve the mutagenic activity of the existing anti-HBV TALENs, the wild-type *Fok*I nuclease domain was replaced by the third generation obligate heterodimeric Sharkey variants. The wild-type S and C TALEN monomer (left and right) plasmids were double digested with *Apa*I and *Bam*HI. This yielded two DNA fragments, the first being the 5284 bp TALE plasmid backbone and the second being the 601 bp *Fok*I nuclease domain-encoding sequence (Figure 3.1). The TALEN plasmid backbones for the S and C monomers (left and right) were extracted and gel purified for subsequent use in the ligation reaction.

Plasmids that contained the Sharkey variants were also double digested with *Apa*I and *Bam*HI to excise the Sharkey *Fok*I nuclease domain encoding sequences (KKR and ELD) (Figure 3.2). Digestion of plasmids yielded the 2699 bp or 5284 bp plasmid backbone and the 601 bp fragments encoding the Sharkey *Fok*I nuclease domain variants (KKR and ELD). The 601 bp fragments were extracted and gel purified. The ELD and KKR sequences were cloned into the left and right S and C TALE backbones respectively. Positive clones were identified by enzymatic digestion using *Dra*I, which cleaves within the left and right S and C Sharkey TALE backbones, *Ava*II for the right S and C Sharkey TALEN monomers and *Eco*RI for the left S and C Sharkey TALEN monomers (Figure 3.3). The S and C Sharkey TALEN plasmids were sequenced to confirm the presence of mutations that make up the left and right Sharkey variants (Appendix 5.8, Figure 5.3 to 5.8).

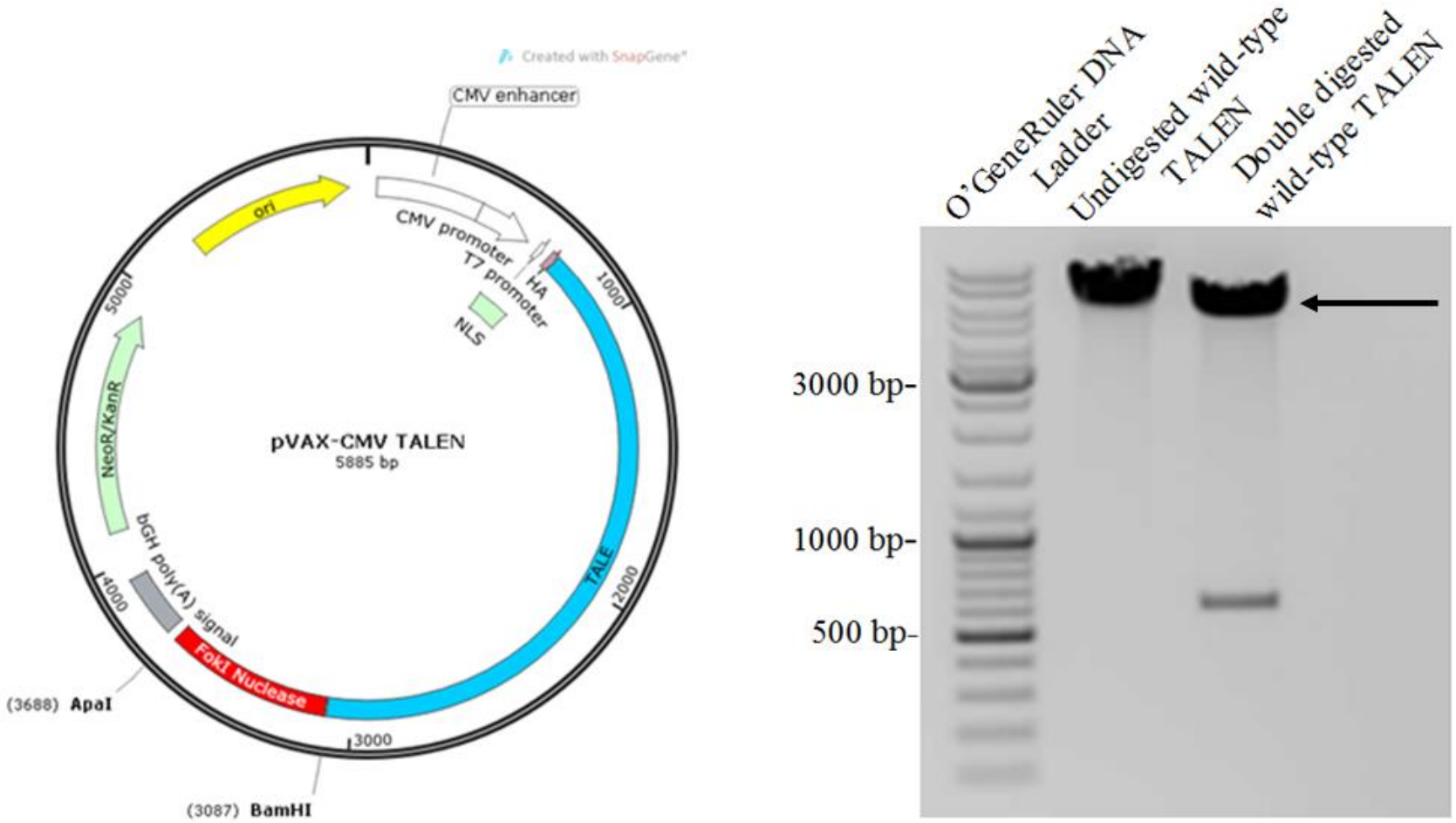

Figure 3.1: Enzymatic digestion of the wild-type TALEN plasmids.

The wild-type TALEN plasmids were double digested with *Apa*I and *Bam*HI to excise the wild-type TALEN backbones (S and C TALEN backbones) indicated by the arrow on the agarose gel. Expected fragment sizes for backbone are 5284 bp and 601 bp for the wild-type nuclease domain-encoding sequences. Lane 1: Molecular weight marker (O'GeneRuler DNA Ladder Mix, Thermo Scientific, CA, USA).

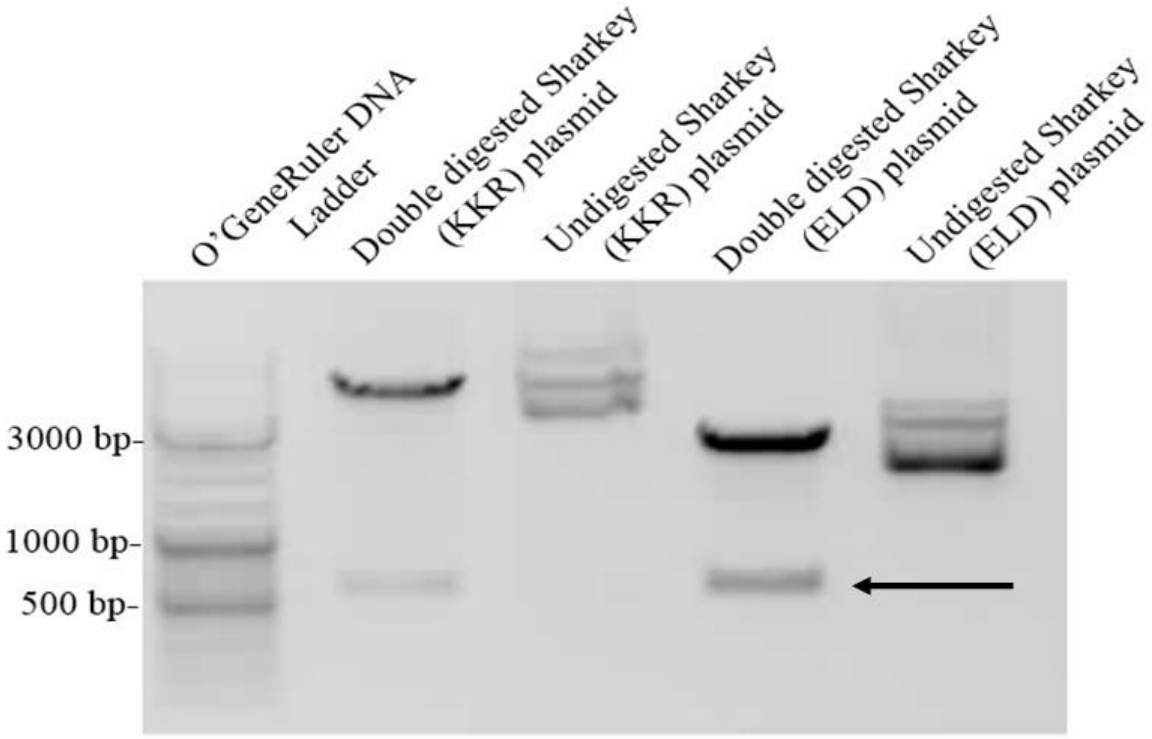

Figure 3.2: Enzymatic digestion of the Sharkey encoding plasmids.

Sharkey encoding plasmids were double digested with *Apa*I and *Bam*HI to excise enhanced Sharkey *Fok*I nuclease domain-encoding fragments indicated by the arrow. Expected fragment sizes for backbone are 5284 bp (KKR) and 2699 bp (ELD) and 601 bp for the enhanced Sharkey *Fok*I nuclease domain-encoding fragments. Lane 1: Molecular weight marker (O'GeneRuler DNA Ladder Mix). Expected banding patterns for the digestion reactions are indicated in Appendix 5.13, Figure 5.11.

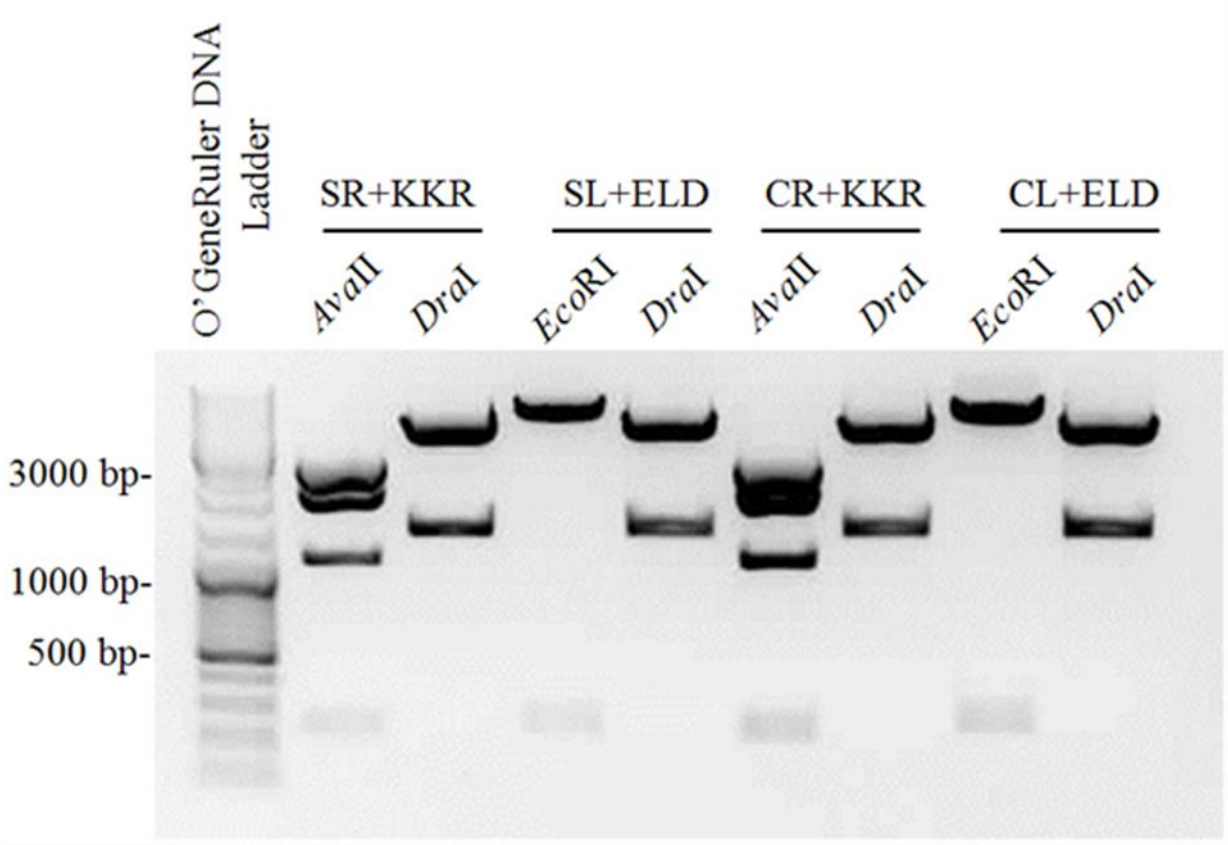

Figure 3.3: Screening of the third generation obligate heterodimeric Sharkey S and C TALEN plasmids by enzymatic digestion.

The right Sharkey TALEN plasmids, SR+KKR and CR+KKR, were digested with *Ava*II and *Dra*I, while the left Sharkey TALEN plasmids, SL+ELD and CL+ELD, were digested with *Eco*RI and *Dra*I. The expected banding patterns for the right and left monomers of the Sharkey S and C TALENs are indicated in Appendix 5.11, Figure 5.10. Lane1: Molecular marker (O'GeneRuler DNA Ladder Mix).

3.2 Anti-HBV Sharkey TALENs efficiently express in liver-derived cells

To examine expression of the nucleases, Huh 7 cells were transiently transfected with wild-type or Sharkey TALEN plasmids. The S and C Sharkey TALENs were directly compared to their wild-type equivalents. A mock transfection with pUC118 plasmid was used as a negative control and a separate pCI-neo-eGFP transfection was performed to determine whether the transfection was successful. To ensure reproducibility, transfections were performed in triplicate. Immunofluorescence detection of the HA tag using monoclonal primary antibody and a fluorescently labelled secondary antibody was used to stain Huh 7 cells.

Huh 7 cells transfected with the pCI-neo-eGFP showed successful and efficient transfection (Figure 3.4). The individual S and C Sharkey TALEN monomers were all expressed in this liver-derived cell line and expression was comparable to wild-type TALENs. As expected, green fluorescence was not detected in cells transfected with pUC118 plasmid.

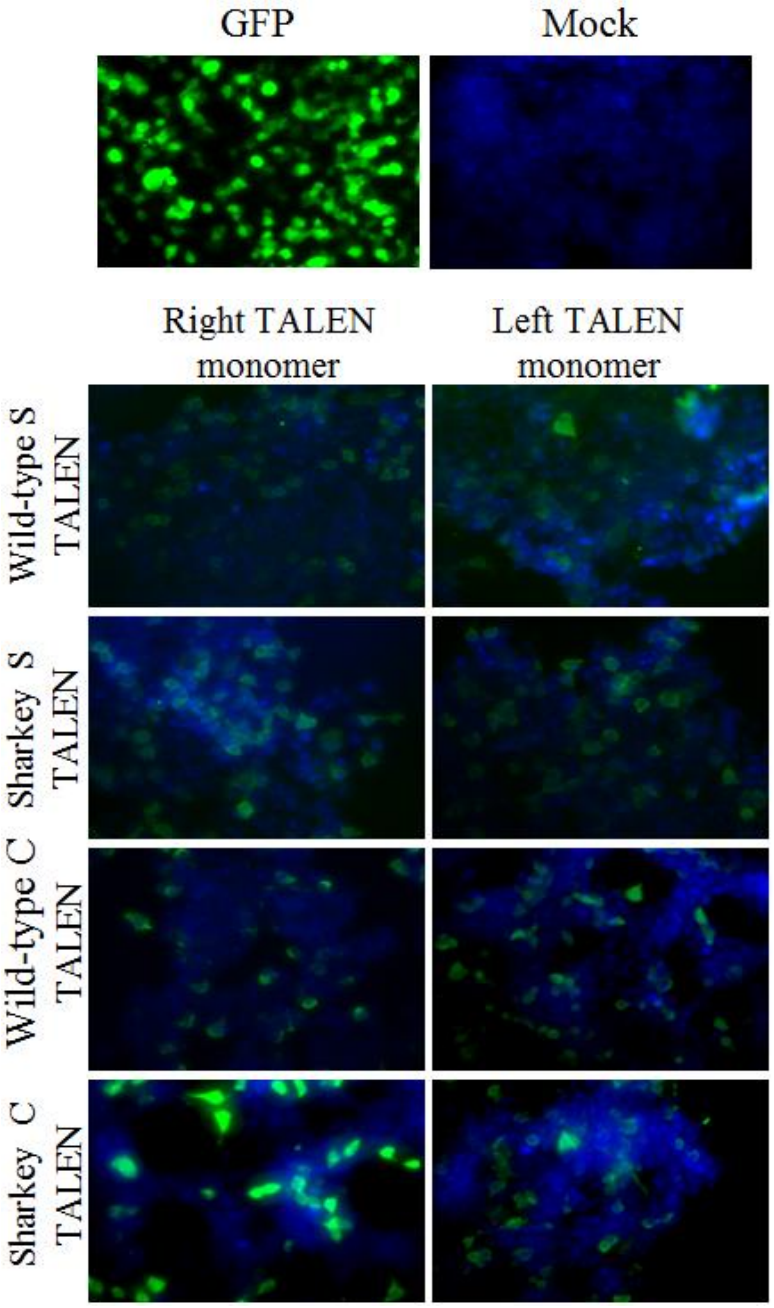

Figure 3.4: Detection of expressed Sharkey and wild-type S and C TALENs in cultured Huh7 cells using immunofluorescence.

Immunofluorescence staining was conducted to examine TALEN expression in a liver-derived cell line. Huh 7 cells were co-transfected with pUC118 (mock transfection) and individual Sharkey and wild-type TALEN monomer plasmids. In parallel, a pCI-neo-eGFP transfection was conducted to assess transfection efficiency. An anti-HA primary antibody together with a fluorescently labelled secondary antibody was used to detect TALEN expression. The nucleus was stained using DAPI. Cells were visualised using fluorescence microscopy at 20× magnification.

3.3 Anti-HBV Sharkey TALEN knockdown HBsAg in liver-derived cells

Once expression of the Sharkey TALENs was confirmed, efficacy of HBV silencing was evaluated in vitro. Huh 7 cells were co-transfected with the Sharkey or wild-type TALEN-encoding plasmids or pUC118 (negative control). Each transfection also included a HBV replication-competent plasmid (pCH-9/3091) and a GFP expressing plasmid (pCI-neo-eGFP) (Appendix 5.14, Figure 5.12). To ensure reproducibility transfections were performed in triplicate. The medium was removed from transfected cells and HBsAg secretion was determined by ELISA.

While both the wild-type and Sharkey S TALENs were able to inhibit HBsAg in Huh 7 cells, the wild-type S TALEN significantly knocked down HBsAg expression by 70% while the Sharkey S TALEN only achieved 25% knockdown (Figure 3.5). This was unexpected as studies have indicated the incorporation of Sharkey variants increase the catalytic efficiency in vitro (Guo et al., 2010). The Sharkey C and wild-type C TALEN transfected cells showed no inhibition of HBsAg expression as expected because the C TALENs target the *C* ORF and not the *S* ORF. Variability in transfection efficiency of the pCH-9/3091 plasmid and C TALENs in the Huh 7 cells (Appendix 5.14, Figure 5.12) could explain the apparent increased expression of HBsAg.

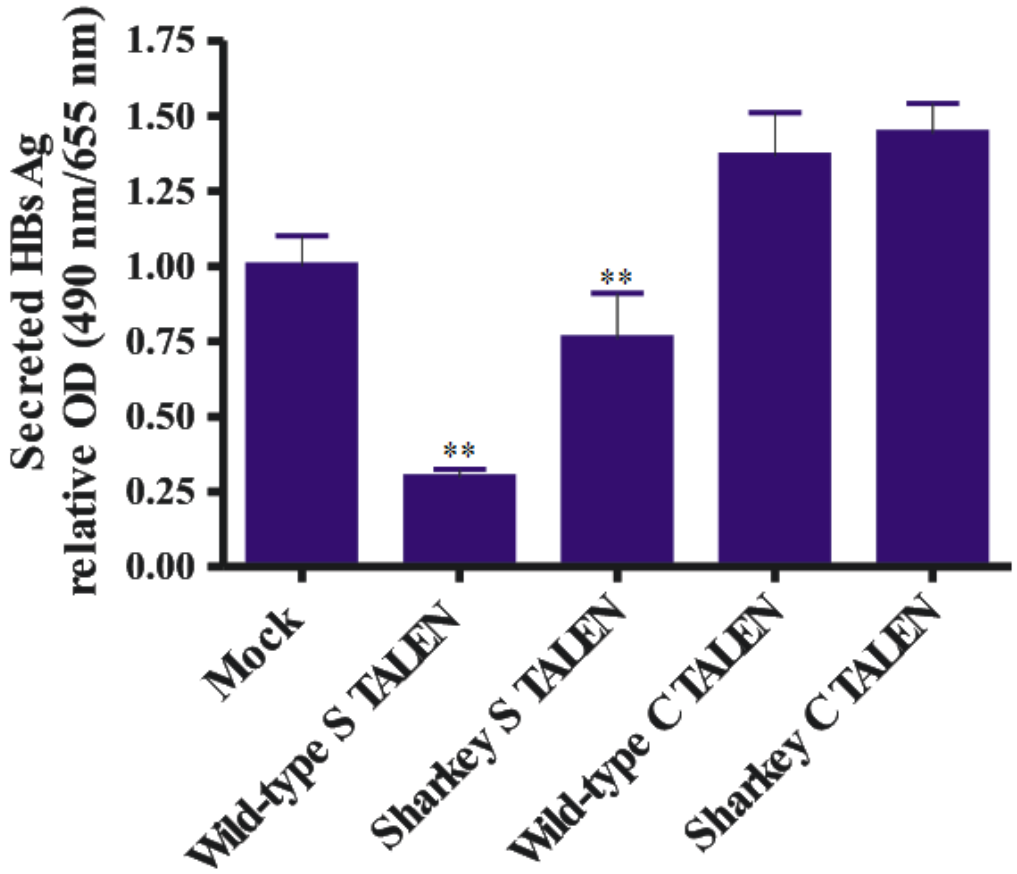

Figure 3.5: Assessment of Sharkey TALEN-mediated knockdown of HBsAg in Huh 7 cells.

To assess Sharkey TALEN efficiency, Huh 7 cells were co-transfected with pCH-9/3091, pCI-neo-eGFP and TALEN plasmids or pUC118 (mock). HBsAg levels in the supernatants were measured using ELISA forty-eight hours after transfection by ELISA. Transfections were performed in triplicate and the error bars indicate the standard error of the mean (SEM) (n=3), ** indicates $p< 0.01$.

3.4 Sharkey TALENs mediated inhibition of HBsAg and targeted disruption of HBV DNA in vitro

3.4.1 Sharkey TALENs mediate efficient HBsAg reduction in HepG2.2.15 cells

The HepG2.2.15 cell line contains a stable integrated HBV sequence and constitutively maintains a viral replicative cycle (Sells et al., 1987, Sells et al., 1988). This cell culture model of persistent viral replication was used to determine the efficacy of the wild-type and anti-HBV Sharkey TALENs. The HepG2.2.15 cells were transfected with the Sharkey or wild-type TALEN-encoding plasmids or pUC118. pCI-neo-eGFP was used to assess transfection efficiency (Appendix 5.15, Figure 5.13) and to ensure reproducibility transfections were performed in triplicate. Cells were triple transfected to increase the probability of targeted mutagenesis by the anti-HBV TALENs. The medium was removed two hours before transfection (day0/baseline) and post transfection for the second (day 8) and third (day 14) transfections from HepG2.2.15 cells and used to determine secreted HBsAg levels.

On day 8, the Mock and TALEN-treated cells show reduced HBsAg expression by 30% to 40% (Figure 3.6) and by day 14 HBsAg levels returned to baseline. Reduction of the HBsAg levels is unexpected as the mock transfected plasmids should not affect HBsAg levels and could indicate a problem with the transfection of the HepG2.2.15 cells. Neither Sharkey nor wild-type TALENs attained complete knockdown of HBsAg expression in HepG2.2.15 cells which was not unexpected as this cell line is characterised by high levels of viral gene expression. Nevertheless the results indicate that the S TALENs were able to moderately reduce HBsAg expression compared to the mock transfected on day 14.

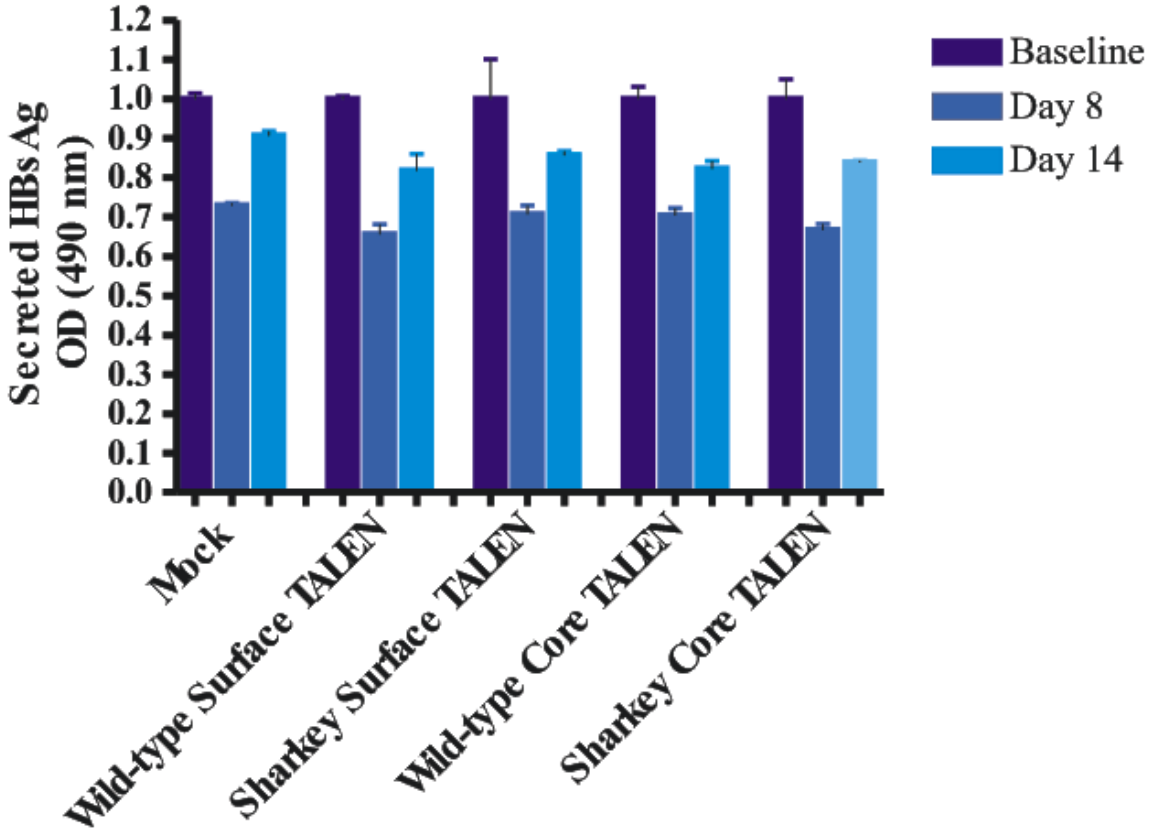

Figure 3.6: Sharkey and wild-type TALEN-mediated HBsAg reduction in HepG2.2.15 cells.

To assess Sharkey TALEN efficiency in a more stringent liver-derived cell line, HepG 2.2.15 cells were transfected with pCI-neo-eGFP and individual TALENs or pUC118. HBsAg levels in the supernatants were measured forty-eight hours post transfection for the baseline, second (day 8) and third (day 14) transfection by ELISA. Transfections were performed in triplicate.

3.4.2 Anti-HBV Sharkey TALENs mediate on-target cleavage in vitro

To examine targeted mutagenesis mediated by Sharkey S and C TALENs, total DNA was extracted from three consecutive transfected HepG2.2.15 cells. DNA from cells transfected with pUC118 was used as a negative control. Sequences spanning approximately 250 bp upstream and downstream of the TALEN target sites were amplified to produce a single band at 520 bp (Appendix 5.16, Figure 5.14 to 5.15). Site-specific Sharkey and wild-type TALEN-mediated cleavage was assessed using the CelI assay. In this assay, sequences spanning the target DNA binding sites were amplified by PCR (Figure 3.7). These PCR amplicons were subsequently denatured to separate the double stranded DNA into single strands and reannealed at room temperature to allow for heteroduplex and/or homoduplex formation. To this the CelI enzyme was added which recognises and cleaves heteroduplexes. Cleavage products are therefore indicative of TALEN-mediated disruption. The CelI-treated samples were resolved on an agarose gel and the density of separated bands was determined to calculate the percentage of targeted disruption (Figure 3.7). To generate a positive control for CelI cleavage, PCR amplicons of wild-type and mutant *HBx* sequences were mixed in equal amounts and processed as described above.

If the TALENs had caused mutagenesis at the target sites, the CelI enzyme will cleave the annealed amplicons (of approximately 520 bp) into a two smaller DNA products (~280 bp) appearing as a single band (Figure 3.8). In vitro analysis indicates the mock transfected cells showed no cleavage as a single band was visible indicating presence of only homoduplexes for both the *S* and *C* ORFs. The Sharkey S and wild-type S TALEN were able to cause targeted mutagenesis to the *S* ORF (Figure 3.8). The Sharkey S and wild-type S TALENs exhibited comparable cleavage activity. Targeted cleavage of 4.6 % and 4.2 % was achieved by the Sharkey S TALEN and wild-type S TALEN respectively. The Sharkey C and wild-type C TALEN appeared to exhibit greater targeted disruption. Targeted cleavage of 16.3 % and 19.2 % was achieved by the Sharkey C TALEN and wild-type C TALEN respectively (Figure 3.8). The data indicated that Sharkey TALENs cause cleavage at the intended site as a result of NHEJ-based targeted disruption, even though the reduction of surface antigen expression was not maintained**.** Increased nuclease activity was expected as the introduction of obligate heterodimeric *Fok*I variants as well as the Sharkey variants has been shown in a study by Doyon and colleagues to have an additive effect thus increasing the nuclease function of TALENs (Doyon et al., 2011). The use of the CelI enzyme could account for the low percentage and possible underestimation of targeted cleavage achieved by the Sharkey

and wild-type S and C TALENs as this enzyme is less sensitive than similarly acting T7E1 enzyme.

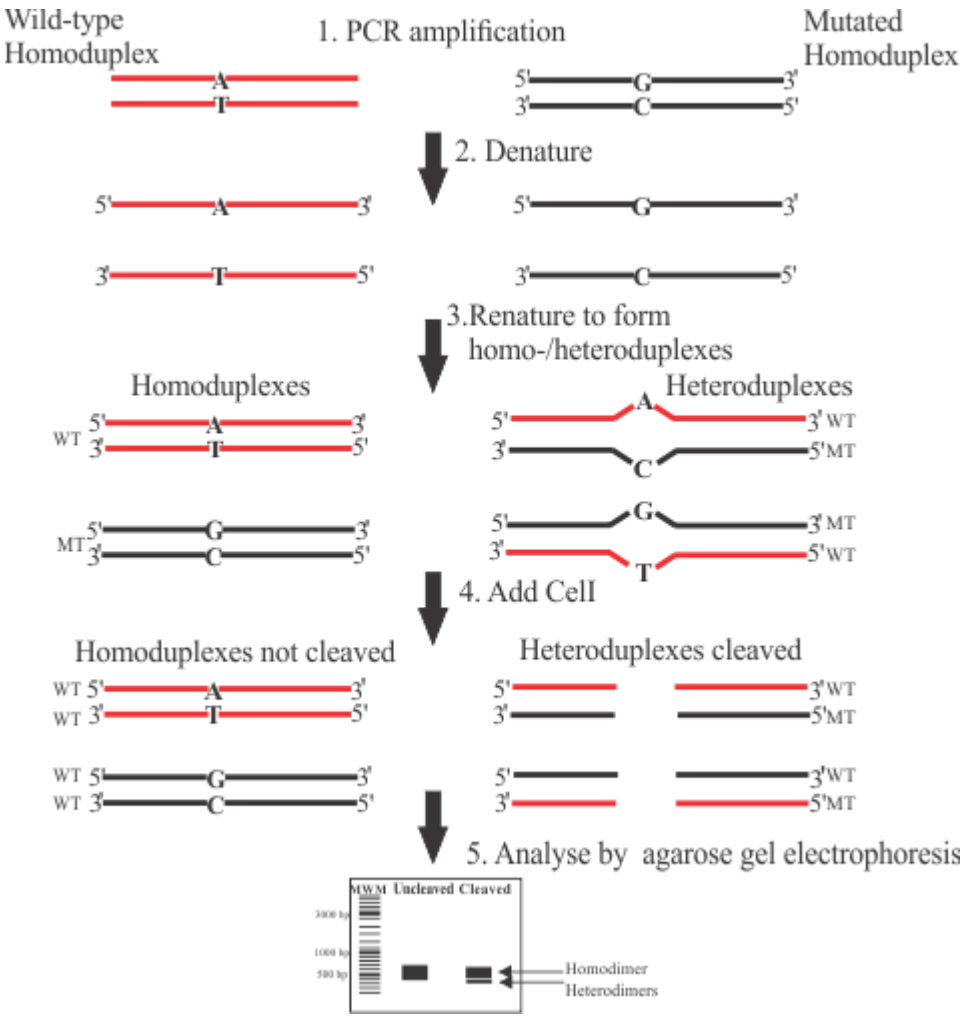

Figure 3.7: CelI-mediated cleavage of heteroduplexes.

(1) Sequences flanking Sharkey TALENs target sites are PCR amplified followed by (2) denaturation and (3) renaturation of the amplified DNA sequences allows the formation of homo- and/or heteroduplexes as a result of indels. (4) The heteroduplexes are recognised by the CelI resulting in cleavage at the nuclease target site. (5) Confirmation of cleavage is carried out by agarose gel electrophoresis and density of separated bands is used to calculate the percentage of targeted disruption. Adapted from (Ehrke-Schulz et al., 2016).

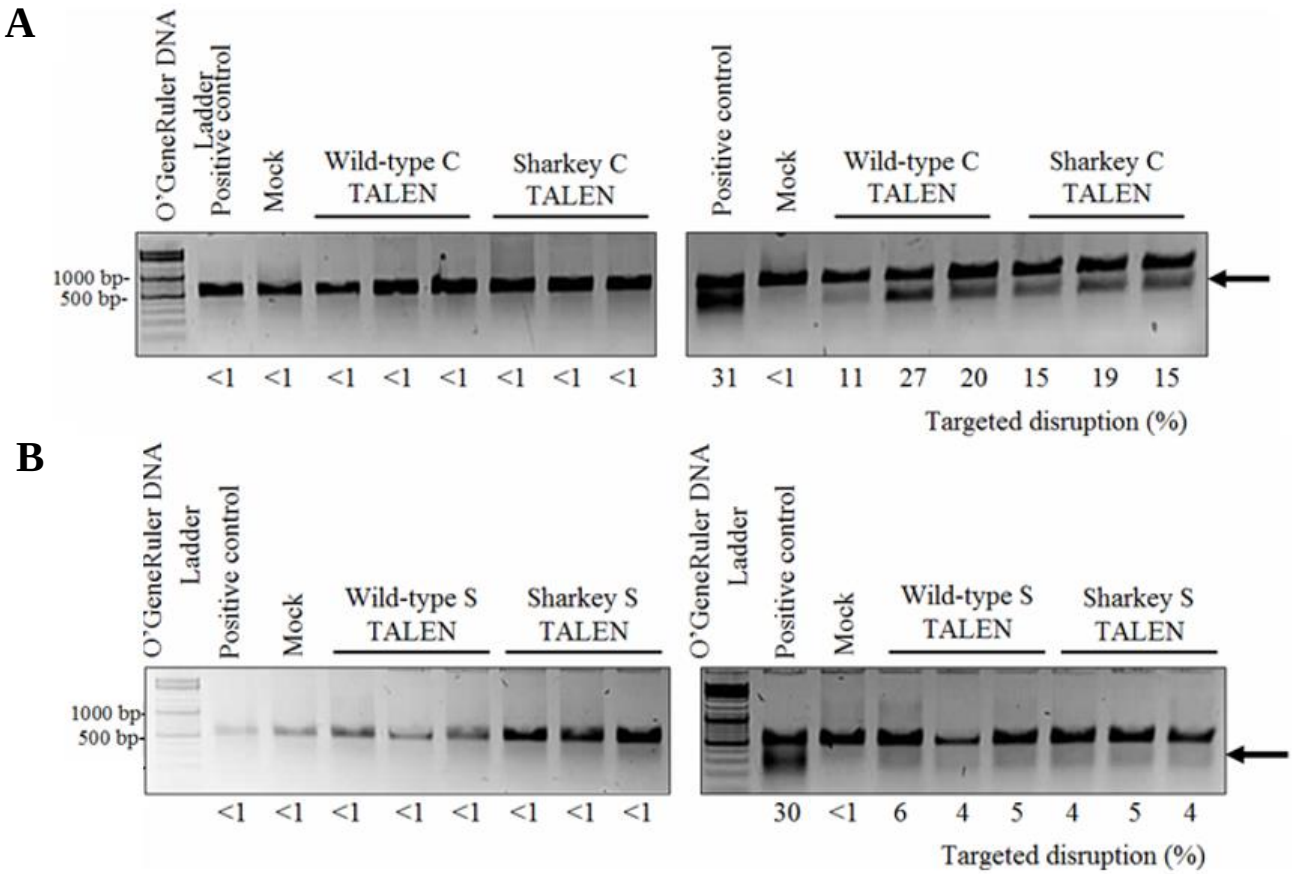

Figure 3.8: Sharkey S and C TALEN-mediated cleavage of HepG2.2.15 DNA.

Total DNA was extracted from HepG2.2.15 cells transfected three times consecutively with Sharkey S or C, wild-type S or C TALENs as well as pUC118 encoding plasmids. The target sites of the TALENs were amplified by PCR and a CelI assay conducted on amplified DNA. Undigested PCR products (~520 bp) indicates no cleavage and the presence of additional bands (~280 bp) shown by the arrow indicates on-target cleavage. The anti-HBV C TALENs are indicated in the top panel **(A)** while the anti-HBV S TALENs are indicated in the bottom panel (**B**). Wild-type and Sharkey TALEN-treated DNA, without CelI enzyme (left) and with CelI enzyme (right). The molecular weight marker is shown with the DNA fragment sizes on the left and the percentage of targeted cleavage is indicated below.

3.5 Lack of anti-HBV Sharkey TALEN-mediated toxicity in vitro

To ensure that the anti-HBV Sharkey TALEN-mediated inhibition of HBsAg is a result of targeted mutagenesis and not toxicity, an MTT assay was conducted. Metabolically active cells are able to use mitochondrial succinic dehydrogenases to reduce the MTT to an insoluble formazan product which are subsequently solubilised in DMSO (Hillegass et al., 2010). This in vitro assay is able to quantify viable cells and was used to evaluate whether the anti-HBV TALENs are toxic. HEK293T cells were co-transfected with pCH-9/3091, pCI-neo-eGFP and the TALEN-encoding plasmids or pUC118 (Appendix 5.17, Figure 5.16). HEK293T cells treated with 50% DMSO served as a positive control for toxicity and untreated cells served as a negative control. To ensure reproducibility control and experimental treatments were carried out in triplicate.

DMSO treatment clearly exhibited toxic effects as evidenced by the low OD reading in comparison to untreated cells (Figure 3.9). Sharkey TALENs are tolerated as well as their wild-type counterparts and were not significantly different from untreated cells. This indicates that the Sharkey TALENs are non-toxic to the cells, as the Sharkey anti-HBV TALENs is most likely acting on the episomal viral replication intermediate. This is likely to account for the absence of measurable cytotoxic events, as endogenous genes are not the targets of these virus-specific TALENs.

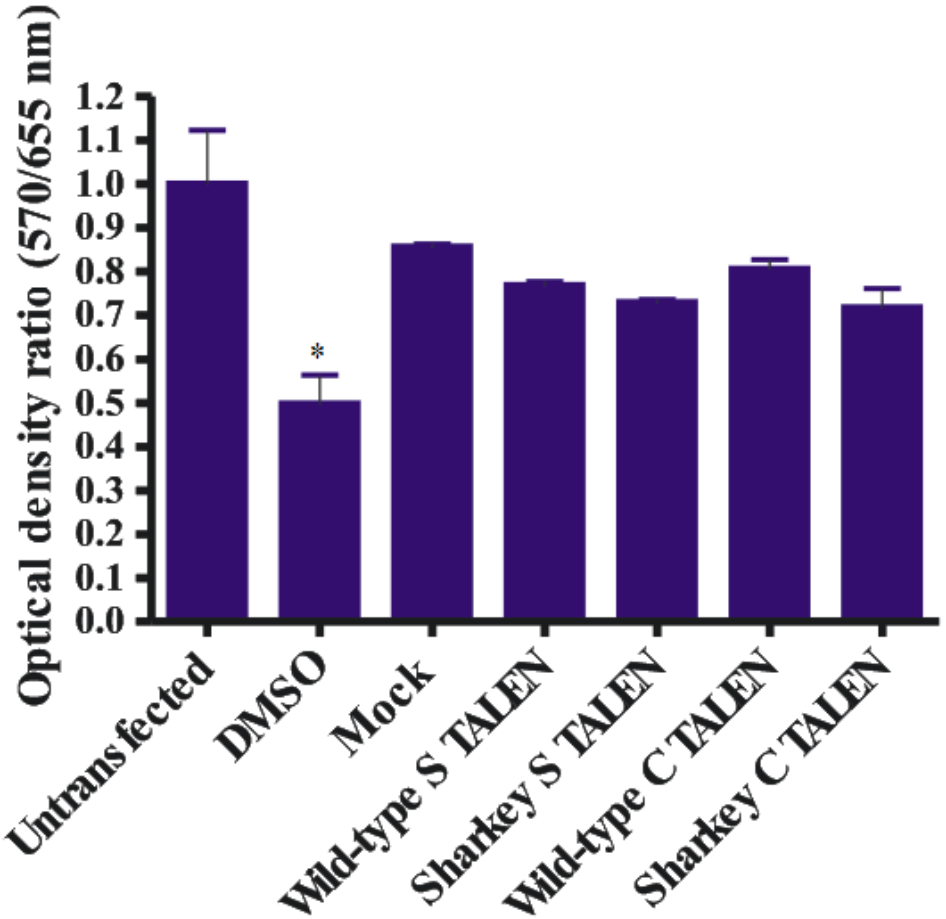

Figure 3.9: In vitro assessment of TALEN mediated cytotoxicity.

To assess potential toxicity of Sharkey TALENs, an MTT assay was conducted 48 hours after co-transfection of HEK293T cells with the indicated plasmids. Transfections were performed in triplicate and the error bars indicate the SEM (n=3). (** indicates $p < 0.01$).

3.6 In vivo Sharkey TALEN-mediated silencing

In vitro assessment of the Sharkey TALENs demonstrated inhibition of HBsAg and targeted mutagenesis of the *S* and *C* ORFs. Therefore to further assess the functionality and efficiency of the Sharkey TALENs, in vivo experiments were preformed to confirm and validate the findings observed in cultured mammalian cells. In vivo assessment of anti-HBV Sharkey TALENs was carried out using the mouse HDI model of HBV replication. The mock and wild-type TALENs were used as negative and positive controls respectively. pCI-neo-FLuc is a reporter plasmid that was used to assess and monitor delivery efficiency. Bioluminescence was detected exclusively in the livers of mice in which hydrodynamic injection was successful (Figure 3.10). Mice in which no bioluminescence signal (Appendix 5.18, Figure 17) detected were excluded from the study as delivery of the plasmids could not be confirmed. Once delivery was confirmed anti-HBV Sharkey TALEN knockdown analysis was performed on samples collected from control and experimental mice 3 and 5 days post-transfection. HBsAg expression was assessed by ELISA.

HBsAg expression was reduced by all the TALENs over the course of a week (Figure 3.11). The wild-type S TALEN knocked down expression in excess of 90% on days 3 and 5 post-injection. Although the Sharkey S TALEN-mediated reduction of HBsAg was statistically significantly different from mock transfected mice ($p<0.05$) it was less effective than the wild-type S TALEN (37% and 57% on day 3 and 5 post-injection). Unexpectedly, significant reduction in HBsAg secretion was observed by both the wild-type (48% and 62% on day 3 and 5 post-injection) and Sharkey (55% and 68% on day 3 and 5 post-injection) C TALENs. This correlated with results obtained in vitro analysis (knockdown analysis in HepG2.2.15 cells, Figure 3.6). This was unexpected as the C TALENs are designed to target the *C* ORF and should not cleave the *S* ORF however similar finding was demonstrated by Bloom and colleagues (Bloom et al., 2013). The observed reduction in HBsAg levels likely reflects transcriptional interference. A similar phenomenon was observed by Bloom and colleagues who observed that the P2 TALEN caused a reduction in HBsAg levels without cleaving its target sites within the *P* ORF (Bloom et al., 2013). In vivo analysis indicates, firstly that the Sharkey S TALENs are able to cause disruption of HBsAg production and secondly the observed reduction of HBsAg correlated with the data obtained from analysis of cells in culture. Greater knockdown efficiency was observed in vivo and may be explained by the different models and mechanisms of delivery.

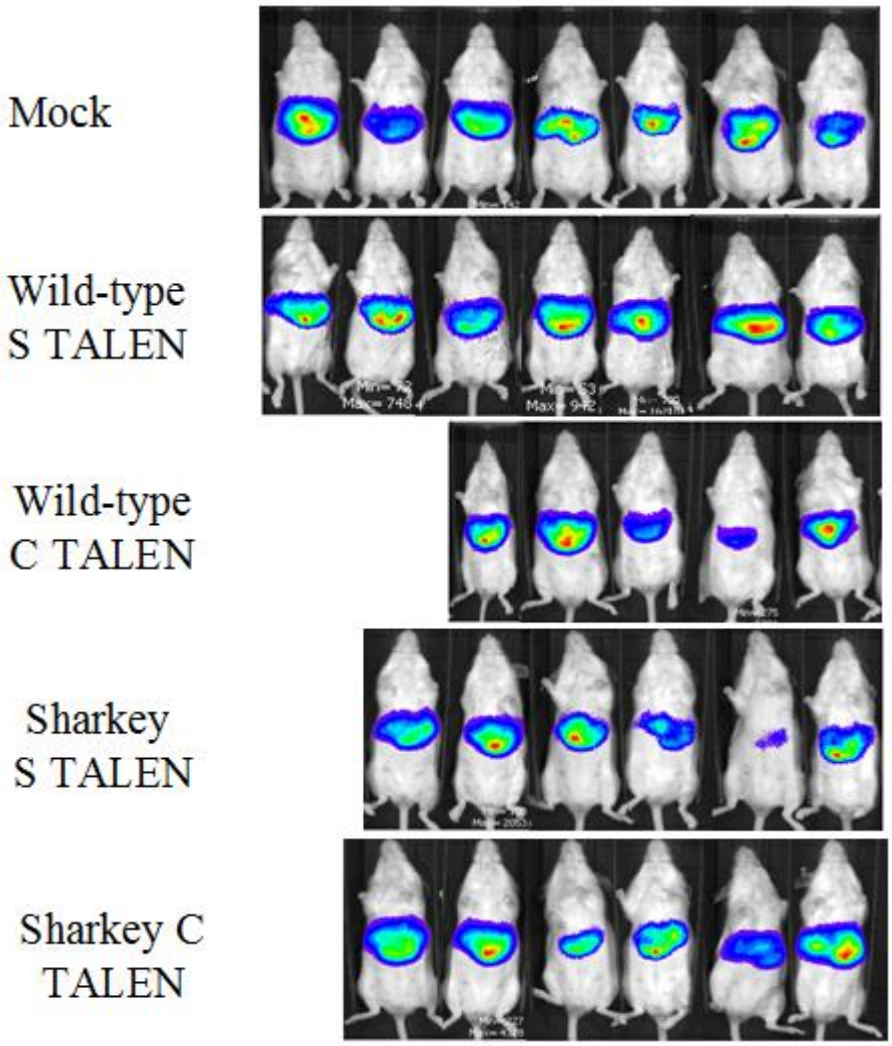

Figure 3.10: Bioluminescence imaging of mice treated with Sharkey TALEN, wild-type TALEN and mock plasmids in vivo.

NMRI mice were hydrodynamically injected in the tail vein with pCH-9/3091, pCI-neo-FLuc and pUC118 or individual TALEN-encoding plasmids. The pCI-neo-FLuc plasmid encoding Firefly luciferase was included to assess delivery efficiency. Bioluminescence imaging was conducted on live mice after administration of 150 mg/kg luciferin 3 days post-infection.

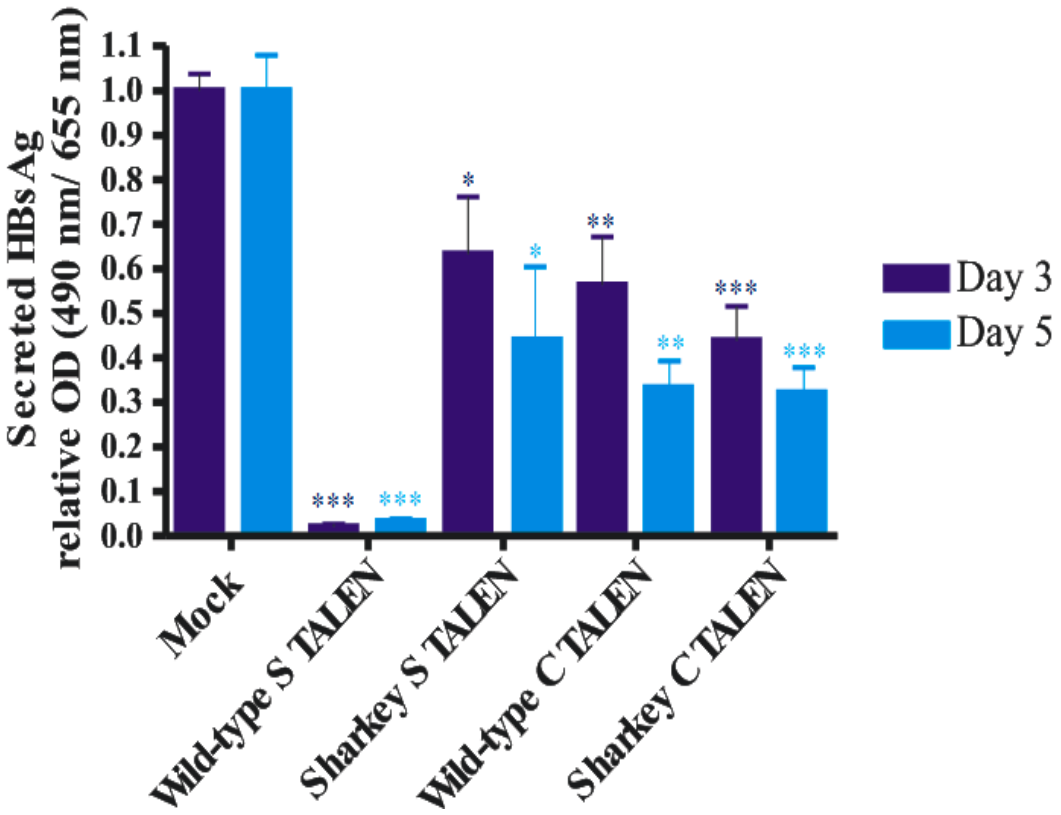

Figure 3.11: Assessment of Sharkey TALEN-mediated knockdown of HBsAg in vivo.

Mice were co-injected with pCH-9/3091 and TALEN plasmids or pUC118. Blood samples were obtained on day 3 and day 5 post-injection and HBsAg levels in the serum were measured using ELISA. The error bars indicate the SEM, * indicates $p< 0.05$, ** $p<0.01$ and *** $p<0.001$.

3.7 Sharkey TALEN-mediated reduction of VPEs in vivo

To assess whether the Sharkey TALENs have an effect on virion secretion, circulating VPEs were measured using real-time PCR. DNA was extracted from serum samples obtained on day 3 and day 5 after injection of control and experimental mice

The Sharkey and wild-type S TALENs were able to significantly decrease circulating VPEs on day 3 by 81% and 90% respectively indicating targeted disruption of the *S* ORF (Figure 3.12). A reduction of 87% and 85% was achieved by the Sharkey C and wild-type C TALENs. By day 5 of the experiment the Sharkey S and C TALENs significantly reduced VPE levels by approximately 99% and suggest that the Sharkey TALENs require a longer period to produce a significant effect. Reduction of approximately 90% was achieved by wild-type S while the wild-type C TALEN exhibited a 60% reduction which was lower than the reduction demonstrated on day 3. These results correlate with the trend of Sharkey TALENs demonstrating lower cleavage efficiency compared to the wild-type TALENs.

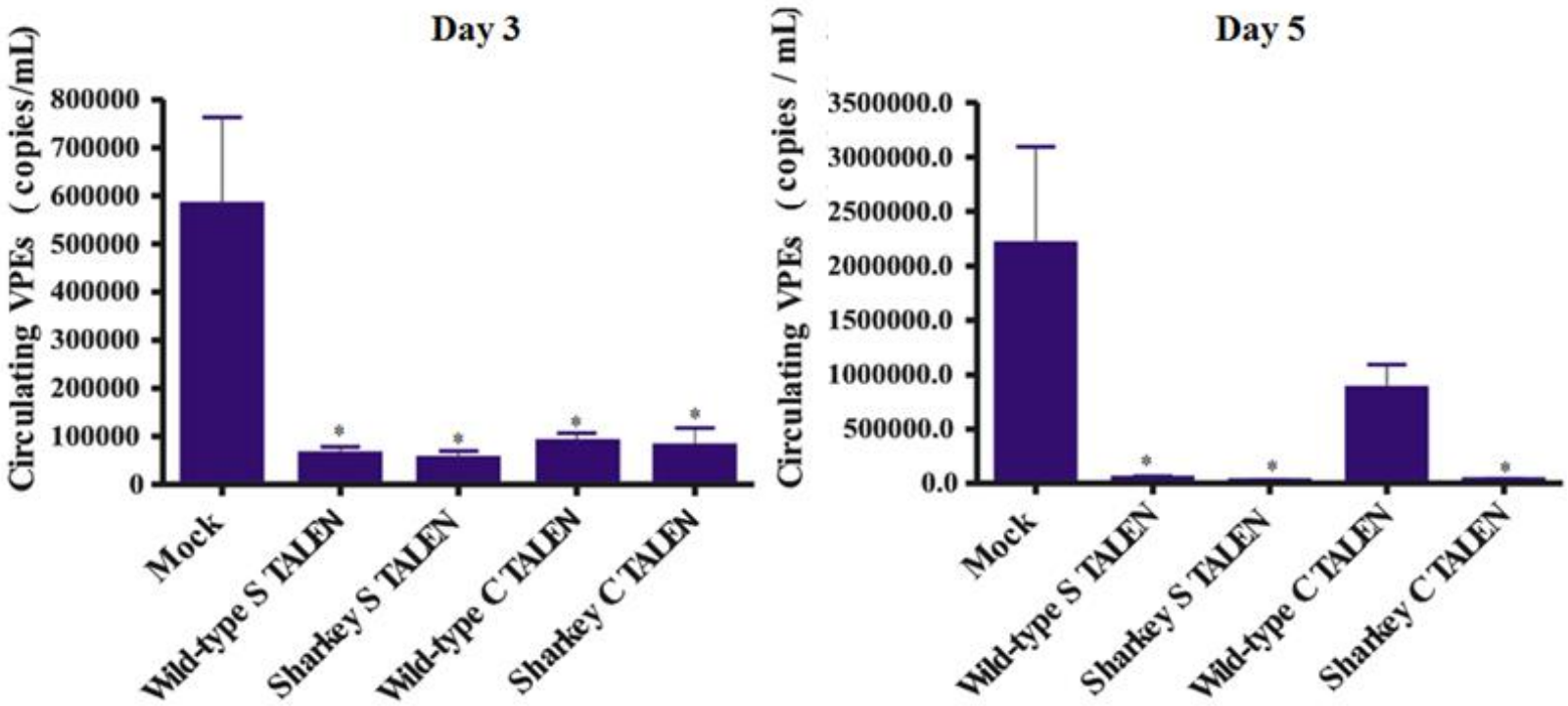

Figure 3.12: Sharkey TALEN-mediated inhibition of HBV viral replication in vivo.

Sharkey TALEN-mediated inhibition of virion secretion was assessed by qPCR. Total DNA was extracted from the serum of mice hydrodynamically injected with the plasmids expressing Sharkey TALENs, wild-type TALENs (positive control) and pUC118 and qPCR used to determine the circulating VPEs. The error bars indicate the SEM, * indicates $p< 0.05$, ** $p<0.01$ and *** $p<0.001$.

3.8 In vivo Sharkey TALEN-mediated reduction of HBV transcription

To determine whether the Sharkey TALENs were able to inhibit the transcription of viral replication, HBV *surface* mRNA and pgRNA levels were measured using reverse transcriptase quantitative PCR (RT-qPCR). RT-qPCR was performed on RNA extracted from livers of mice injected with the different treatments. qPCR was performed to measure the viral *surface* and pgRNA levels relative to a house-keeping gene murine *glyceraldehyde-3-phosphate dehydrogenase* (m*GAPDH*) mRNA (Figure 3.13).

The TALENs were designed to target the *S* and *C* ORFs of HBV in an attempt to disrupt cccDNA. The wild-type S TALEN reduced *surface* mRNA by 74% in comparison to the 35% reduction exhibited by the Sharkey S TALEN. This was unexpected as the wild-type S and Sharkey S TALEN constructs contain the same TALE backbone however the variation reduction of *surface* mRNA observed could be a result of the third generation Sharkey variant. Both the wild-type C and Sharkey C TALENs inhibited expression of *surface* mRNA by 45% and 48% respectively. TALENs are designed to bind DNA and cause cleavage thereby disrupting the targeted ORF. The protein will still be produced but will likely not be functional. The observed data indicating reduction in surface mRNA and pgRNA levels are unexpected and indicate that viral transcription is altered by the TALENs. Transcriptional interference can be caused by a number of factors, which includes modification to the promoter such as methylation (Delaval and Feil, 2004), repressor binding to its operator overlapping a promoter (Rojo, 2001) and shielding of an enhancer site (Kuhn and Geyer, 2003). The *S* ORF is divided into the *S*, *pre-S1* and *pre-S2* regions that codes for the 3 surface envelope proteins and the *C* ORF encodes core and precore proteins. Gene expression is regulated by four promoters which include the pre-S1, pre-S2 and X promoters and the BCP. The anti-HBV TALENs could transcriptionally interfere with the Pre-S1 and Pre-S2 promoters as well as the BCP as these promoters are exclusively responsible for the expression of *surface* mRNA and pgRNA.

The wild-type S and C TALENs reduced pgRNA levels by approximately 89% of pgRNA expression individually; this level of inhibition however was not exhibited by the Sharkey TALENs. Nevertheless, significant reduction of approximately 73% and 75% was achieved by Sharkey S and C TALENs respectively. Greater inhibition of viral pgRNA compared to

surface mRNA was exhibited by the Sharkey TALENs. Nonetheless, the results indicate the anti-HBV TALENs are affecting HBV viral *surface* mRNA and pgRNA expression in vivo.

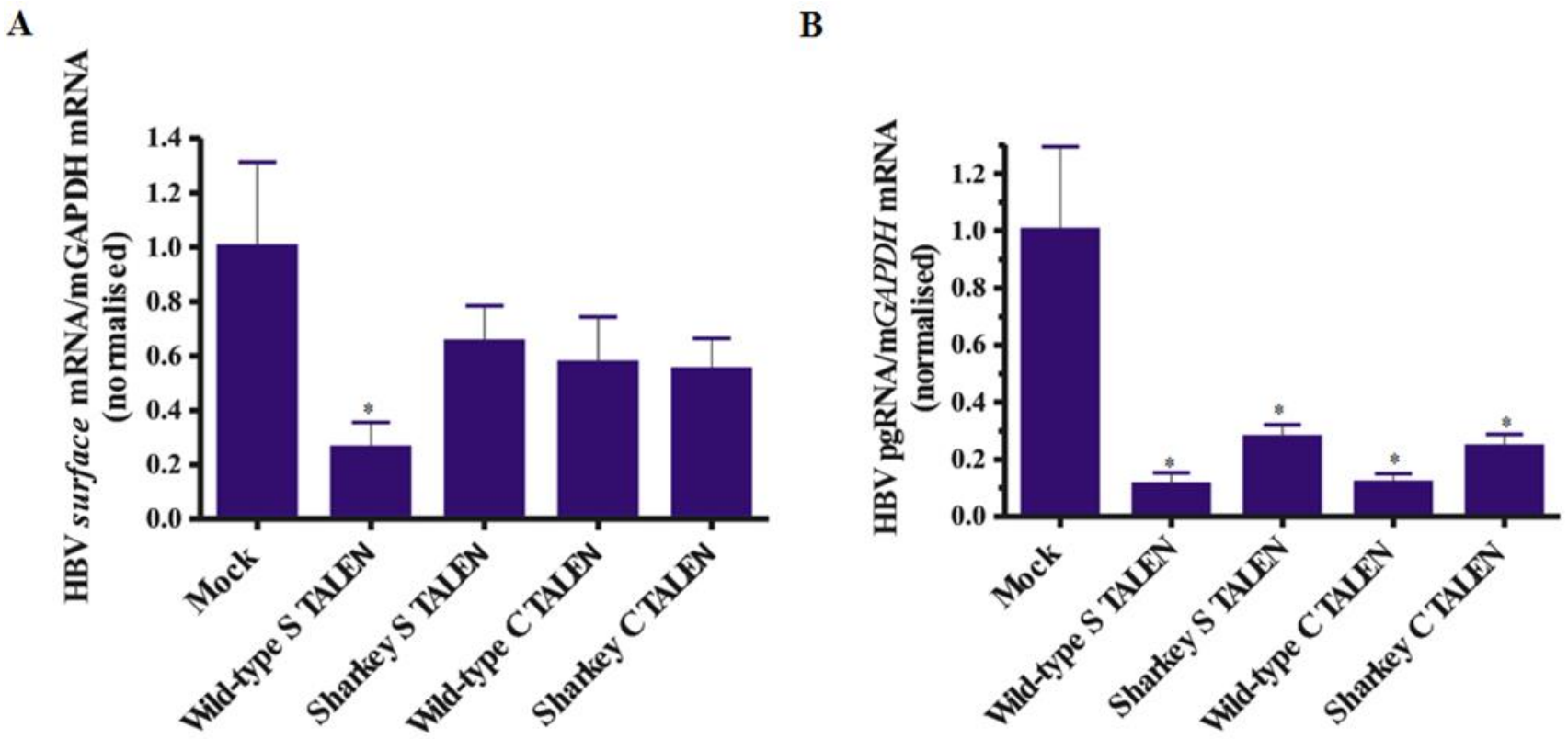

Figure 3.13: Sharkey TALEN-mediated knockdown of HBV mRNA expression in vivo.

To evaluate Sharkey TALEN efficiency in vivo, mice were hydrodynamically injected with the Sharkey TALEN plasmids, wild-type TALEN plasmids and pUC118 (mock). RNA was extracted from the livers of the treated mice. Primers designed against the *S* and *C* ORFs were used to measure (**A**) *surface* mRNA and (**B**) pgRNA levels relative to m*GAPDH* mRNA. The error bars indicate the SEM, * indicates $p < 0.05$, ** $p<0.01$ and *** $p<0.001$.

3.9 In vivo Sharkey TALEN-mediated on-target cleavage

To assess sequence-specific mutagenesis mediated by the Sharkey TALENs in vivo, total DNA was extracted from mouse livers. PCR amplification of the S and C TALEN target sites was carried out and produced a single band of 520 bp (Appendix 5.19, Figure 5.18 to 5.19). The PCR amplified DNA for the *S* and *C* target regions was purified and cleavage was assessed using CelI (Figure 3.14 and 3.15).

The CelI assay indicates mock treated mice exhibited no cleavage as expected (Figure 3.14 and 3.15). In contrast five of the wild-type C TALEN-treated mice and six of the Sharkey C TALEN-treated mice exhibited cleavage as a result of on-target mutagenesis. The Sharkey S and C TALENs yielded 11.6% and 21.67% cleavage whereas the wild-type S and C TALENs yield 15.4% and 30.6% cleavage respectively. This indicates wild-type TALENs exhibited greater targeted cleavage compared to the Sharkey TALENs. Targeted cleavage obtained in vivo was greater compared to in vitro cleavage obtained by the Sharkey S and C TALENs. Overall results indicate that the Sharkey TALENs caused targeted mutagenesis to result in disruption of HBV replication.

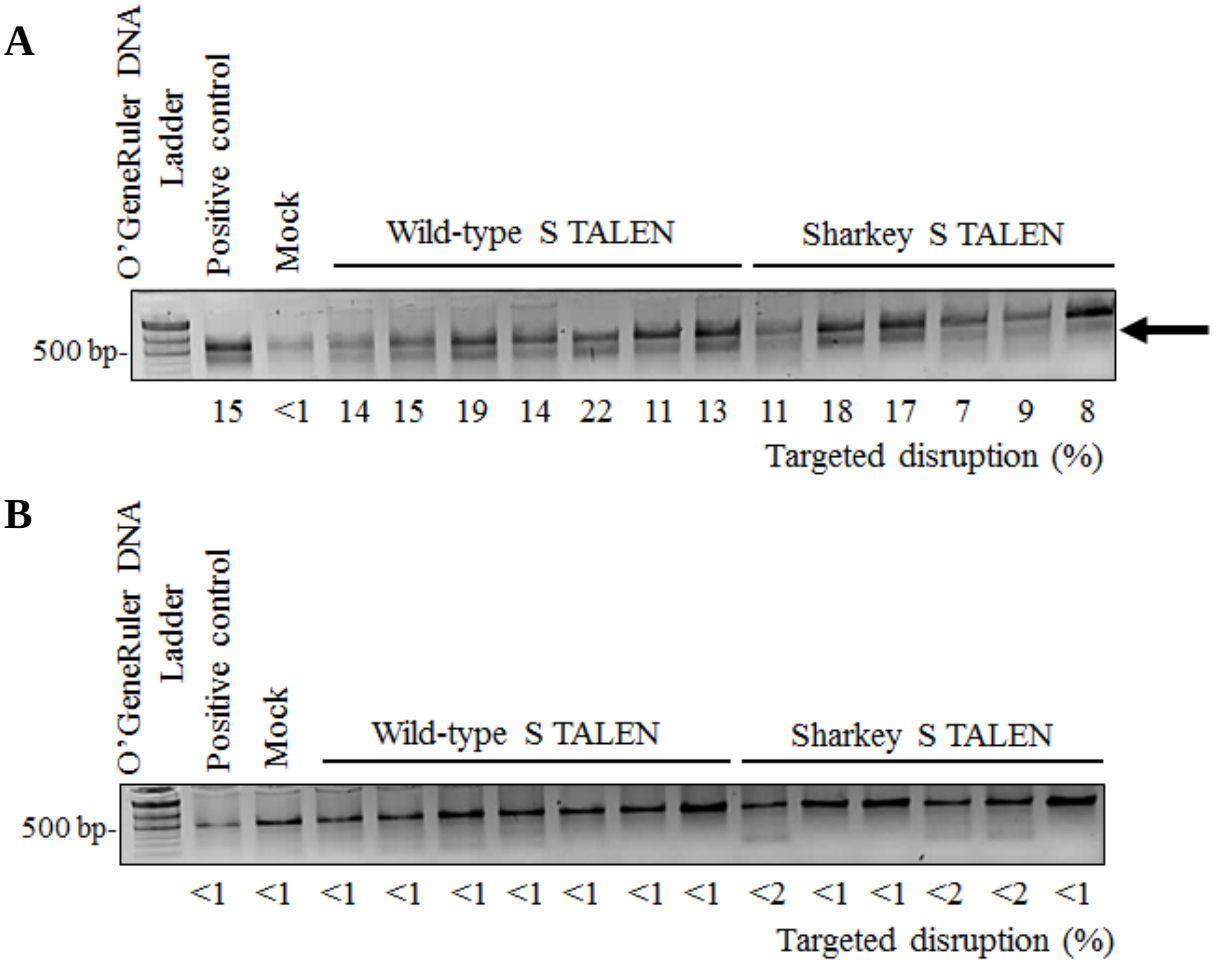

Figure 3.14: Wild-type and Sharkey S TALEN-mediated in vivo on-target cleavage.

Total DNA was extracted from control and experimental mice. PCR amplification of S TALEN target sites was carried out and CelI assay was conducted on each of the samples. The undigested PCR products (~520 bp) present no cleavage and the presence of an additional band indicates on-target cleavage. Wild-type and Sharkey S TALEN-treated samples with **(A)** and without **(B)** CelI treatment. The molecular weight marker is shown with the DNA fragment sizes on the left and the percentage targeted cleavage is indicated below.

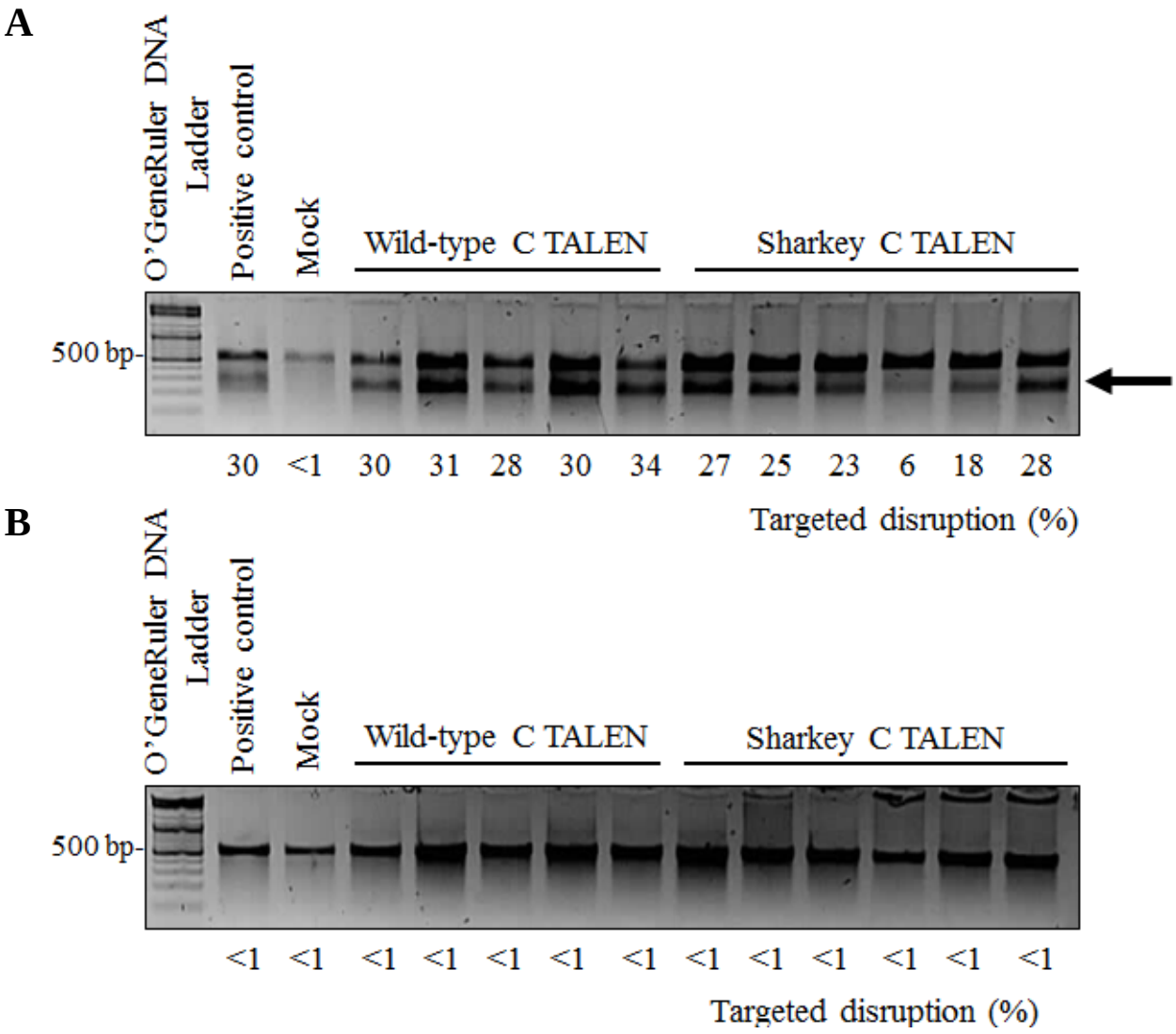

Figure 3.15: Wild-type and Sharkey C TALEN-mediated in vivo on-target cleavage.

Total DNA was extracted control and experimental mice. PCR amplification of C TALEN target sites was carried out and CelI assay was conducted on each of the samples. The undigested PCR products (~520 bp) present no cleavage and the presence of an additional band indicates on-target cleavage. Wild-type C and Sharkey C TALEN-treated samples with **(A)** and without **(B)** CelI treatment. The molecular weight marker is shown with the DNA fragment sizes on the left and the percentage targeted cleavage is indicated below.

3.10 Lack of Sharkey TALEN-mediated toxicity in vivo.

Serum samples from day 5 of the experiment were used to measure alanine aminotransferase (ALT) activity as an indication of toxicity (Figure 3.16). The standard/normal range of ALT may vary slightly based on age and gender but is generally accepted to range between 10-40 IU/L and levels above 100 IU/L is indicative of toxicity (Wang et al., 2012)

Measurement for mock, wild-type S TALEN, wild-type C TALEN, Sharkey S and C TALENs treated mice were all below the threshold of 100 IU/L (Figure 3.16). This indicates little if any hepatocellular damage or toxicity associated with the effects of the Sharkey TALENs. The results indicates that reduction of HBV markers HBsAg, *surface* mRNA, pgRNA and VPEs is not a result of induced toxicity but rather are an effect of targeted binding and cleavage of *S* and *C* ORFs.

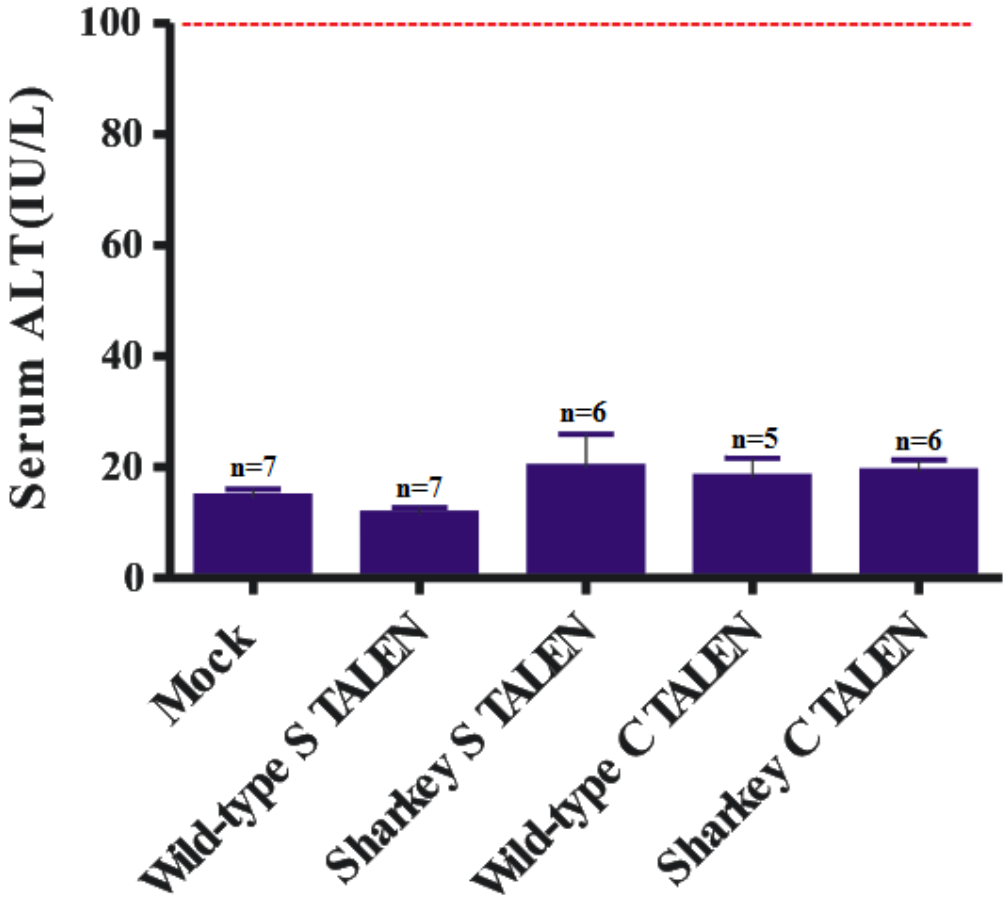

Figure 3.16: Assessment of Sharkey TALEN-associated liver toxicity.

To determine whether there is any toxicity associated with the Sharkey and wild-type TALENs, serum samples were used to determine ALT activity in control and experimental mice. The red line represents the threshold above which liver damage is evident.

Chapter 4

4 Discussion

4.1 Targeting cccDNA of HBV by Sharkey TALENs

The inability to achieve a functional cure for chronic hepatitis B is believed to be a result of the persistence of the cccDNA and the failure of current available anti-viral therapeutics to completely eliminate cccDNA (Allweiss and Dandri, 2017). HBV cccDNA is formed through the repair of rcDNA and will continue to exist as an episome through interactions with non-histone and histone proteins (Guo et al., 2012). It assembles into chromatin-like structures designated as minichromosomes within the nucleus (Newbold et al., 1995, Nassal, 2008). This episomal minichromosome accumulates within infected hepatocytes and functions as a permanent template for virus replication by providing a continuous supply of pgRNA and viral mRNAs (Revill and Locarnini, 2016).

The reactivation of cccDNA has been shown to be the main cause for HBV recurrence and persistence (Bock et al., 1994). To date, there are two main pathways responsible for maintaining cccDNA within infected cells. The first pathway is the infection and re-infection of hepatocytes (Revill and Locarnini, 2016) and the second pathway occurs when newly assembled nucleocapsid translocates to the nucleus to replenish cccDNA (Köck et al., 2010, Yang and Kao, 2014). Current therapies are limited as they are not able to eliminate cccDNA. Although current therapies have been able to strongly suppress viral replication these treatments are not curative and are only able to slow down the development of cirrhosis and progression to HCC (Wursthorn et al., 2006, Durantel and Zoulim, 2016). Therefore, the ideal strategy to cure chronic HBV infections would be the elimination or permanent disruption of the stable cccDNA minichromosome within hepatocytes without causing hepatotoxicity (Yang and Kao, 2014). The DNA sequence of cccDNA which is distinct from host cellular chromatin can be targeted with genome editing technologies such as TALENs (Hoeksema and Tyrrell, 2010).

The use of designer nucleases in gene therapy is an active field of research. Thus it is critical to evaluate the catalytic activity (efficiency), on-target binding and cleavage (specificity and safety) of these gene editing technologies. As a result of the small and compact nature of the HBV genome the virus' sequence plasticity is limited. The use of TALENs to induce mutations within the HBV genome would therefore most likely affect viral fitness making this an attractive strategy to disable cccDNA. Several studies have shown genome editing tools are capable of targeting HBV and disrupt cccDNA (Bloom et al., 2013, Chen et al., 2014). Accumulating evidence has demonstrated the effectiveness of designer nucleases (Cradick et al., 2010, Dong et al., 2015). However, several strategies have shown that the efficiency of sequence-specific designer nucleases can be improved (Miller et al., 2007, Guo et al., 2010, Doyon et al., 2011) This includes the extensive evaluation and development of modified *Fok*I nuclease domains. Therefore the aim of this study was the development of engineered nucleases with improved efficiency and safety by incorporating third generation Sharkey variants into existing anti-HBV TALENs.

The third generation obligate heterodimeric Sharkey TALENs targeted two conserved target sites, namely the *S* and *C* ORFs in an attempt to disrupt cccDNA. Immunodetection of the HA epitope within the Sharkey TALENs validated TALEN expression in liver-derived Huh 7 cells. In vitro assessment demonstrated the Sharkey TALENs were able to inhibit HBsAg expression in Huh 7 cells. Analysis of target sites revealed on-target mutagenesis of TALEN target sites. This suggests the Sharkey TALENs bound to their targets and caused targeted disruption, thereby affecting the formation of HBsAg in both liver-derived cell lines. In vivo analysis of Sharkey TALEN indicated a reduction of HBsAg, reduction of viral RNA and targeted mutagenesis by both Sharkey S and C TALENs as a result of targeted disruption of HBV replication.

4.2 Efficiency of Sharkey TALENs

Engineered nucleases have the potential to treat both infectious and hereditary genetic disorders that conventional treatments have not been able to effectively combat (Heslop et al., 1994, Manickan et al., 1995, Davis et al., 1996). The use of genome editing tools has been investigated as a gene therapy strategy against a number of diseases. Several clinical trials have used engineered sequence-specific nucleases for the treatment of various diseases (Qasim et al., 2017, Reardon, 2016). There are currently two clinical trials using ZFNs to cause targeted mutagenesis of the CCR5 gene, which is used during the early stage of HIV

infection (DiGiusto et al., 2016) and the second trial involves targeted disruption of the glucocorticoid receptor gene as a potential treatment for glioblastoma (Reik et al., 2008). The first clinical trial evaluating TALENs has been for the modification of T-cells for treatment of $CD19^+$ acute lymphoblastic leukemia (Qasim et al., 2017). The first CRISPR/Cas9 clinical trial has also recently been approved (Reardon, 2016). These clinical trials demonstrate the utility of nucleases as potential treatments for various diseases. Furthermore nucleases have also been reported to target non-human genomes and therefore function as antiviral therapies for the treatment of chronic infections. Cradick and colleagues were one of the first groups to assess the use of designer nucleases to cleave and disrupt HBV DNA. ZFNs were used to induce targeted mutations in an HBV-containing plasmid and this resulted in inhibition of the production of pgRNA in vitro (Cradick et al., 2010). Since this first study, numerous groups have employed similar strategies to target HBV. Some of these studies focused on the use of other designer nucleases such as TALENs and CRISPR/Cas as well as focused on the delivery of designer nucleases (such as ZFNs). These studies demonstrate that engineered nucleases not only serve as a powerful research tool but also show promise for clinical use.

TALEN specificity and versatility is mediated by the well-characterised DNA-binding domain that can be engineered to target a wide range of DNA sequences (Miller et al., 2007) whereas the mutagenic efficiency of TALENs is dependent on catalytic activity of the *Fok*I nuclease domain (Bibikova et al., 2001). In this study enhanced third generation obligate heterodimeric Sharkey nuclease domains (KKR and ELD) were incorporated into existing HBV TALENs to further improve efficiency and ultimately increase the safety of these TALENs. The third generation heterodimeric nuclease-encoding domains as well as the Sharkey variants were first developed within the ZFN architecture (Miller et al., 2007). Although the data are limited, incorporation of third generation variants, Sharkey variants or a combination of both within TALENs generally increased nuclease activity while simultaneously reducing toxicity (Guo et al., 2010, Doyon et al., 2011).

The third generation *Fok*I nuclease domains (ELD and KKR) were generated to favour heterodimerisation of left and right monomers. By reducing the likelihood of homodimerisation potential off-target effects are reduced and overall specificity of ZFNs and TALENs is improved. These nucleases have proven to be safer and more efficient in comparison to their homodimeric counterparts (Doyon et al., 2011). The Sharkey variant contains two amino acid mutations (S418P and K441E) that have been shown to enhance cleavage activity as compared to the wild-type *Fok*I nuclease domain (Guo et al., 2010). The enhanced activity of the Sharkey variants is believed to be due to the placement of the

mutation at a turn region in the protein. The introduction of a proline at the onset of α-helix 3 could have influenced the rigidity of the nuclease structure enabling rapid recognition and substrate turnover (Guo et al., 2010). The Sharkey variants have been incorporated into existing third generation nuclease encoding domains (ELD and KKR) producing 3rd generation obligate heterodimeric Sharkey *Fok*I nuclease domains (ELD+Sharkey and KKR+Sharkey). Studies have demonstrated a synergism between the ELD+Sharkey and KKR+Sharkey thus demonstrating compatibility of the various mutations (Miller et al., 2007). Doyon and colleagues confirmed the incorporation of the Sharkey variants produced an additive effect (Doyon et al., 2011).

In this study, the functionality and efficiency of Sharkey TALENs were investigated both in vitro and in vivo. Hydrodynamic injection of mice was used to simulate viral replication in vivo using plasmids containing a replication competent HBV sequence. The Sharkey S and C TALENs reduced HBsAg by 35% on day 3 to 57% on day 5 respectively. These results suggest greater reduction of HBsAg was achieved over time however the wild-type TALENs were more efficient than the Sharkey TALENs. The Sharkey S and C TALENs reduced viral *surface* mRNA by 35% and 48% respectively whereas a reduction of 73% and 75% of pgRNA was observed. The production of new virions (VPEs) was reduced by approximately 99% by the Sharkey S and C TALEN respectively on day 5. The CelI assay was used to assess on-target mutagenesis of HBV DNA by the Sharkey TALENs which was quantified at 11.6% and 20.2% for the S and C Sharkey TALEN respectively. Overall the wild-type TALENs demonstrated greater inhibition of HBsAg and viral mRNA compared to Sharkey TALENs which was unexpected as a study by Pillay and colleagues showed that in zebrafish embryos the Sharkey TALENs exhibited a 26-fold increase in indel mutations compared to wild-type (Pillay et al., 2013). This was further demonstrated when Sharkey variants exhibited a three- to six-fold increase in the mutagenic activity compared to the wild-type TALEN in vitro (Pillay et al., 2013). However a study by Guo and colleagues indicated reduced efficiency of the TALENs incorporated with the Sharkey variants in vivo in zebrafish and correlates with the findings of this study (Guo et al., 2010). In this study, while capable of inhibiting markers of HBV replication in vitro and in vivo, the third generation obligate heterodimeric Sharkey nuclease domains did not prove to increase the catalytic function of anti-HBV TALENs.

4.3 Safety of Sharkey TALENs

Engineered sequence-specific nucleases have therapeutic potential, nonetheless major concern associated with use of any engineered sequence-specific nucleases is the potential to cleave non-specifically (Stone et al., 2016). Unintended cleavage by these nucleases is seen as one of the major contributors to toxicity. Cleavage at unintended sites within the genome could lead to genomic instability, unwanted chromosomal rearrangements and cell death (Scott et al., 2014, Jackson and Bartek, 2009, Karran, 2000). Furthermore, the potential for off-target activity to cause inactivation of tumour suppressors and or activation of oncogenes is of great concern. A high level of specificity is therefore a crucial feature required by any engineered nuclease. Increased specificity of engineered nucleases reduces the potential for unintended cleavage at non-target sites thus increasing the safety of engineered nucleases as a potential therapeutic.

The first TALEN construct contained the AvrBs4 TALE architecture fused to a wild-type *Fok*I nuclease domain (Kim et al., 1996). The wild-type nuclease domain is prone to homodimerisation which has been associated with off-target cleavage (Halford et al., 2011). Several types of heterodimeric nuclease domains have been developed thus far to further reduce toxicity, decrease off-target cleavage while simultaneously optimising the efficiency and specificity of TALENs. Nonetheless, existing data suggests that TALENs may not be associated with significant toxicity and this correlates with the in vitro and in vivo results obtained in this study. In this study an MTT assay indicated no cytotoxicity was caused by the use of the Sharkey TALENs in vitro. A study by Pillay and colleagues further demonstrated, the incorporation of Sharkey variants into ZFNs caused no morphological defects or mortality of zebrafish embryos in comparison to the wild-type *Fok*I nuclease domain-containing ZFNs (Pillay et al., 2013). This assessment was based on the number of normal embryo after the injection of the TALEN encoding mRNA (Doyon et al., 2011). Serum ALT levels of mice treated with wild-type and Sharkey TALENs were well within the acceptable range indicating that these nucleases have negligible toxic effects in vivo. The results in this study demonstrate the observed reduction of markers of HBV replication was exhibited by the activity of the Sharkey TALEN and not due to toxicity of the Sharkey TALENs.

4.4 Future Work

4.4.1 Off-target analysis

Despite the successes of using engineered nucleases to edit pathology causing genes, translating these technologies for clinical application requires significant improvements to efficacy, specificity and safety. The safety of designer nucleases is of major concern as potential off-target effects could lead to serious complications. Despite inhibition of HBV markers of replication, on-target cleavage and reduced toxicity observed in this study, the efficiency of the Sharkey TALENs cannot be fully assessed without off-target analysis.

At approximately 3 billion base pairs the human genome is quite large, creating a high probability of it containing sites that may be unintentionally targeted by engineered nucleases. Numerous tools exist to evaluate the efficiency of on- and off-target cleavage and include design parameters to minimise off-targets effects (Lee et al., 2016). The use of in silico methods involves the application algorithms based on in vitro and in vivo data to predict potential off-targets (Lee et al., 2016). This includes a range of web-based design tools and a range of bioinformatics- and experimental-based nuclease design tools. The three main parameters these tools aid include (i) selection of target site of sequence-specific nuclease, (ii) predicting the level of on-target and off-target cleavage rates and (iii) off-target site prediction. Examples of these tools include PROGNOS which is used to predict off-targets for ZFNs and TALENs (Fine et al., 2013).

Several in vitro and in vivo methods have been developed for the detection of off-target cleavage and include systematic evolution of ligands by exponential enrichment (SELEX), Sanger sequencing and high-throughput sequencing. Although powerful, these tools are associated with a number of limitations, one of which is the inability to detect off-target cleavage at sequences that form DNA or RNA bulges (Pattanayak et al., 2011, Pattanayak et al., 2013). In addition these methods are generally time consuming and careful attention needs to be taken when deciphering data for false-positive sequence reads (Cho et al., 2014).

In vivo detection methods include use of integrase-deficient lentivirus (IDLV) capture. IDLVs are able to enter cells efficiently but, unlike their wild-type counterparts, are not able to integrate and typically remain in the nucleus as an episome (Vink et al., 2009). These episomal IDLVs can integrate into DSBs and as such can be used to detect off-target cleavage in an unbiased way (Gabriel et al., 2011). However, the efficiency at which IDLV are captured at a particular site is much lower than the mutation frequency at that site resulting in

the loss of detection of potential off-targets (Koo et al., 2015). Cross-linking chromatin immunoprecipitation (ChIP) sequencing is another method that can be used to detect in situ nuclease interactions with target DNA (Park, 2009). This method has been shown to be less efficient at locating *bona fide* off-target sites because it is associated with false positives and is less sensitive at detecting low levels of off-target cleavage (Kuscu et al., 2014, Guilinger et al., 2014).

Genome-wide unbiased identification of DSBs evaluated by sequencing (GUIDE-seq) has seen increased use as it is able to identify off-target cleavage occurring at a frequency of 0.1% in a cell population (Tsai et al., 2015). This technique involves use of small, modified double-stranded oligonucleotides (dsODNs) which are incorporated at DSBs. Capture of the dsODNs at a DSB allows the surrounding sequences to be amplified and identified by sequencing. Since this method relies on the incorporation of dsODNs into DSBs, which only occurs in 30-50% of cases, some off-target sites can be missed (Tsai et al., 2015). While these methods effectively detect off-target cleavage occurring at low frequency, the gold standard for detection of off-targets is whole genome sequencing (WGS). While WGS is expensive, it is a powerful tool that allows the identification and detection of small indels, single nucleotide polymorphisms and structural variants such as rearrangements, inversions, major deletions and duplications (Veres et al., 2014).

4.4.2 Delivery of anti-HBV Sharkey TALENs

To enable clinical application of sequence-specific designer nucleases like anti-HBV Sharkey TALENs an efficient hepatotropic delivery system is required. Several viral and non-viral vectors have been developed that are capable of delivering designer nuclease-encoding sequences in vivo. Non-viral delivery systems have the ability to deliver large genetic sequences and production can be scaled up easily. Nevertheless, clinical assessment of non-viral vectors has been associated with low transduction efficiency and reduced target specificity.

Recombinant viruses are the vectors of choice for delivering gene therapeutics as these vectors have high transduction efficiency (Gray et al., 2010) and excellent expression profiles (Bouard et al., 2009). The delivery of TALENs using lentiviral and adenoviral vectors has been successfully demonstrated (Yang et al., 2013, Holkers et al., 2014). Despite successful

delivery of TALENs, the use of viral vectors is associated with a number of limitations that include, small carrying capacity, immunogenicity and general costs associated with viral production (Boeke et al., 2013). Despite these limitations, the use of viral vectors has been successful in clinical application, particularly AAV vectors. Recombinant AAVs have emerged as a highly promising gene delivery system as a result of their low immunogenicity and ability to mediate persistent gene expression in non-dividing cells (Howarth et al., 2010). AAV vectors can use be used to deliver therapeutic sequences to different cell types as the various serotypes exhibit a range of cell tropism and transduction efficiencies (Burger et al., 2004). It is reasonable to envision that recombinant AAV vectors can be used to deliver anti-HBV Sharkey TALENs to infected hepatocytes where these nucleases can disable cccDNA as a means to treat chronic hepatitis B.

4.5 Conclusion

Developing a curative approach to target HBV cccDNA is crucial as chronic hepatitis B infection is a major health burden. Current treatments are ineffective at eliminating viral cccDNA which is responsible for persistence of chronic infection. This is the first study to generate and evaluate Sharkey TALENs targeting the HBV genome. Anti-HBV Sharkey TALENs targeting two conserved sites within the *S* and *C* ORFs were generated. The Sharkey TALENs mediated inhibition of HBV replication and transcription in vitro and in vivo with minimal toxicity. Targeted mutagenesis was observed indicating that the anti-HBV Sharkey TALENs functioned as intended. Despite significant reduction of markers of HBV replication exhibited by the anti-HBV Sharkey TALENs, overall efficiency was lower than their wild-type counterparts. This indicates that the incorporation of the third generation obligate heterodimeric Sharkey variants into TALEN architecture did not improve the efficiency of the TALENs. Nevertheless, this study further validates the use of genome editing tools, in particular TALENs, as a potential therapy for HBV as both Sharkey and wild-type TALENs were able to target cccDNA of HBV without causing toxicity. Permanently disabling cccDNA is an important first step in developing a functional cure for chronic HBV infection.

Chapter 5

Appendix

5.1 Preparation and transformation of chemically competent E. coli

Materials

- ***Luria-Bertani media***

Ten grams of Bacto-tryptone (Thermo Scientific, CA, USA), 5 g NaCl and 5 g yeast extract (Oxoid, UK) were added to 1 litre of distilled water. This solution was autoclaved for 20 minutes at 121 °C and 1 kg/cm^2 and stored at room temperature.

- ***Transformation buffer (100 mM $CaCl_2$, 10 mM PIPES-HCl, 15% glycerol***)

To prepare transformation buffer, 0.3024 g PIPES, 1.4702 g of $CaCl_2$ and 15 ml glycerol was added to 80 ml of ddH_2O. The pH of the buffer was adjusted to 7.0 using NaOH and adjusted to a final volume of 100 ml. The transformation buffer was autoclaved for 20 minutes at 121 °C and 1 kg/cm^2 and stored at -20 °C.

- ***1000 × ampicillin (Roche Applied Science, Mannheim, Germany)***

One hundred milligrams of ampicillin was dissolved in 10 ml of 50% ethanol and stored at -20 °C.

- ***1000 × kanamycin (Thermo Scientific, CA, USA)***

Two hundred and fifty milligrams of kanamycin powder was added to 5 ml of double distilled water (ddH_2O) and was filter sterilised. This was stored as 1 ml aliquots at -20 °C in the dark.

- ***1% agar***

One percent (w/v) agar was mixed in Luria-Bertani medium and autoclaved at 121 °C for 20 minutes. The agar solution was cooled to approximately 50 °C. A final concentration of 100 µg/ml for ampicillin and 50 µg/ml for kanamycin was added to the agar solution. The agar solution was poured into petri dishes and allowed to solidify at room temperature and the plates were stored at 4 °C. Kanamycin plates were also stored in the dark.

Protocol

Preparation of chemically competent E. coli

Ten millilitres of Luria-Bertani media was inoculated with 10 µl of *E. coli* and incubated at 37 °C in a shaking incubator overnight. The 10 ml of culture was added to 150 ml of Luria-Bertani media and incubated with shaking at 37 °C for 4 hours until it reached an absorbance at 600 nm of approximately 0.4. The culture broth was split into 50 ml centrifuge tubes and centrifuged at 3000 ×g for 15 minutes. The pellet was re-suspended in 1 ml of transformation buffer, the volume adjusted to 35 ml with transformation buffer and incubated on ice for 20 minutes. After 20 minutes the cell suspension was centrifuged at 1000 ×g for 15 minutes at 4 °C. The pellet was re-suspended with 2 ml of transformation buffer, transferred to sterile microcentrifuge tubes in 100 µl aliquots and stored at -80 °C.

Transforming chemically competent E. coli

Ten microlitres of plasmid DNA was added to one hundred microlitres of competent *E. coli* and incubated on ice for 30 minutes. Thereafter the cells were heat shocked for 90 seconds at 42 °C. After heat shock treatment the cells were placed on ice for 5 minutes. The transformed *E. coli* were then plated on Luria-Bertani agar plates containing selective antibiotics.

5.2 Large-scale plasmid preparation

Materials

- ***Luria-Bertani media***
- ***Plasmid Maxi Kit (Qiagen, Hilden, Germany)***
- ***1000× ampicillin and 1000× kanamycin***

Protocol

A single colony containing the plasmid DNA of interest was used to inoculate 150 ml of Luria-Bertani media that was supplemented with ampicillin (100 μg/ml) or kanamycin (50 μg/ml). The bacterial culture was incubated overnight at 37 °C in a shaking incubator. The following day the bacterial culture was centrifuged at 6000 ×g for 20 minutes. The pellet was re-suspended in 10 ml of buffer P1. Ten millilitres of buffer P2 was added, mixed gently by inverting the tube 4-6 times and allowed to incubate for 5 minutes at room temperature. Ten millilitres of chilled buffer P3 was added and mixed gently by inverting the tube 4-6 times and then incubated on ice for 20 minutes. After 20 minutes the samples were centrifuged at 20 000 ×g for 40 minutes. A Qiagen-tip 500 column was equilibrated by adding 10 ml buffer QBT and allowed to empty by gravity flow. Supernatant was added to the column and allowed to enter the resin by gravity flow. The column was washed twice with 30 ml of buffer QC. The Qiagen-tip 500 column was transferred to a sterile 50 ml collection tube and 15 ml of buffer QF was added to elute the DNA. The DNA was precipitated by adding 10.5 ml of isopropanol, mixed and centrifuged at 15 000 ×g for 30 minutes at 4 °C. The isopropanol was discarded and the DNA pellet was washed by adding 5 ml of 70% ethanol and centrifuging the sample at 15 000 ×g for 20 minutes at 4 °C. The ethanol was discarded, the pellet was left to air dry for 5 minutes and then re-suspended in 100 μl of distilled water and stored at -20 °C.

5.3 Digestion of the Sharkey encoding plasmids

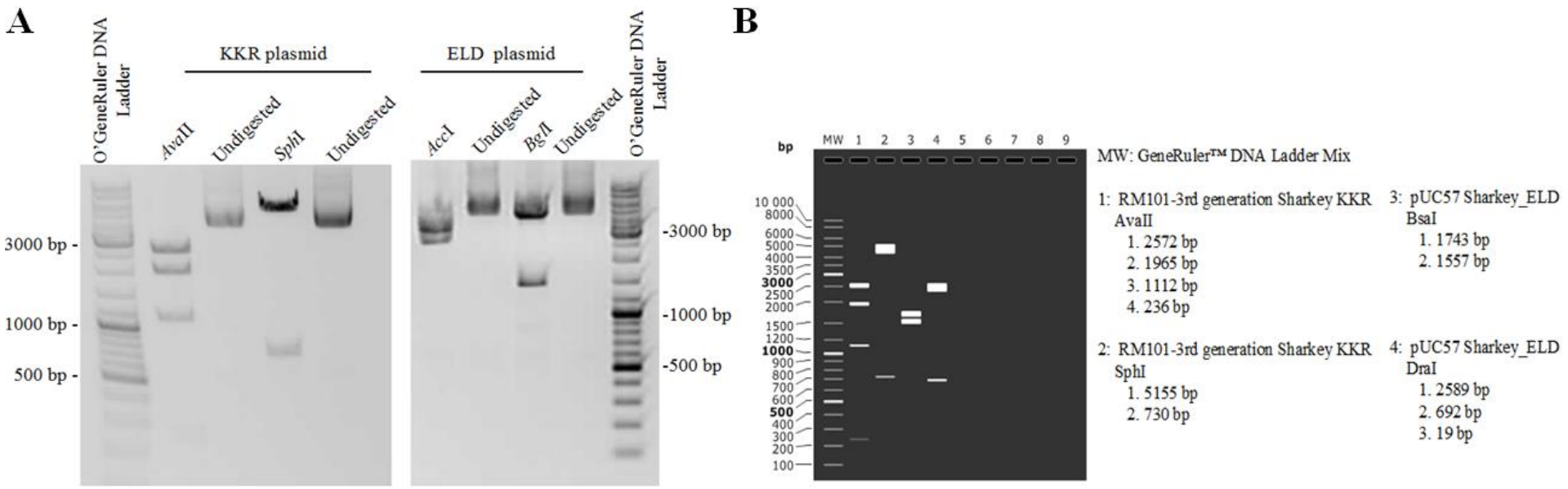

Figure 5.1: Restriction enzyme digestion of the plasmids encoding the Sharkey variants (KKR and ELD).

(**A**) The plasmid encoding the right Sharkey variant (KKR) was digested with *Ava*II and *Sph*I while the plasmid encoding the left Sharkey variant (ELD) was digested with *Acc*I and *Bgl*I to ensure the KKR and ELD encoding sequences were present within the plasmid. Molecular weight marker (O'GeneRuler DNA Ladder Mix). (**B**) **Simulated digestion of Sharkey encoding plasmids**. A simulated 1% agarose gel was generated and indicates the expected fragment sizes for the digest of RM101-3rd generation Sharkey KKR (the right Sharkey variant) with *Ava*II (lane 1) and *Sph*I (lane 2) and pUC57 Sharkey ELD (left Sharkey variant) with *Bsa*I (lane 3) and *Dra*I (lane 4). The fragments sizes for each band are indicated on the right and the molecular weight marker (MW) is the O'GeneRuler DNA Ladder Mix. SnapGene® software (from GSL Biotech; available at snapgene.com) was used to generate the simulated gel.

*5.4 Bgl*I digestion of the wild-type TALEN plasmids

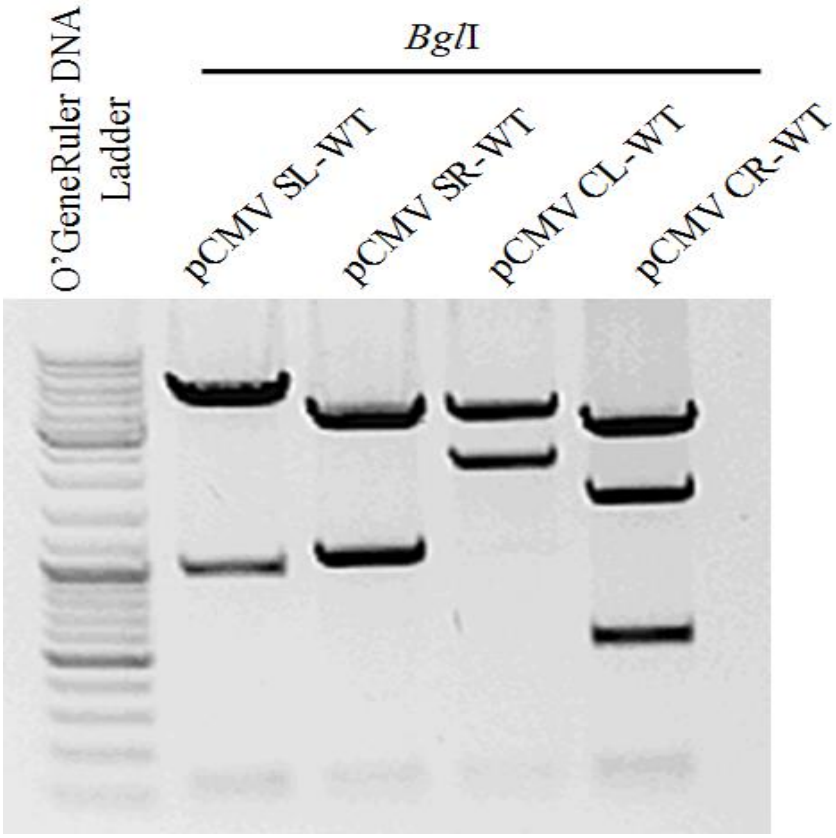

Figure 5.2: Enzymatic digestion of wild-type TALEN plasmids.

The wild-type TALEN (SR, SL, CR, CL) plasmids were digested with *Bgl*I enzyme and was used to distinguish the different TALEN monomers. Expected banding pattern was produced. Lane1: molecular weight marker (MW) is the O'GeneRuler DNA Ladder Mix.

5.5 Agarose Gel Electrophoresis

Materials

- ***50× Tris Acetate EDTA (TAE) Buffer***

Two hundred and forty-two grams of Tris base, 57.1 ml glacial acetic acid, 100 ml of 0.5 M EDTA (pH 8.0) was added to double distilled water (ddH_2O). The TAE buffer was made to a total volume of 1 L using ddH2O.

- ***Agarose* (Lonza, BS, Switzerland)**

- ***Ethidium bromide (10 mg/ml*) *(Sigma-Aldrich, MO, USA)***

Protocol

To prepare a 1% gel, 1 g of of agarose was added to 100 ml of 1× TAE and dissolved by heating in a microwave. The mixture was allowed to cool at room temperature and ethidium bromide solution to a final concentration of 0.5 µg/ml. The mixture was poured into a gel casting chamber and allowed to set at room temperature. Once set, the gel was placed in a running chamber containing 1× TAE buffer and subjected to electrophoresis at 100 volts for 45 minutes. The gel was visualised using a G:BOX UV transilluminator (Syngene, Cambridge, UK)

5.6 Extraction of DNA fragments from agarose gel (Gel extraction)

Materials

- ***MinElute Gel Extraction kit (Qiagen, Hilden, Germany)***
- ***Isopropanol***

Protocol

The DNA fragment of interest was excised from the agarose gel and each gel slice was placed in a microcentrifuge tube and weighed. To each tube, 3 volumes of Buffer QG was added to 1 volume of gel (100 mg ~ 100 µl) and the tubes were incubated at 50 °C for 10 minutes with periodic mixing to dissolve the gel slice. The microcentrifuge tubes were centrifuged briefly, 1 gel volume of isopropanol was added to the samples, mixed briefly and centrifuged. Samples were transferred to a QIAquick spin column that was inserted into a 2 ml collection tube and centrifuged for 1 minute at maximum speed in a standard bench-top microcentrifuge. The flow-through was discarded and the QIAquick spin column was placed back into the collection tube. Five hundred microlitres of Buffer QG was added to the column and centrifuged at maximum speed for 1 minute. The flow-through was discarded and 750 µl of Buffer PE of was added to the QIAquick spin column to wash the DNA and centrifuged at 10 000 ×g for 1 minute. The samples were centrifuged at 13 000 rpm for an additional 2 minutes to remove excess wash buffer. The QIAquick spin column was transferred into a clean centrifuge tube and 30 µl of ddH2O was added to the QIAquick spin column and incubated for 5 minutes at room temperature. After incubation the samples were centrifuged at 10 000 ×g. The eluted DNA was stored at -20 °C.

5.7 Small scale plasmid preparation

Materials

- ***Luria-Bertani media***
- ***EconoSpin™ All-in-One Mini Spin Columns (Epoch Life Sciences, MO, USA)***

Protocol

A single colony containing the plasmid DNA of interest was used to inoculate 10 ml of Luria-Bertani media that was supplemented with ampicillin (100 µg/ml) or kanamycin (50 µg/ml). The bacterial culture was left to incubate overnight at 37 °C on a shaking incubator. The following day the bacterial culture was centrifuged at 4000 ×g for 20 minutes. The supernatant was removed and the pellet was re-suspended in 250 µl buffer MX1. Two hundred and fifty microlitres of lysis buffer (MX2) was added to the re-suspension, mixed gently by inverting the tube 4-6 times and allowed to incubate for 5 minutes at room temperature. Three hundred and fifty microlitres of chilled neutralisation buffer (MX3) was added and mixed gently by inverting the tube 4-6 times and then incubated on ice for 5 minutes. After 5 minutes the samples were centrifuged at 6000 ×g for 20 minutes. The supernatant was transferred to EconoSpin™ columns and centrifuged at maximum speed (10 000 ×g) for 1 minute using a standard bench-top centrifuge. The flow-through in the collection tube was discarded and 700 µl of wash buffer (WS) was added to the column. The samples were centrifuged at maximum speed (10 000 ×g) for 1 minute, the flow-through was discarded and the samples were centrifuged again to remove excess wash buffer. The column was placed in a sterile microcentrifuge tube, 50 µl of ddH_2O was added to the column and centrifuged at 10 000 ×g for 1 minute. The eluted plasmid DNA was stored at -20 °C.

5.8 Sequence analysis of the anti-HBV TALENs

5.8.1 Confirmation of Sharkey mutations in the FokI nuclease domain of the Sharkey TALEN monomers

```
WT        GSQLVKSELEEKKSELRHKLKYVPHEYIELIEIARNSTQDRILEMKVMEFFMKVYGYRGK
KKR       GSQLVKSELEEKKSELRHKLKYVPHEYIELIEIARNPTQDRILEMKVMEFFMKVYGYRGE
SR+KKR    GSQLVKSELEEKKSELRHKLKYVPHEYIELIEIARNPTQDRILEMKVMEFFMKVYGYRGE
CR+KKR    GSQLVKSELEEKKSELRHKLKYVPHEYIELIEIARNPTQDRILEMKVMEFFMKVYGYRGE
          ************************************ ***********************:

WT        HLGGSRKPDGAIYTVGSPIDYGVIVDTKAYSGGYNLPIGQADEMQRYVEENQTRNKHINP
KKR       HLGGSRKPDGAIYTVGSPIDYGVIVDTKAYSGGYNLPIGQADEMQRYVKENQTRNKHINP
SR+KKR    HLGGSRKPDGAIYTVGSPIDYGVIVDTKAYSGGYNLPIGQADEMQRYVKENQTRNKHINP
CR+KKR    HLGGSRKPDGAIYTVGSPIDYGVIVDTKAYSGGYNLPIGQADEMQRYVKENQTRNKHINP
          ************************************************:***********

WT        NEWWKVYPSSVTEFKFLFVSGHFKGNYKAQLTRLNHITNCNGAVLSVEELLIGGEMIKAG
KKR       NEWWKVYPSSVTEFKFLFVSGHFKGNYKAQLTRLNRKTNCNGAVLSVEELLIGGEMIKAG
SR+KKR    NEWWKVYPSSVTEFKFLFVSGHFKGNYKAQLTRLNRKTNCNGAVLSVEELLIGGEMIKAG
CR+KKR    NEWWKVYPSSVTEFKFLFVSGHFKGNYKAQLTRLNRKTNCNGAVLSVEELLIGGEMIKAG
          ************************************: ***********************

WT        TLTLEEVRRKFNNGEINF*GP
KKR       TLTLEEVRRKFNNGEINF*GP
SR+KKR    TLTLEEVRRKFNNGEINF*GP
CR+KKR    TLTLEEVRRKFNNGEINF*GP
          ********************


WT        GSQLVKSELEEKKSELRHKLKYVPHEYIELIEIARNSTQDRILEMKVMEFFMKVYGYRGK
ELD       GSQLVKSELEEKKSELRHKLKYVPHEYIELIEIARNPTQDRILEMKVMEFFMKVYGYRGE
SL+ELD    GSQLVKSELEEKKSELRHKLKYVPHEYIELIEIARNPTQDRILEMKVMEFFMKVYGYRGE
CL+ELD    GSQLVKSELEEKKSELRHKLKYVPHEYIELIEIARNPTQDRILEMKVMEFFMKVYGYRGE
          ************************************ ***********************:

WT        HLGGSRKPDGAIYTVGSPIDYGVIVDTKAYSGGYNLPIGQADEMQRYVEENQTRNKHINP
ELD       HLGGSRKPDGAIYTVGSPIDYGVIVDTKAYSGGYNLPIGQADEMERYVEENQTRDKHLNP
SL+ELD    HLGGSRKPDGAIYTVGSPIDYGVIVDTKAYSGGYNLPIGQADEMERYVEENQTRDKHLNP
CL+ELD    HLGGSRKPDGAIYTVGSPIDYGVIVDTKAYSGGYNLPIGQADEMERYVEENQTRDKHLNP
          ************************************************:*********:** **

WT        NEWWKVYPSSVTEFKFLFVSGHFKGNYKAQLTRLNHITNCNGAVLSVEELLIGGEMIKAG
ELD       NEWWKVYPSSVTEFKFLFVSGHFKGNYKAQLTRLNHITNCNGAVLSVEELLIGGEMIKAG
SL+ELD    NEWWKVYPSSVTEFKFLFVSGHFKGNYKAQLTRLNHITNCNGAVLSVEELLIGGEMIKAG
CL+ELD    NEWWKVYPSSVTEFKFLFVSGHFKGNYKAQLTRLNHITNCNGAVLSVEELLIGGEMIKAG
          ************************************************************

WT        TLTLEEVRRKFNNGEINF*GP
ELD       TLTLEEVRRKFNNGEINF*GP
SL+ELD    TLTLEEVRRKFNNGEINF*GP
CL+ELD    TLTLEEVRRKFNNGEINF*GP
          ********************
```

Figure 5.3: **Multiple sequence alignment of S and C Sharkey nuclease domains.**

Anti-HBV Sharkey S and C TALEN monomer plasmids were sequenced to confirm presence of the left or right Sharkey nuclease domain-encoding sequence. The top sequence represents the wild-type *Fok*I nuclease domain, the second sequence represents the left or right Sharkey *Fok*I variants, the third sequence represents the *Fok*I domain generated from sequencing left and right S Sharkey plasmids and the bottom sequence *Fok*I domain generated from sequencing left and right C Sharkey plasmids. The wild-type *Fok*I and the Sharkey *Fok*I were used as reference sequences to confirm the presence of the S418P, E441K, E490K, I538K and H537R mutations in the right monomer and the S418P, E441K, Q486E, I499L and N496D mutations in the left monomer. The amino acids highlighted in yellow represents the wild-type sequences, and the sequences highlighted in green represent mutated amino acid sequence. Raw sequencing data can be seen below.

5.8.2 Chromatograms of the anti-HBV TALEN plasmids

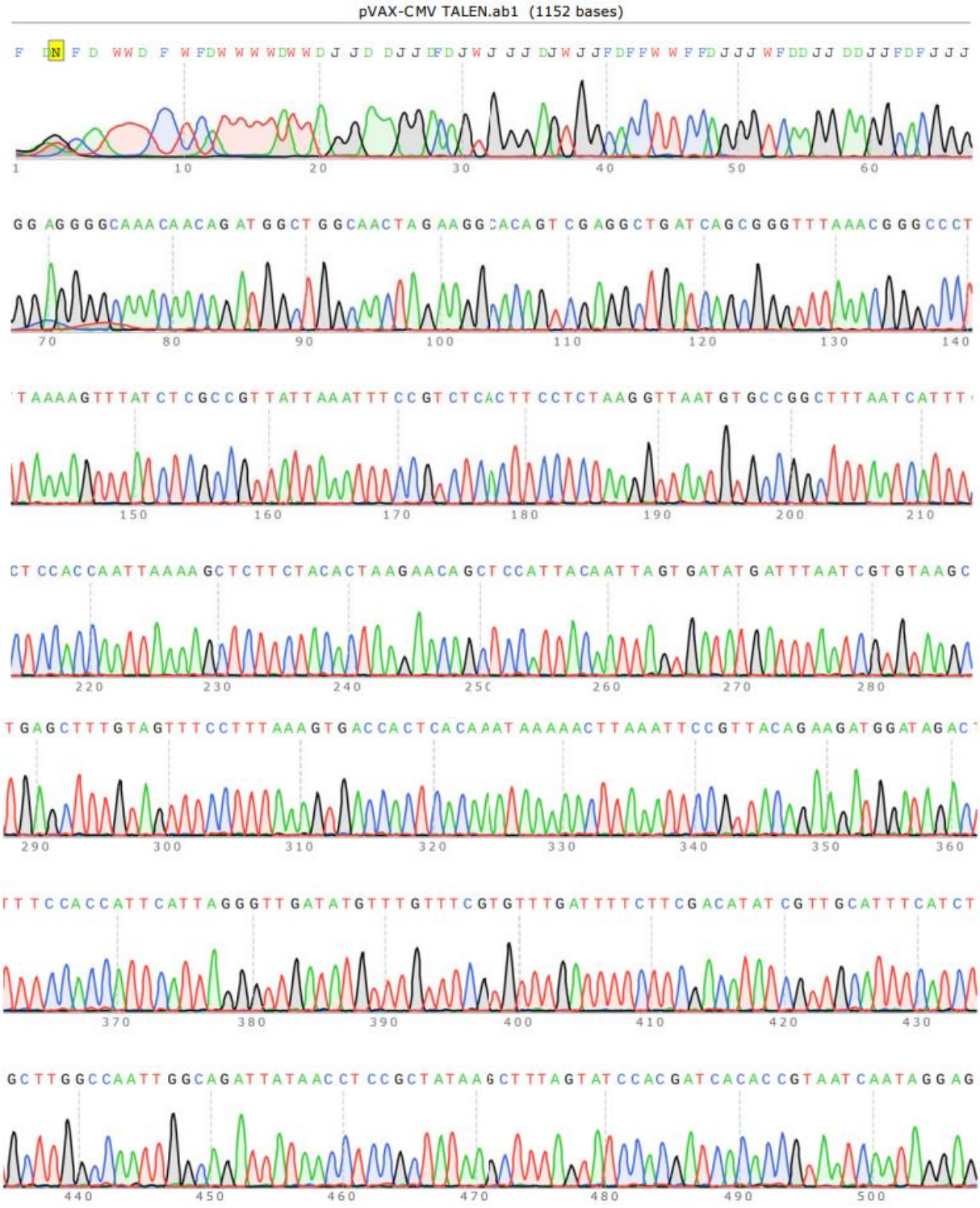

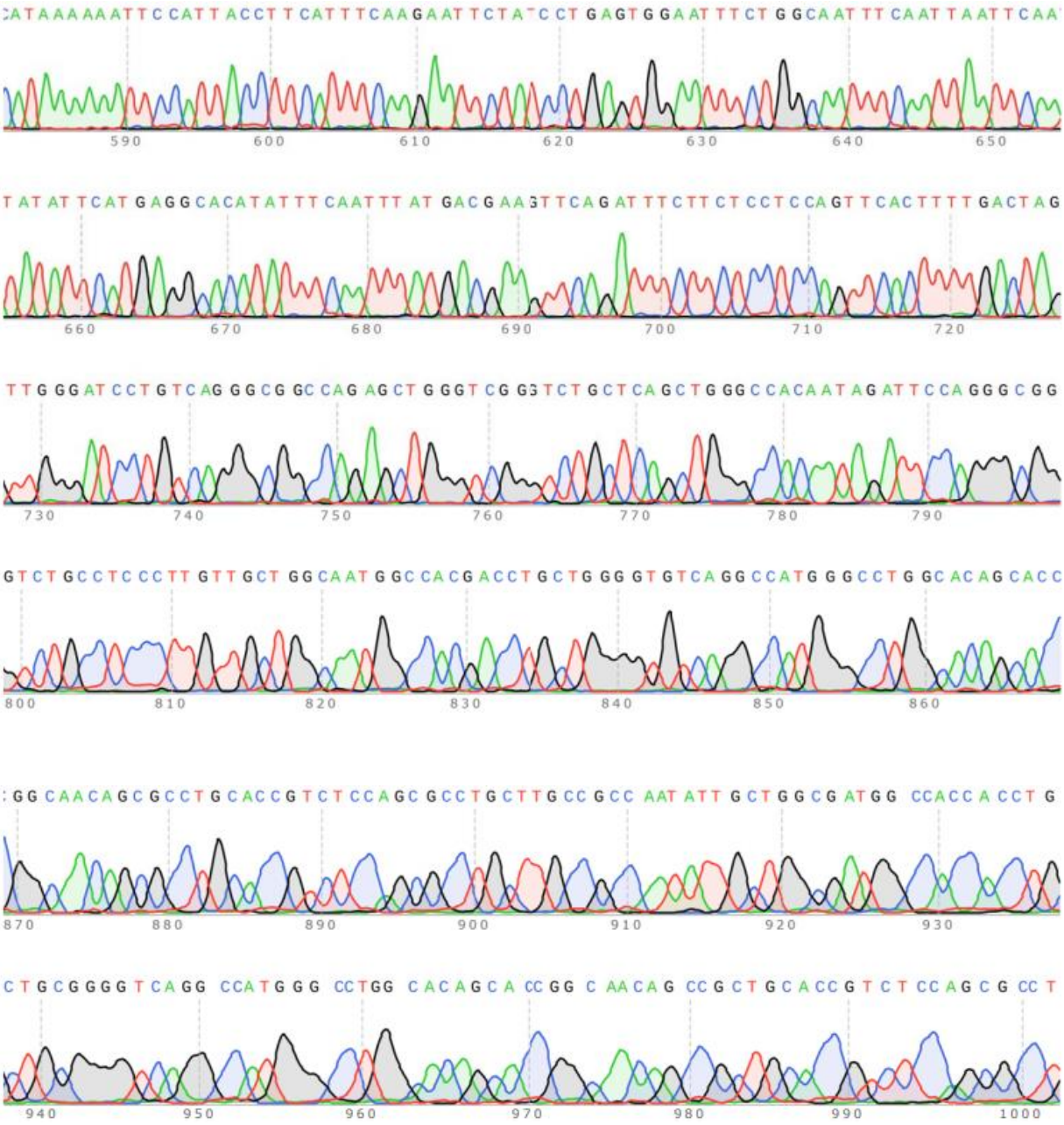
590 600 610 620 630 640 650
660 670 680 690 700 710 720
730 740 750 760 770 780 790
800 810 820 830 840 850 860
870 880 890 900 910 920 930
940 950 960 970 980 990 1000

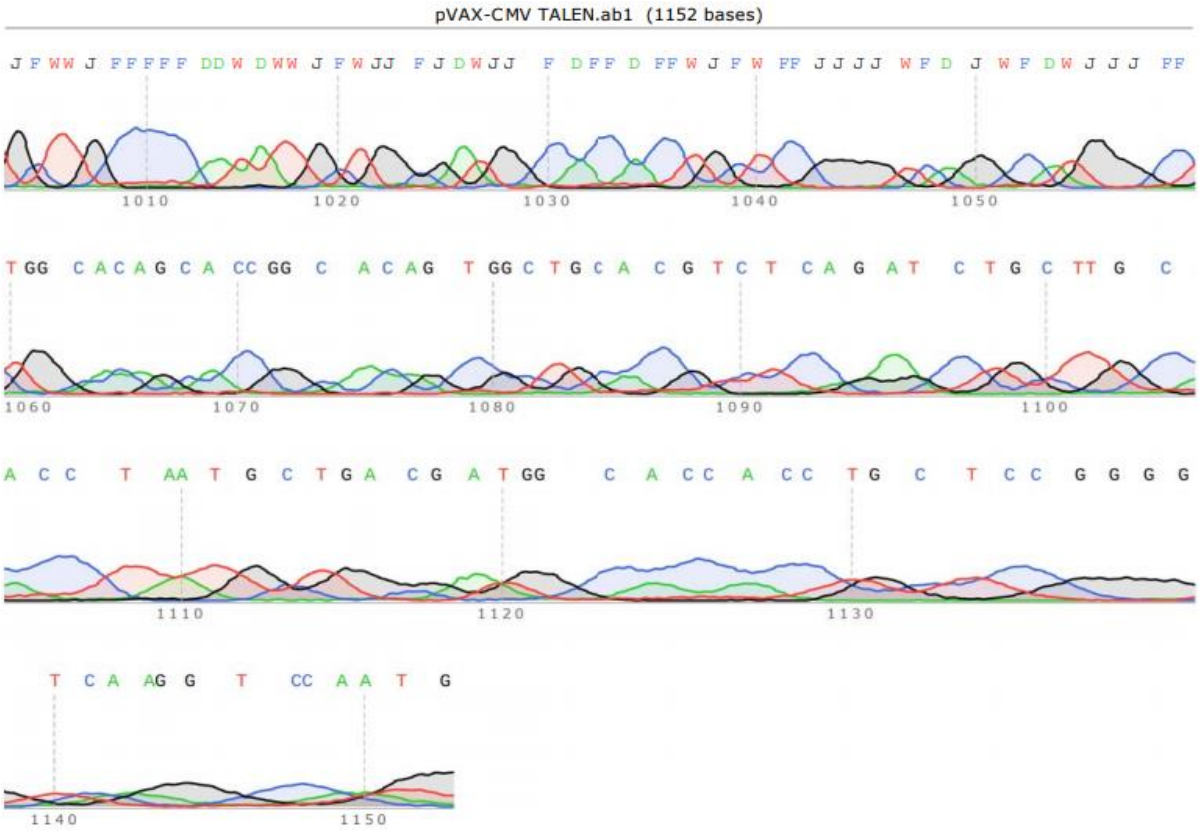

Figure 5.4: A chromatogram of the wild-type S TALEN sequence.

The chromatogram represents the data from sequencing the wild-type S TALEN plasmids using a reverse primer that binds downstream of the *Fok*I nuclease domain-encoding sequence.

Chapter 5- Appendix

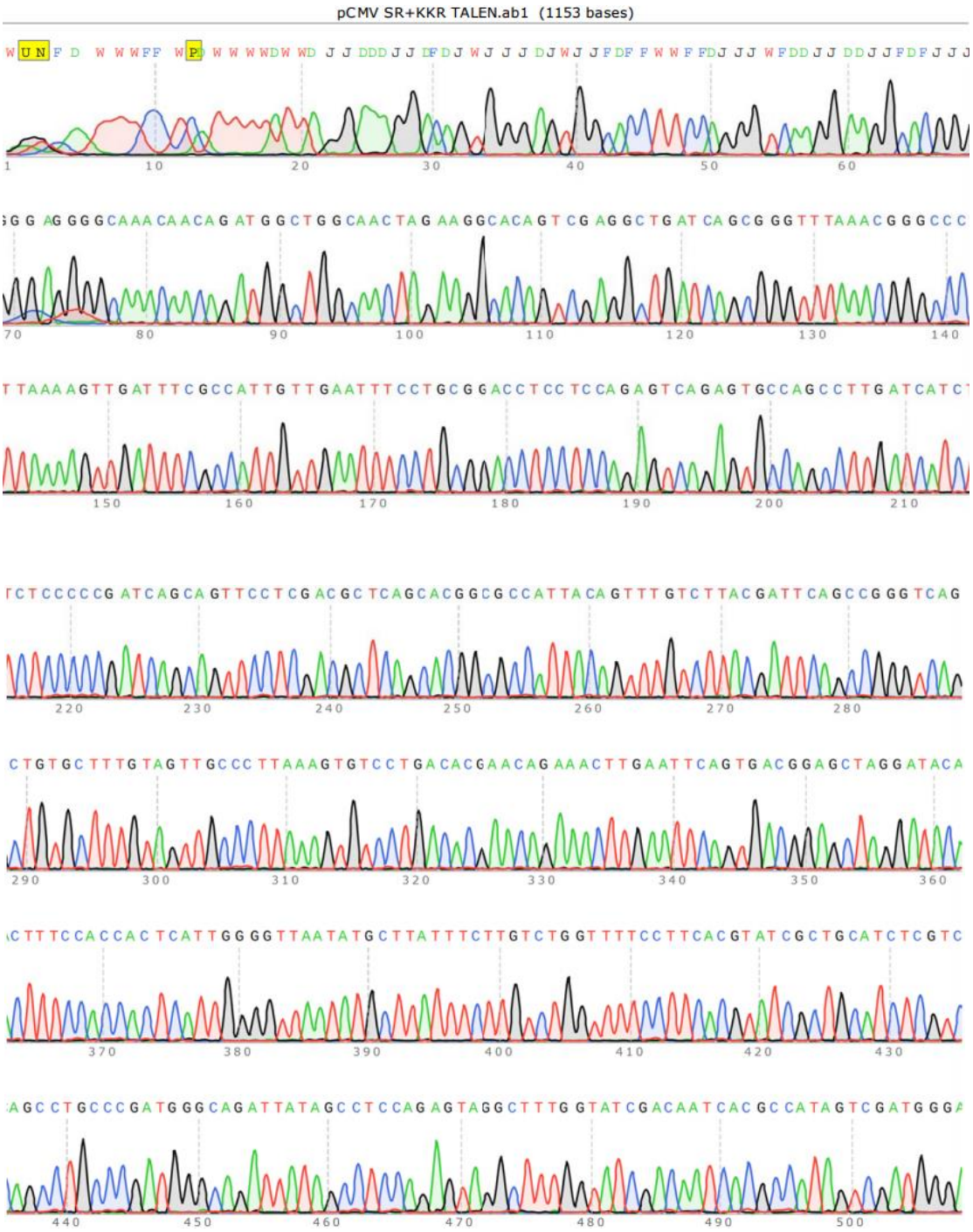

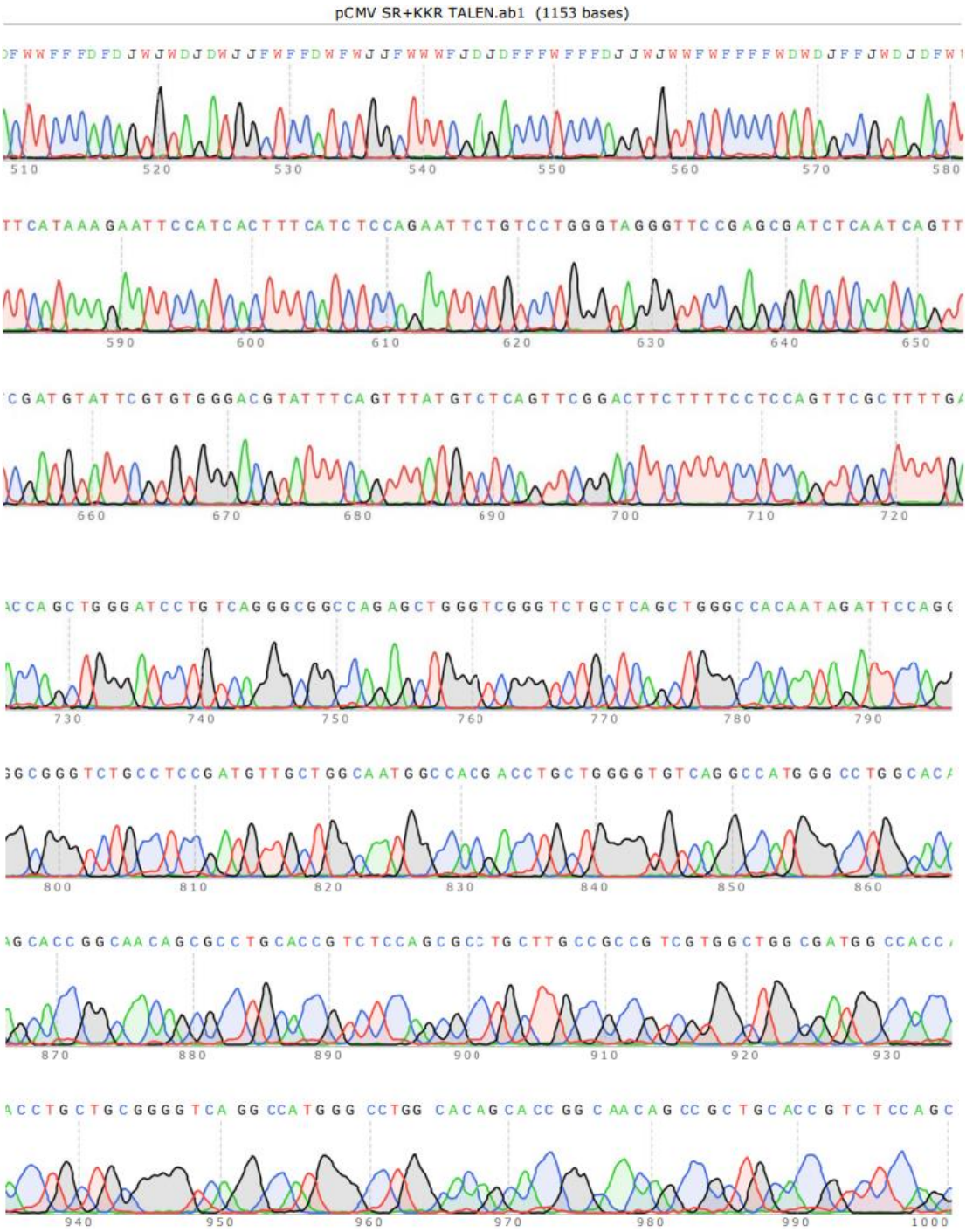
pCMV SR+KKR TALEN.ab1 (1153 bases)

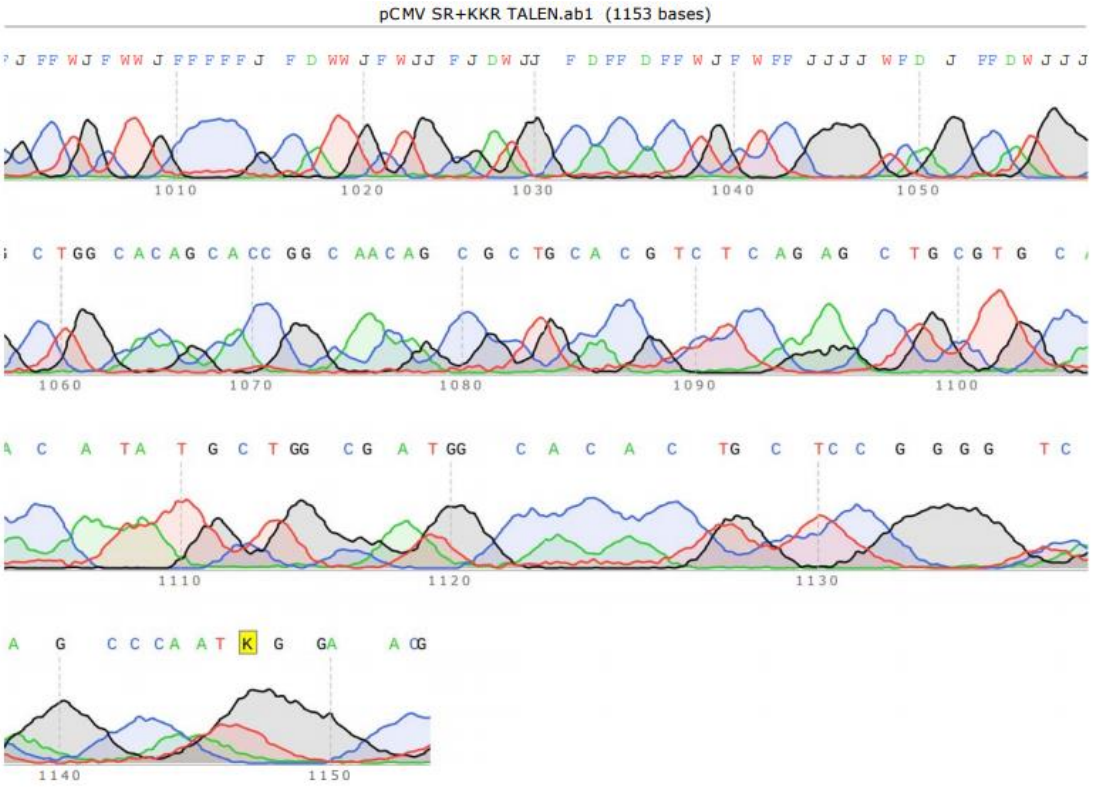

Figure 5.5: **A chromatogram of the right Sharkey S TALEN sequence.**

The chromatogram represents the data from sequencing the right Sharkey S TALEN plasmid using a reverse primer that binds downstream of the *Fok*I nuclease domain-encoding sequence.

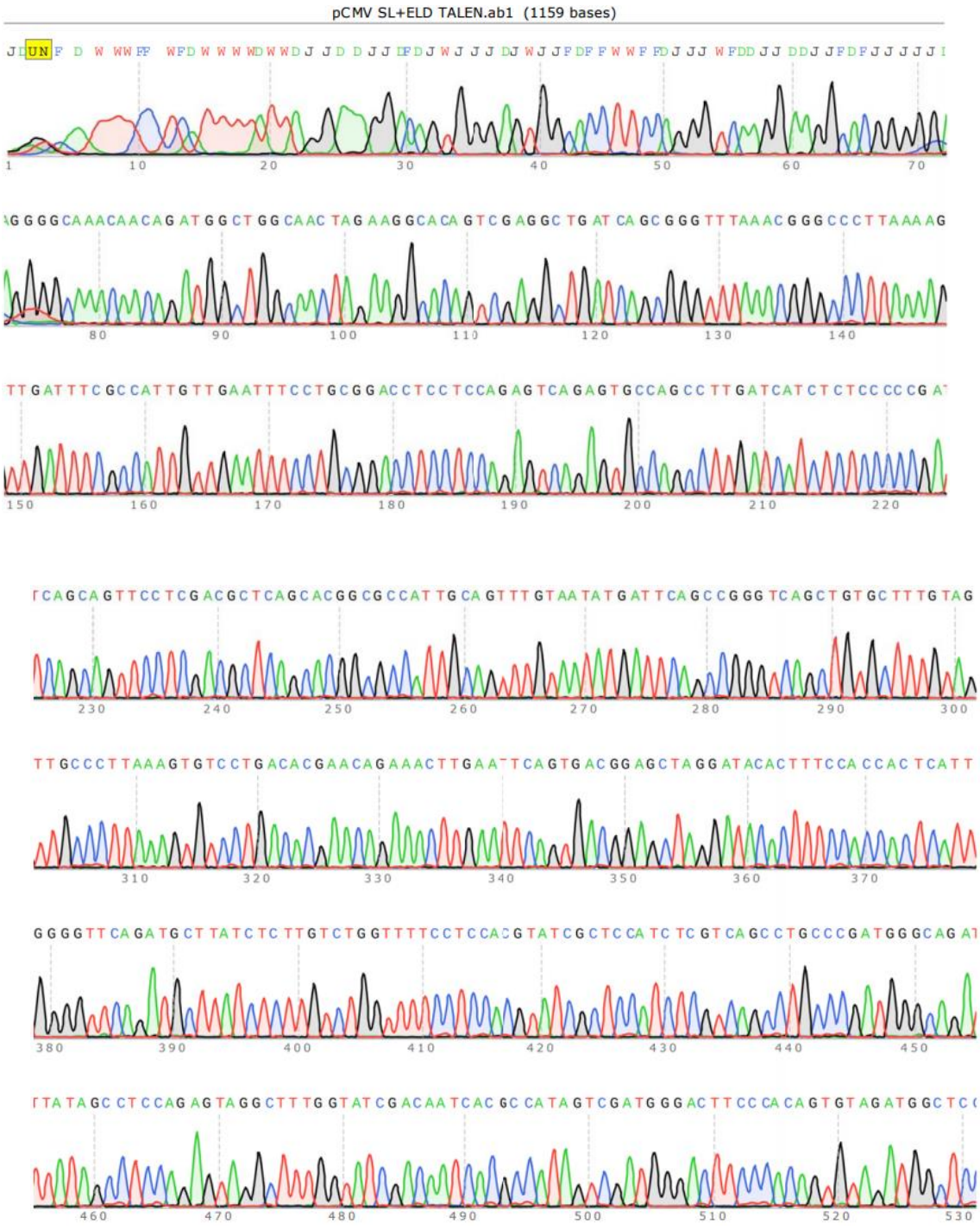
pCMV SL+ELD TALEN.ab1 (1159 bases)

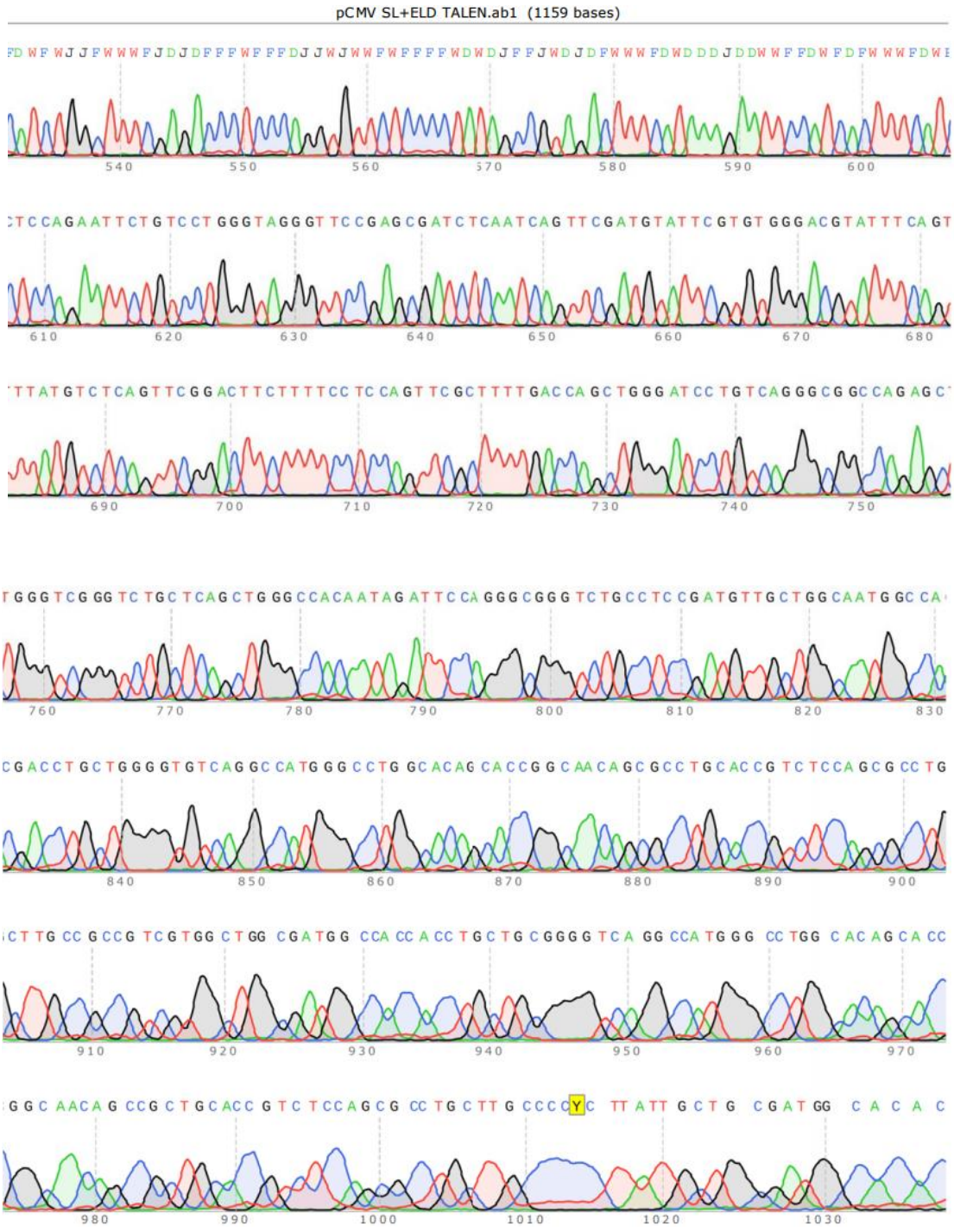
pCMV SL+ELD TALEN.ab1 (1159 bases)
540 550 560 570 580 590 600
610 620 630 640 650 660 670 680
690 700 710 720 730 740 750
760 770 780 790 800 810 820 830
840 850 860 870 880 890 900
910 920 930 940 950 960 970
980 990 1000 1010 1020 1030

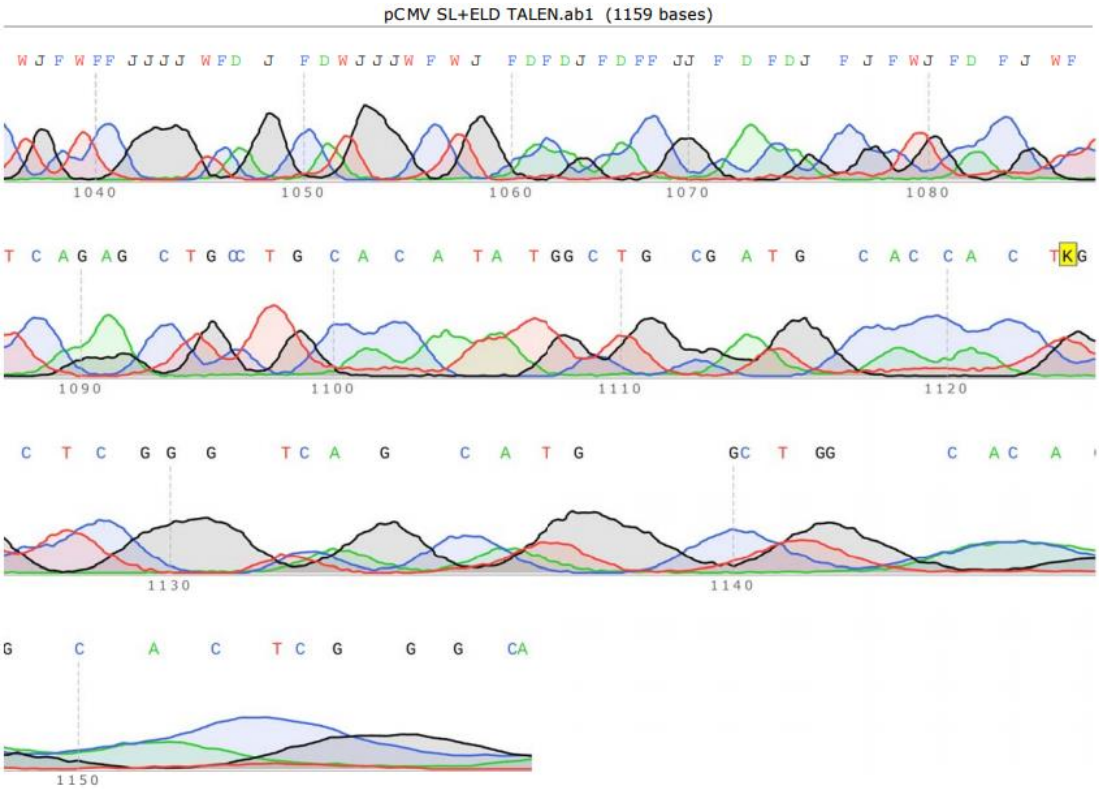

Figure 5.6: A chromatogram of the left Sharkey S TALEN sequence.

The chromatogram represents the data from sequencing the left Sharkey S TALEN plasmid using a reverse primer that binds downstream of the *Fok*I nuclease domain-encoding sequence.

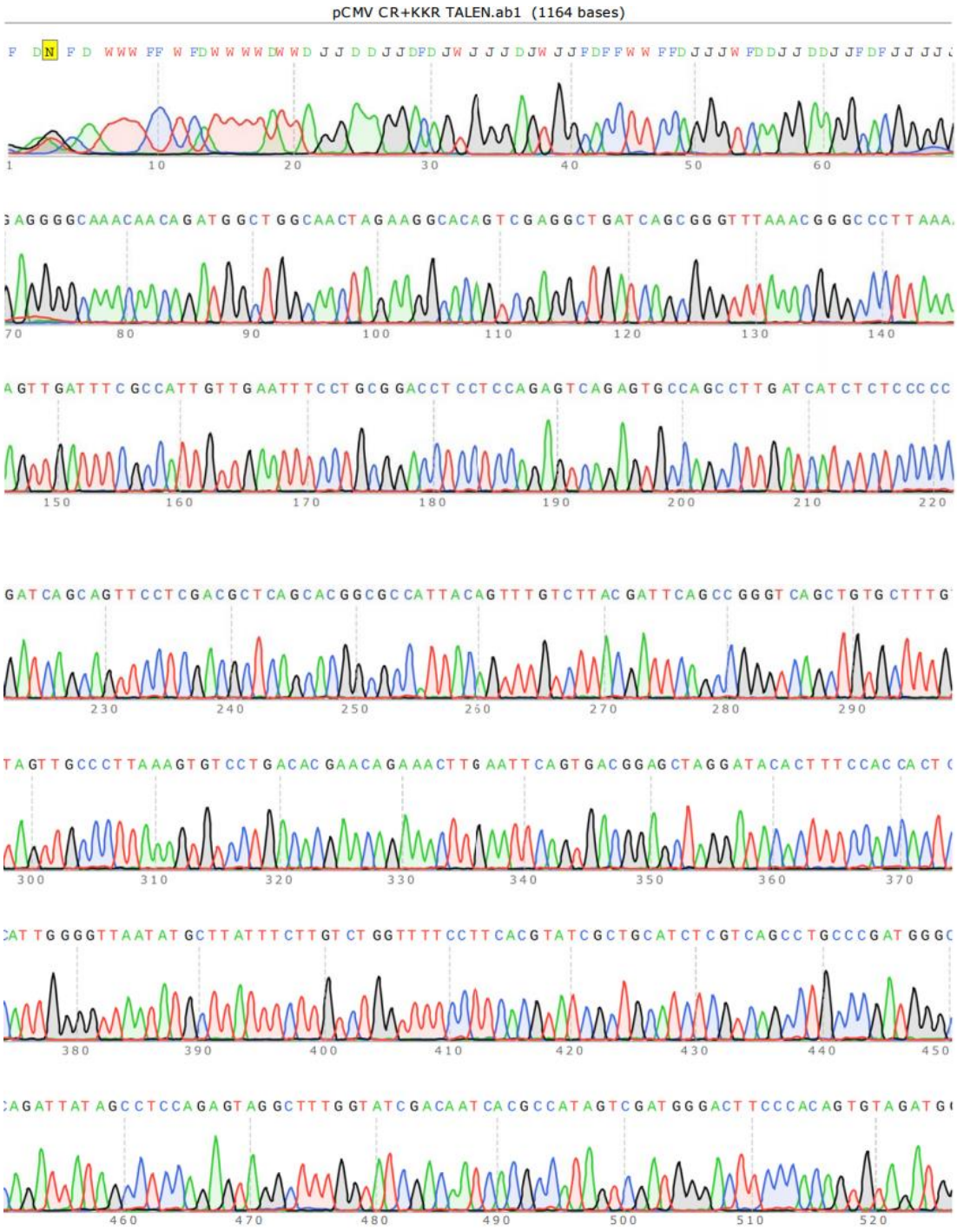
pCMV CR+KKR TALEN.ab1 (1164 bases)

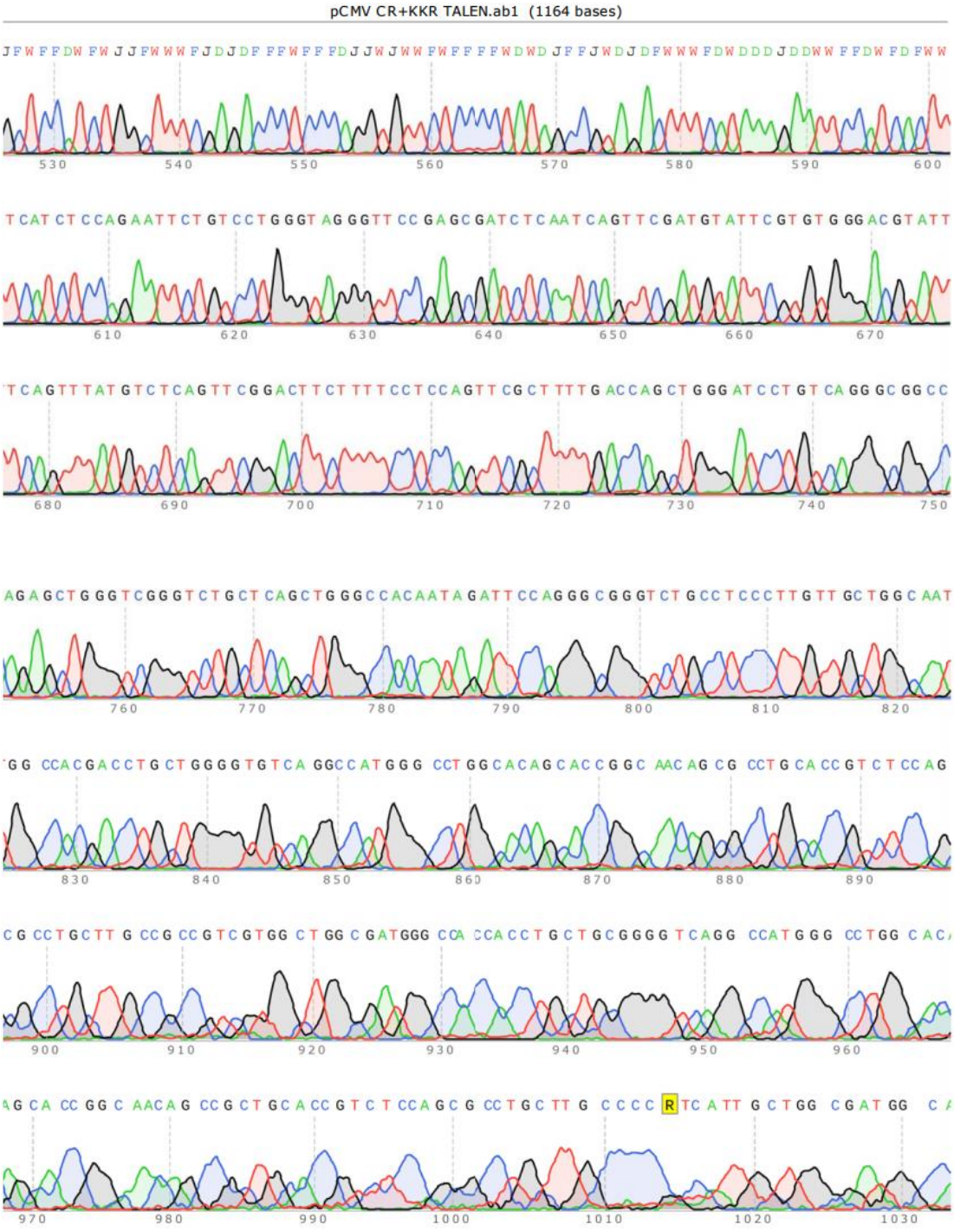
pCMV CR+KKR TALEN.ab1 (1164 bases)
530 540 550 560 570 580 590 600
610 620 630 640 650 660 670
680 690 700 710 720 730 740 750
760 770 780 790 800 810 820
830 840 850 860 870 880 890
900 910 920 930 940 950 960
970 980 990 1000 1010 1020 1030

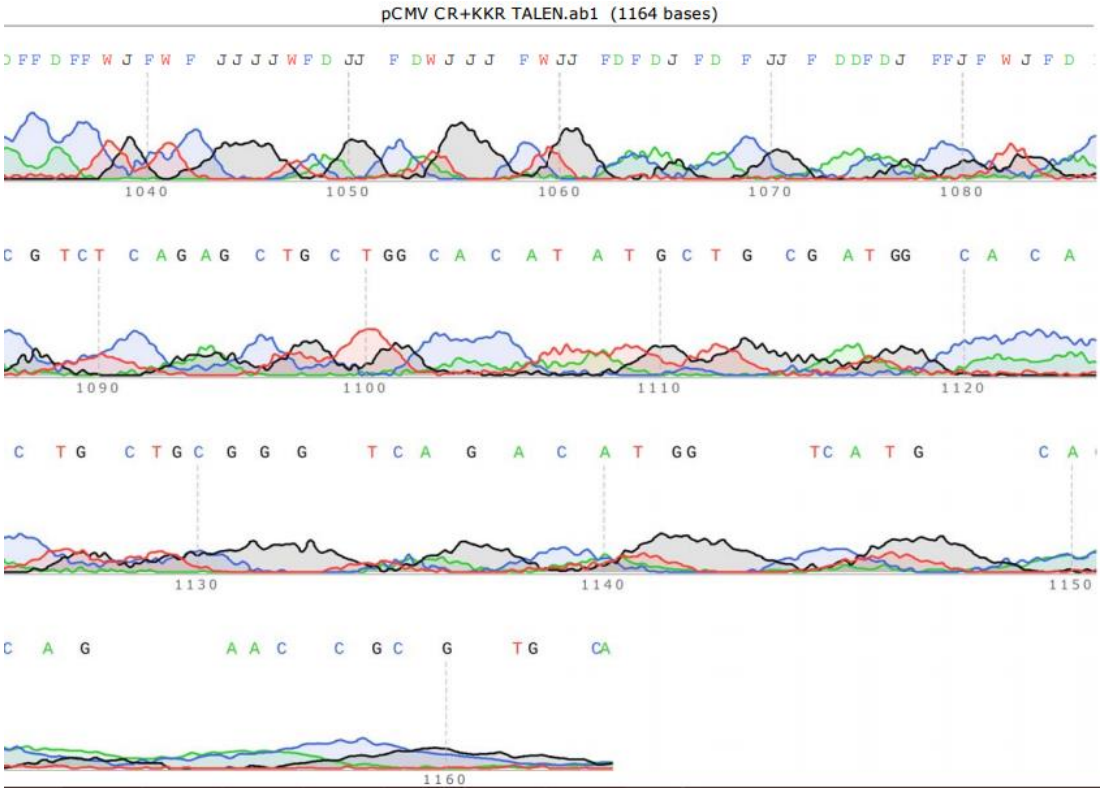

Figure 5.7: A chromatogram of the right Sharkey C TALEN sequence.

The chromatogram represents the data from sequencing the right Sharkey C TALEN plasmid using a reverse primer that binds downstream of the *Fok*I nuclease domain-encoding sequence.

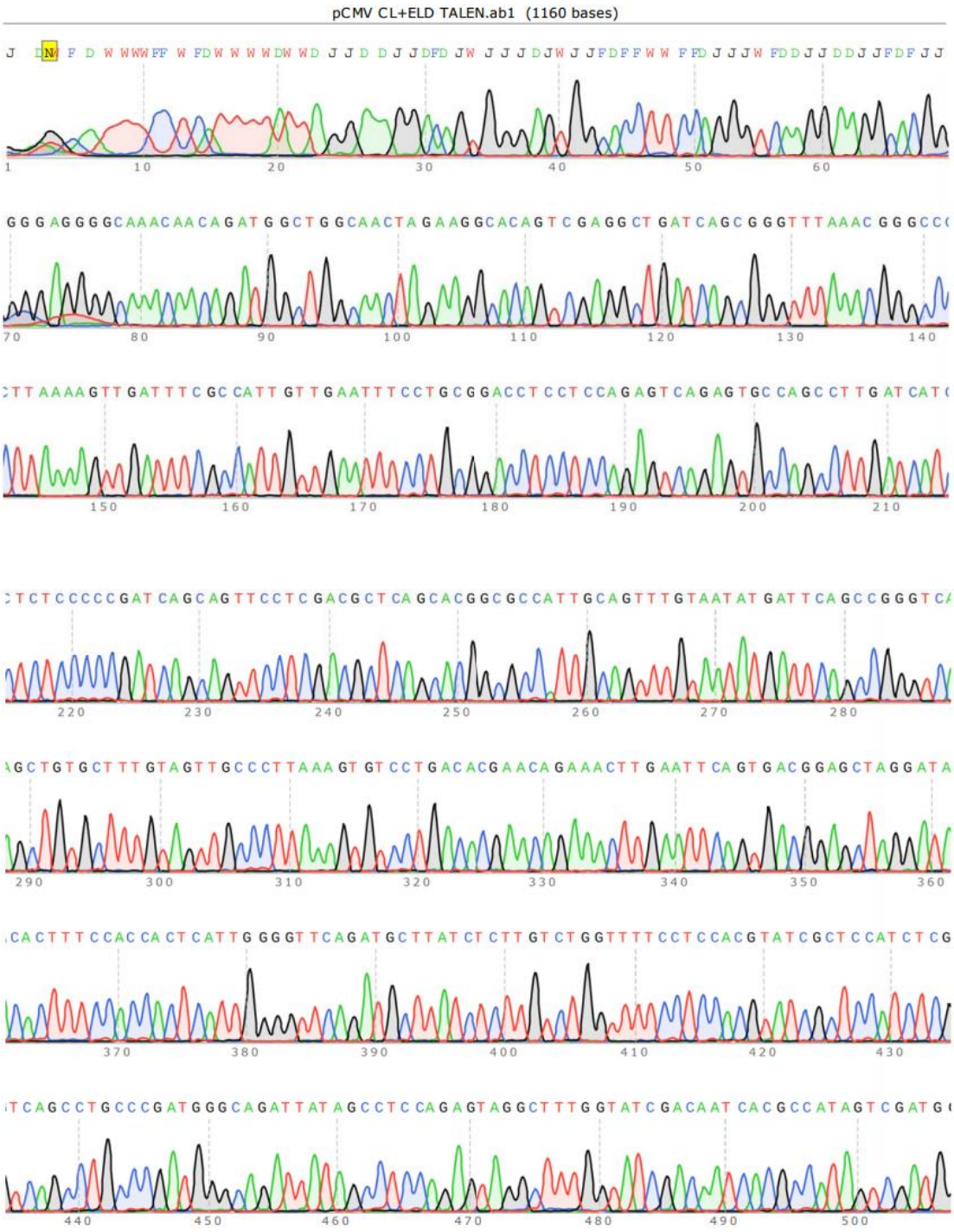
pCMV CL+ELD TALEN.ab1 (1160 bases)

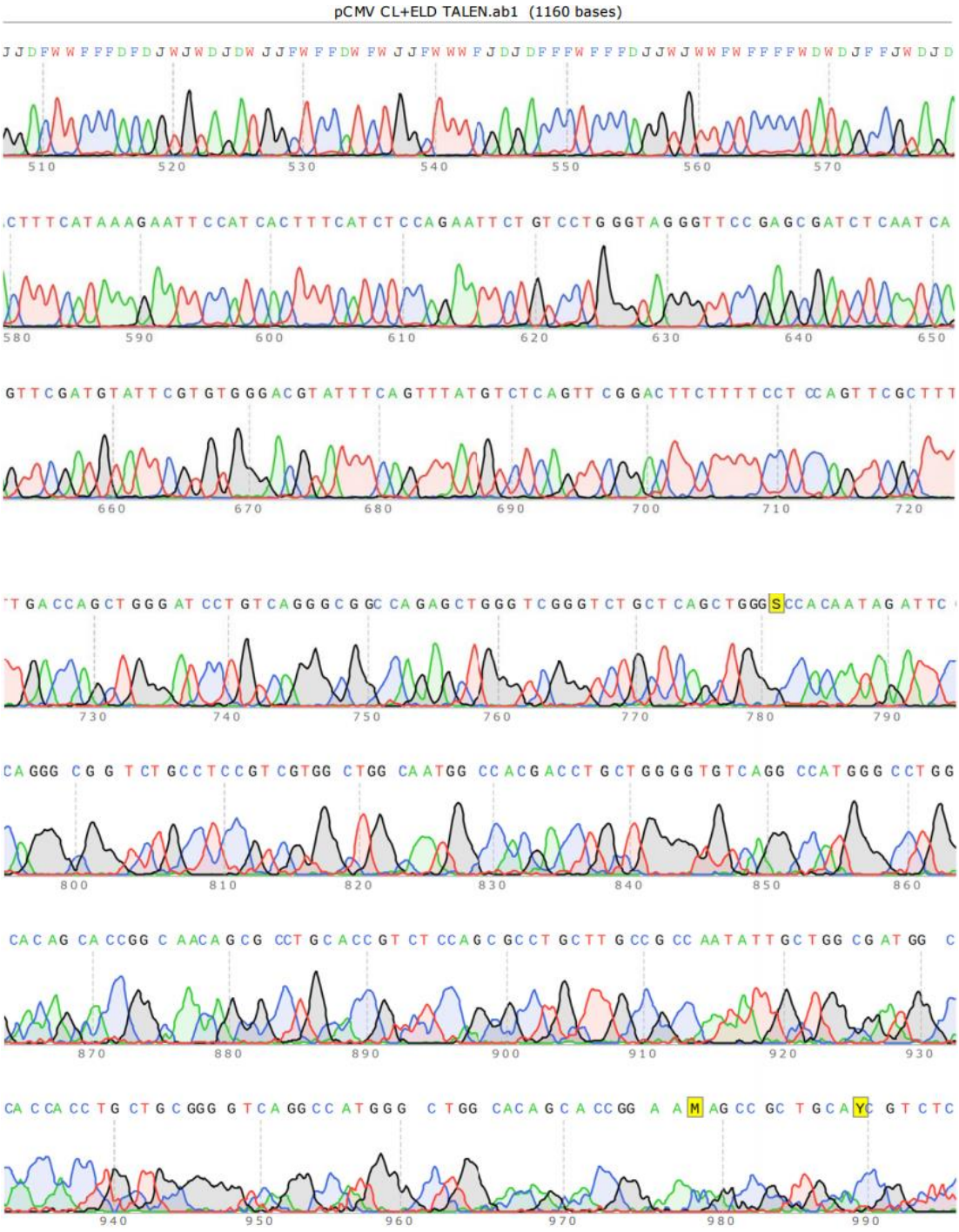
pCMV CL+ELD TALEN.ab1 (1160 bases)

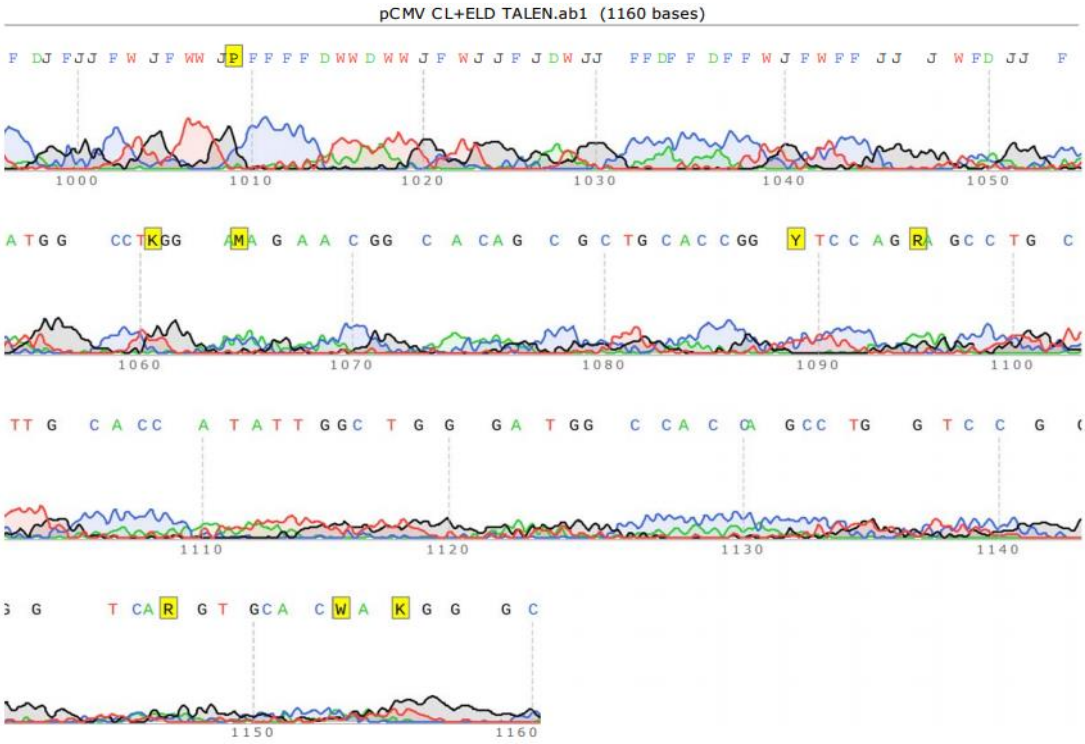

Figure 5.8: A chromatogram of the left Sharkey C TALEN sequence.

The chromatogram represents the data from sequencing the left Sharkey C TALEN plasmid using a reverse primer that binds downstream of the *Fok*I nuclease domain-encoding sequence.

5.9 Cell Culture

5.9.1 Culturing and growth of mammalian cells

Materials

- ***Preparation of 1000 × penicillin/streptomycin (100 000 U/mL; 100 000 µg/mL)***

The pen/strep solution was prepared by dissolving 0.9 g of penicillin and 15 g of streptomycin in 15 ml of PBS. The solution was filter sterlised and stored in 1 ml aliquots at -20 °C.

- ***Complete DMEM***

Consist of 449 ml of DMEM, 50 ml of 10% FBS (foetal bovine serum) and 1 ml of Pen/Strep (penicillin 100 U/ml; streptomycin 100 µg/ml). Medium was filter sterilised and stored 4°C.

- ***Saline/0.01% EDTA solution***

Protocol

Liver-derived human hepatoma 7 (Huh 7) and HepG2.2.15 cells as well as kidney-derived human embryonic kidney 293T (HEK293T) cells were used. The HepG2.2.15 and HEK293T cells were grown in 75 cm^2 CellStar® cell culture flasks (Greiner Bio-One, Frickenhausen, Germany) and maintained in Dulbecco's Modified Eagle's Medium (DMEM) (Gibco™, Thermo Scientific, CA, USA) while the Huh 7 cells were maintained in low glucose (1 g/L) DMEM (Gibco™, Thermo Scientific, CA, USA). The DMEM was supplemented with penicillin (100 U/ml), streptomycin (100 µg/ml) and 10% foetal calf serum (FCS). The cells were incubated in a humidified incubator at 37 °C and 5% CO_2. The Olympus CKX31 light microscope (Olympus, Tokyo, Japan) was used to monitor the cells.

5.9.2 General procedure used for seeding or passaging cells

Protocol

Media was removed from cells and wash with 10 ml of saline/EDTA. Saline/EDTA solution was discarded. An additional 5 ml of saline/EDTA solution was added to the cells and incubated at 37°C (5% CO_2) for approximately 10 minutes. After incubation, the saline /EDTA solution was discarded. Approximately 3 ml of TrypLE™ Express was added, swirl gently and was incubate at 37°C (5% CO_2) for approximately 5 minutes. TrypLE™ Express was not required for the HEK 293T cells. After incubation, the flask was gently tapped to lift cells. Seven millilitres of complete DMEM was added to suspense the cells, the cell suspension was transferred into in sterile 15 mL tube and centrifuged for 3 minutes at 200 ×g. Supernatant was discarded and 1 ml of complete DMEM was added to re-suspend the pellet. Cells were split according to appropriate ratio and the appropriate volume of complete DMEM was added into new flask/plate. Approximately 10 ml complete DMEM was added to the new flask. Cells maintained were incubated at 37°C (5% CO_2) in a humidified incubator.

5.10 Large-scale plasmid preparation (Endotoxin-free)

Materials

- ***Luria-Bertani media***
- ***EndoFree® Plasmid Maxi Kit (Qiagen, Hilden, Germany)***
- ***1000× ampicillin and 1000× kanamycin***

Protocol

To prepare the endotoxin-free plasmids, the large scale plasmid preparation (Appendix 5.2) protocol was followed with one additional step. After addition of buffer P3 and clearing the supernatant by centrifugation, 2.5 ml of Buffer ER was added, the solution mixed and incubated for 30 minutes on ice. The supernatant was processed as described above using endotoxin-free solutions. The DNA pellet was washed with 5 ml of endotoxin-free room-temperature 70% ethanol and re-suspended in 100 µl endotoxin-free Buffer TE and stored at -20 °C.

5.11 Digestion of endotoxin-free plasmids

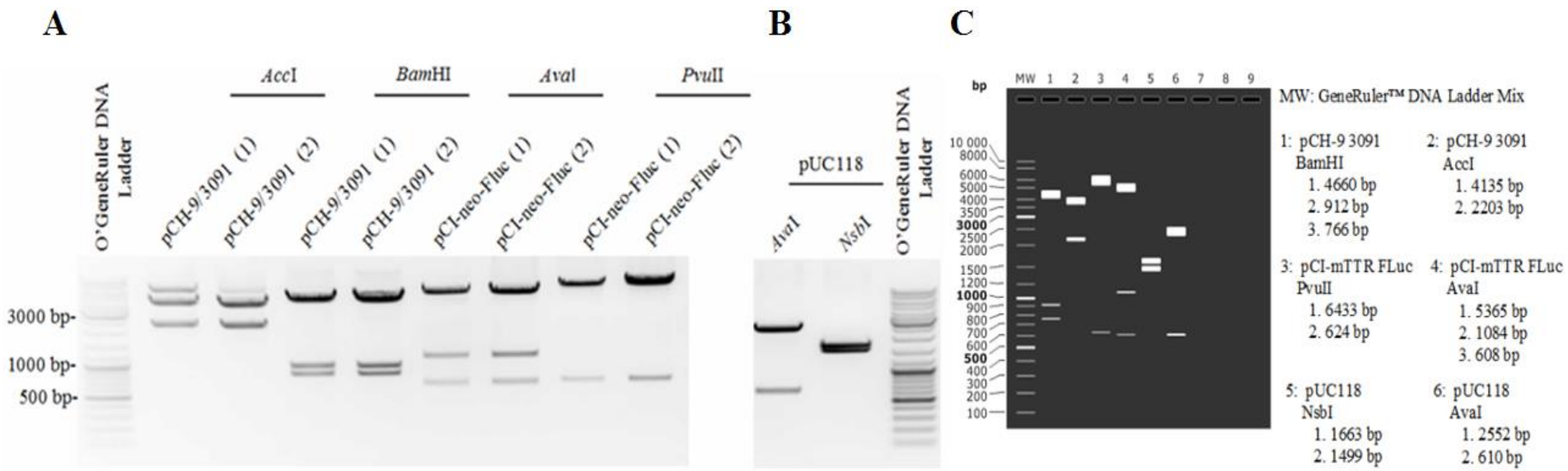

Figure 5.9: Restriction enzyme digestion of the marker and control endotoxin-free plasmids.

The endotoxin-free plasmids were screened before use. (**A**) The pCH-9/3091 plasmids were digested with *Bam*HI and *Acc*I while the pCI-neo-FLuc plasmids were digested with *Pvu*II and *Ava*I. Lane1: Molecular weight marker (O'GeneRuler DNA Ladder Mix). (**B**) The single negative control plasmid pUC118 was digested with *Nsb*I and *Ava*I. Lane 3: Molecular weight marker (O'GeneRuler DNA Ladder Mix). (**C**) **Simulated double digestion of marker, HBV and control plasmids**. A simulated 1% agarose gel was generated and indicates the expected fragment sizes for the digest of pCH-9/3091 with *Bam*HI (lane 1) and *Acc*I (lane 2), pCI-neo-FLuc with *Pvu*II (lane 3) and *Ava*I (lane 4) and pUC118 with *Nsb*I (lane 5) and *Ava*I (lane 6). The fragments sizes for each band are indicated on the right and the molecular weight marker (MW) is the O'GeneRuler DNA Ladder Mix.

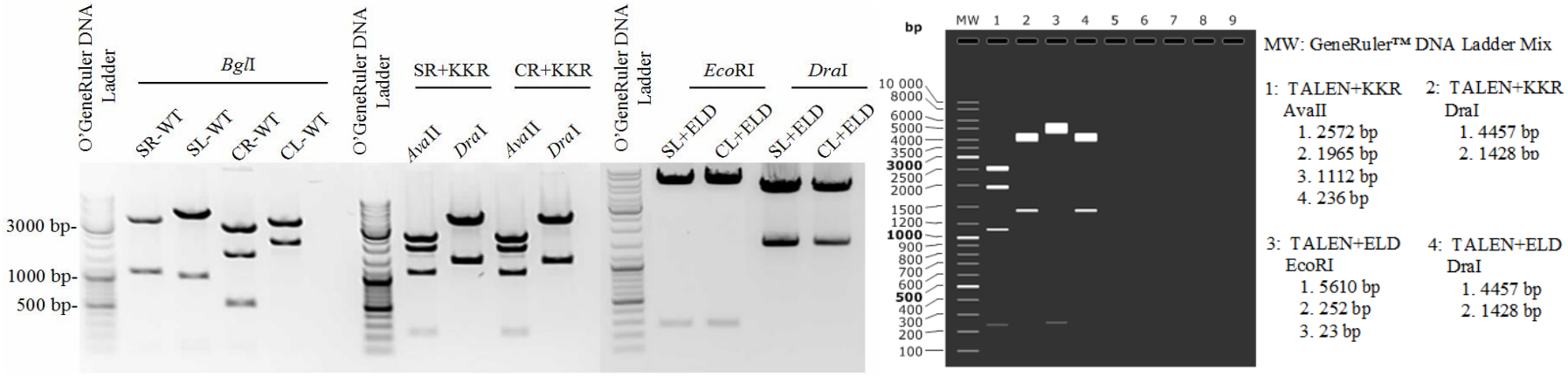

Figure 5.10: Screening of endotoxin-free wild-type and Sharkey TALEN plasmids.

The endotoxin-free plasmids were screened before use. (**A**) The monomers of the wild-type S and C TALENs were digested with *Bgl*I. The right Sharkey S and C TALEN monomer plasmids, SR+KKR and CR+KKR, were digested with *Ava*II and *Dra*I, while the left monomer plasmids, SL+ELD and CL+ELD, were digested with *Eco*RI and *Dra*I. Lane 1, 7 and 13: Molecular weight marker (O'GeneRuler DNA Ladder Mix). (**B**) **Simulated double digestion of Sharkey encoding plasmids**. A simulated 1% agarose gel was generated and indicates the expected fragment sizes for the digest of Sharkey S and C TALEN plasmids. The right S and C Sharkey TALEN monomers were digested with *Ava*II (lane 1) and *Dra*I (lane 2) while the left S and C Sharkey TALEN monomers were digested with *Eco*RI (lane 3) and *Dra*I (lane 4). The fragments sizes for each band are indicated on the right and the molecular weight marker is O'GeneRuler DNA Ladder Mix. SnapGene® software (from GSL Biotech; available at snapgene.com) was used to generate the simulated gel.

5.12 Ethics Certificate

STRICTLY CONFIDENTIAL

ANIMAL ETHICS SCREENING COMMITTEE (AESC)

CLEARANCE CERTIFICATE NO. 2016/11/45/B

APPLICANT: Ms P Singh

SCHOOL: Molecular Medicine and Haematology
DEPARTMENT:
LOCATION:

PROJECT TITLE: Inactivation of hepatitus virus (HBV) using heterodimeric transcription activator-like effector nucleases (TALENs) delivered by hydrodynamic injection to mice livers

Number and Species

60 3-5 week old NMRI Mice

Approval was given for the use of animals for the project described above at an AESC meeting held on 2016/11/29. This approval remains valid until 2019/01/30.
Unreported changes to the application may invalidate the clearance given by the AESC

The use of these animals is subject to AESC guidelines for the use and care of animals, is limited to the procedures described in the application form and is subject to any additional conditions listed below:

None

Signed: _____ (Chairperson, AESC) Date: 31/01/2017

I am satisfied that the persons listed in this application are competent to perform the procedures therein, in terms of Section 23 (1) (c) of the Veterinary and Para-Veterinary Professions Act (19 of 1982)

Signed: _____ (Registered Veterinarian) Date: 31-01-17

cc: Supervisor: Professor P Arbuthnot
Director: CAS

Works 2000/lain0015/AESCCert.wps

5.13 Simulated agarose gel showing double digestion of Sharkey encoding plasmids

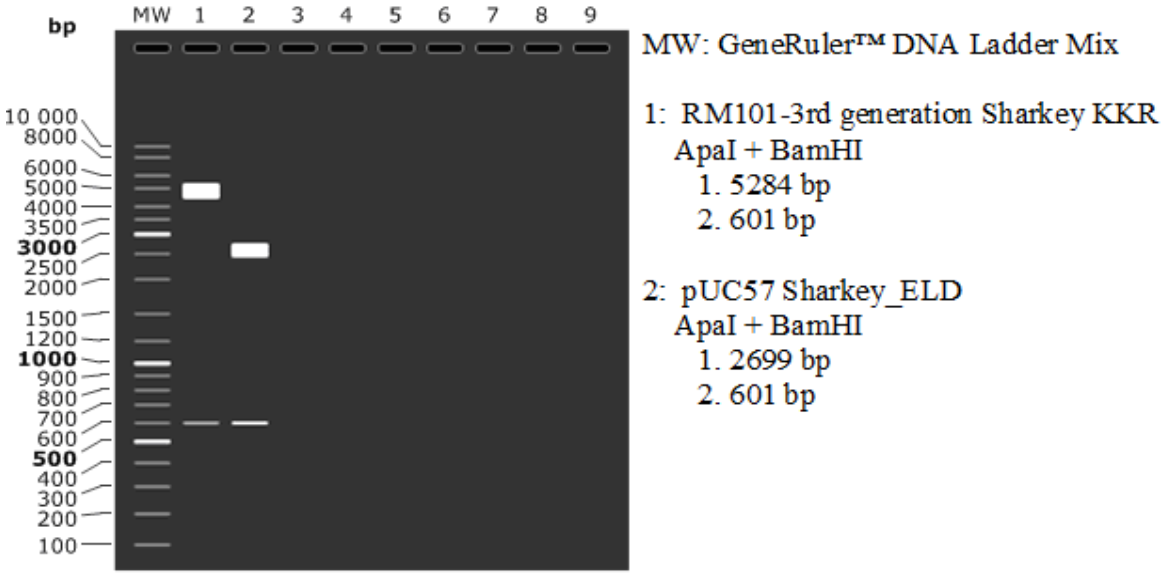

Figure 5.11: Simulated double digestion of Sharkey encoding plasmids.

A simulated 1% agarose gel was generated and indicates the expected fragment sizes for the double digest of RM101-3rd generation Sharkey KKR (the right Sharkey variant) and pUC57 Sharkey ELD (left Sharkey variant) with *Apa*I and *Bam*HI. The size of each band is indicated on the right and the molecular weight marker (MW) is the O'GeneRuler DNA Ladder Mix. SnapGene® software (from GSL Biotech; available at snapgene.com) was used to generate the simulated gel.

5.14 Transfection efficiency of anti-HBV TALENs in Huh 7 cells

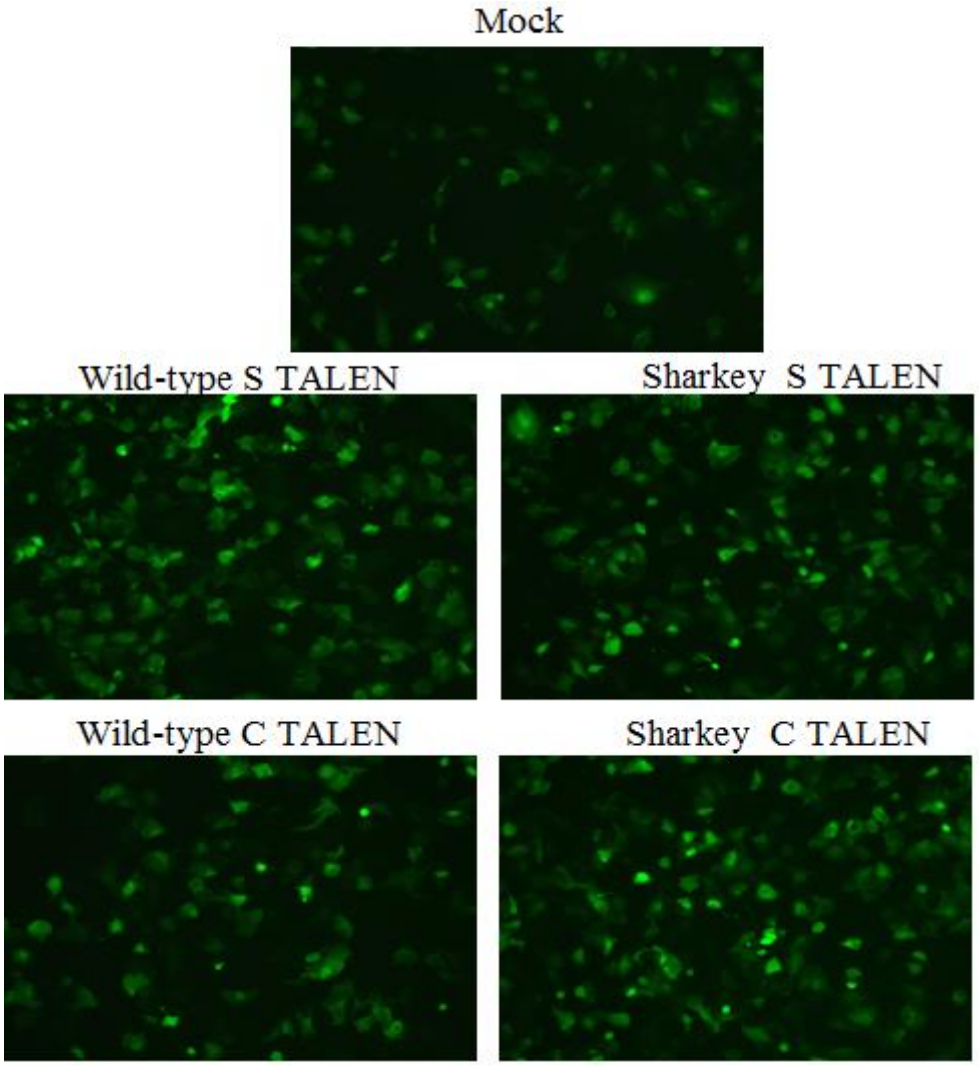

Figure 5. 12: Transfection efficiency of Sharkey and wild-type TALENs in Huh 7 cells.

Assessment of the transfection efficiency for ELISA was evaluated using the pCI-neo-eGFP plasmid. The pCI-neo-eGFP plasmid was included in the individual transfection mixes. GFP expression was visualised using fluorescence microscopy at 20× magnification

5.15 Transfection efficiency of anti-HBV TALENs in HepG2.2.15 cells

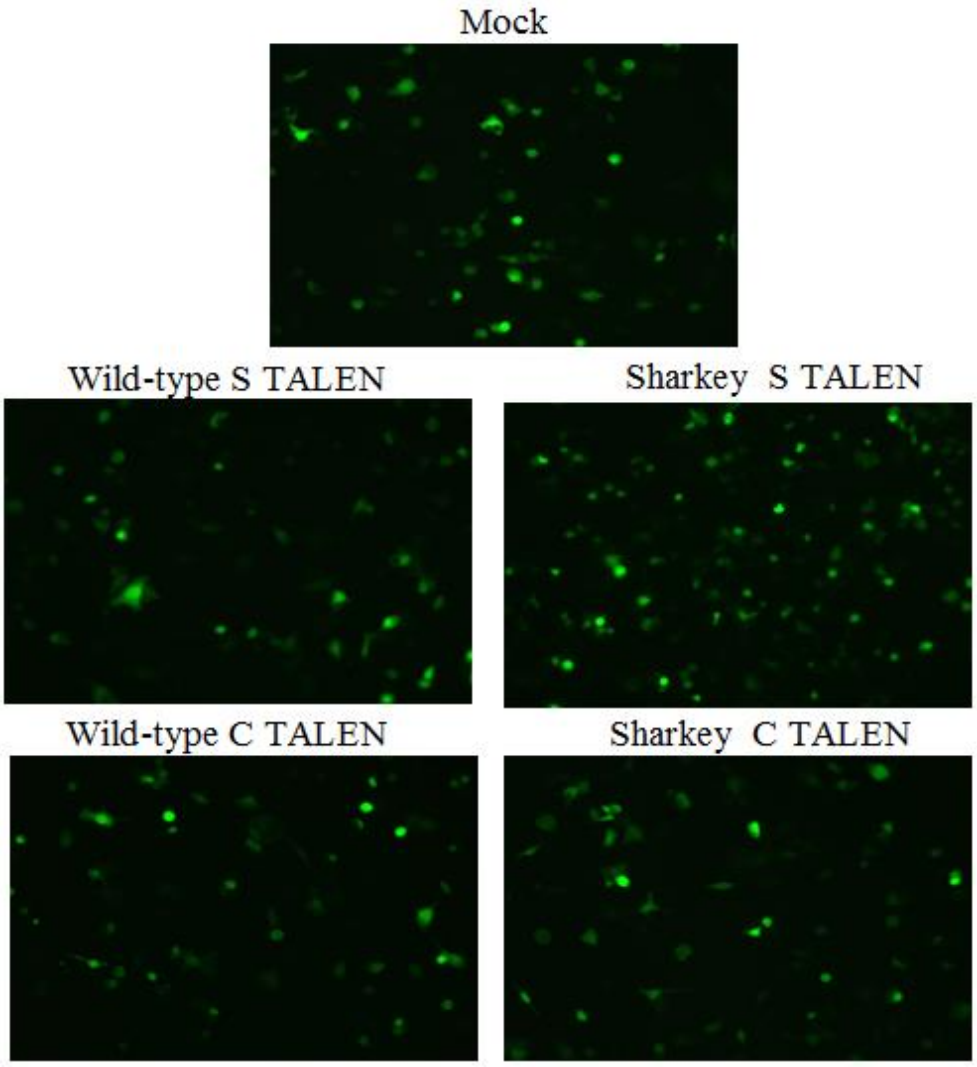

Figure 5. 13: Transfection efficiency of Sharkey and wild-type TALENs in HepG2.2.15 cells.

Assessment of the transfection efficiency in triple transfected HepG2.2.15 cells was evaluated by co-transfecting pCI-neo-eGFP. GFP expression was visualised 48 hours post-transfection using fluorescence microscopy at 20× magnification. The images represents day 14 of triple transfected HepG2.2.15 cells.

5.16 PCR amplification of sequences for the CelI assay

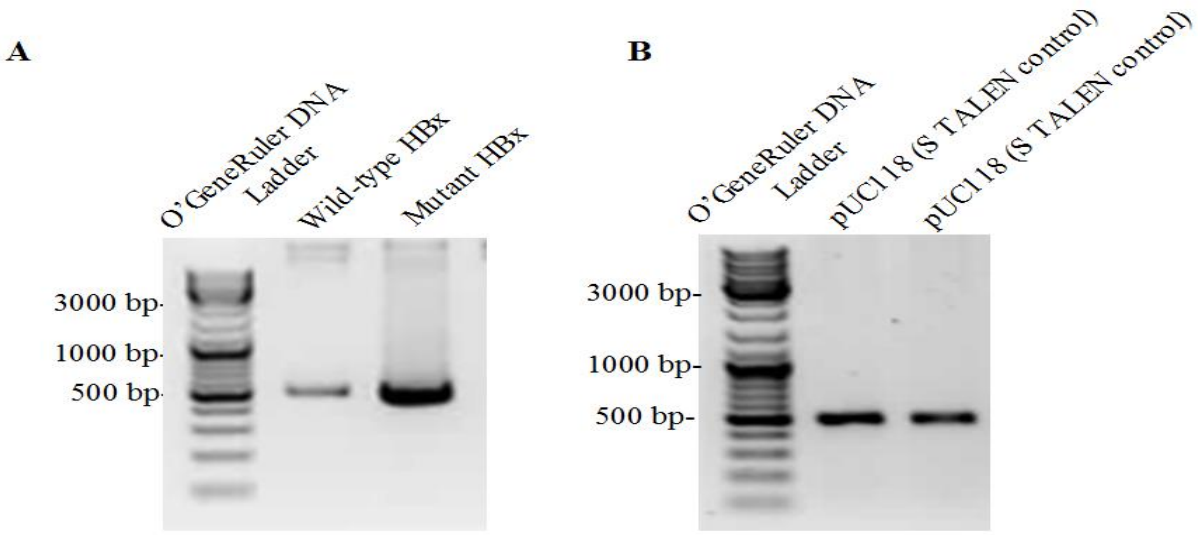

Figure 5.14: PCR amplification of the *HBx* positive control and target sites for S and C TALENs.

(**A**) The wild-type HBx as well as the mutant *HBx* sequence was PCR amplified. The amplicons produced the expected band of ~ 520 bp. The amplicons were mixed at equimolar concentrations and used in the CelI assays. Lane 1: O'GeneRuler DNA ladder. (**B**) HepG.2.2.15 cells were transfected in triplicate with the pUC118 plasmid which functioned as the mock (negative) control. Total DNA from HepG2.2.15 cells transfected with pUC118 plasmid were extracted and PCR amplification was carried out to amplify C and S TALEN targets sites. PCR amplicons produced the expected band of ~520 bp. Lane 1: O'GeneRuler DNA ladder.

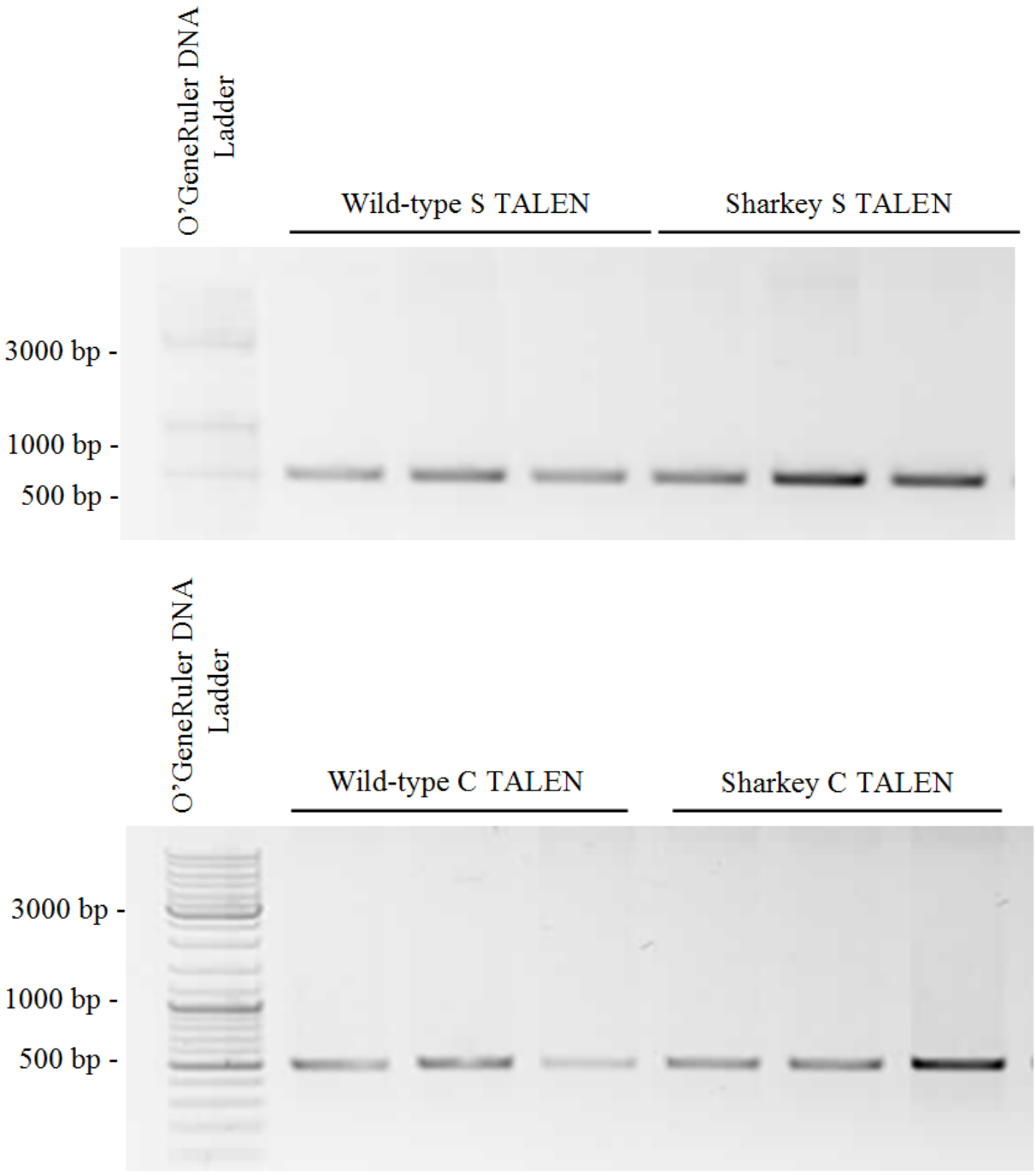

Figure 5.15: PCR amplification of S and C TALEN target site from experimental transfections.

HepG.2.2.15 cells were transfected in triplicate with the various anti-HBV TALEN plasmids. Total DNA from HepG2.2.15 cells transfected with Sharkey and wild-type TALENs were extracted and amplified. PCR amplification produced the expected band of ~520 bp. Lane 1: O'GeneRuler DNA ladder.

5.17 Transfection efficiency of anti-HBV TALENs in HEK293 cells

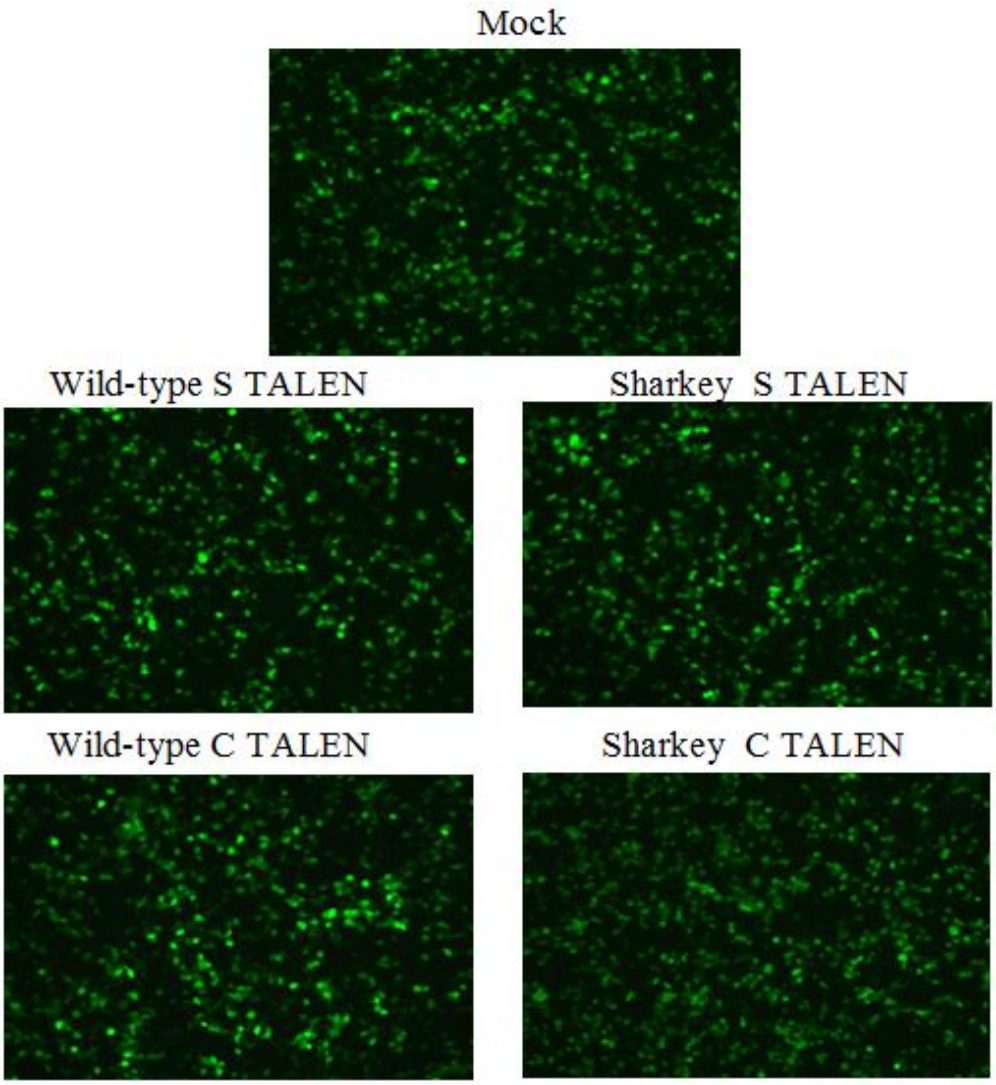

Figure 5.16: Transfection efficiency of Sharkey and wild-type TALENs in HEK 293 cells.

Assessment of the transfection efficiency for MTT assay was evaluated using the pCI-neo-eGFP plasmid. GFP expression was visualised using fluorescence microscopy at 20× magnification.

5.18 Detection of anti-HBV TALENs in vivo lack

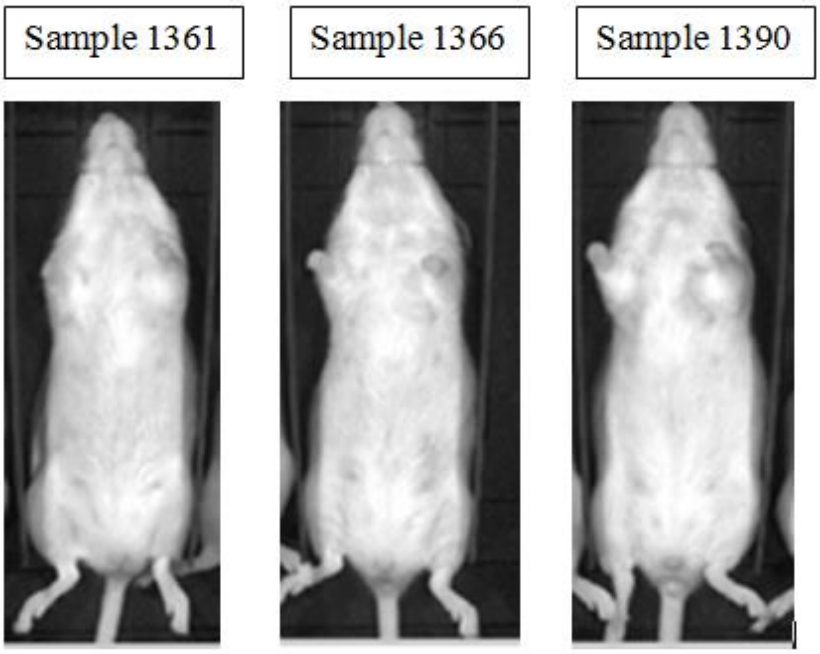

Figure 5.17: Delivery of anti-HBV TALENs in vivo.

Mice were hydrodynamically injected with the wild-type and Sharkey TALENs along with pCI-neo-FLuc that was used to assess and monitor delivery efficiency. Bioluminescence imaging was carried out 72 hours post injection. The lack of bioluminescence indicates delivery of the plasmids to the liver did not occur.

5.19 PCR amplification of in vivo sequences for the CelI assay

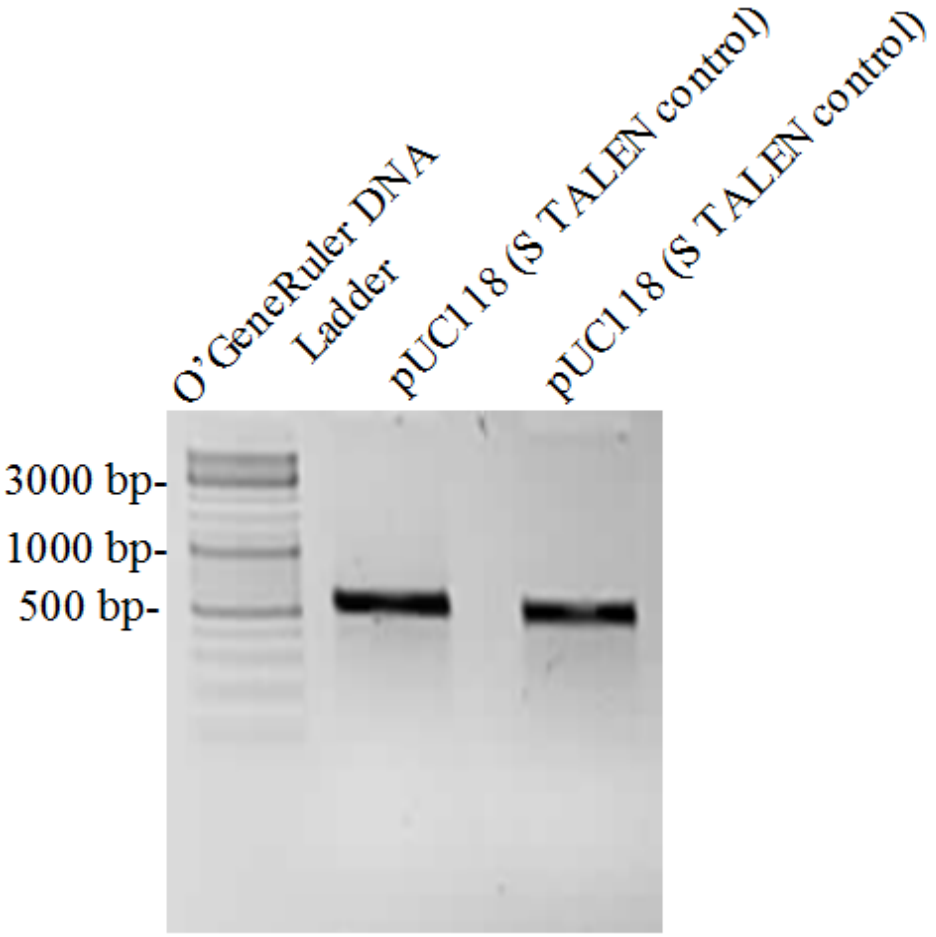

Figure 5.18: PCR amplification of the *HBx and pUC118* region in vitro.

Mice hydrodynamically injected with pUC118 plasmid served as the mock (negative) control. Total DNA from liver was extracted and PCR amplification of S and C TALEN targets sites was carried out. Lane 1: O'GeneRuler DNA ladder

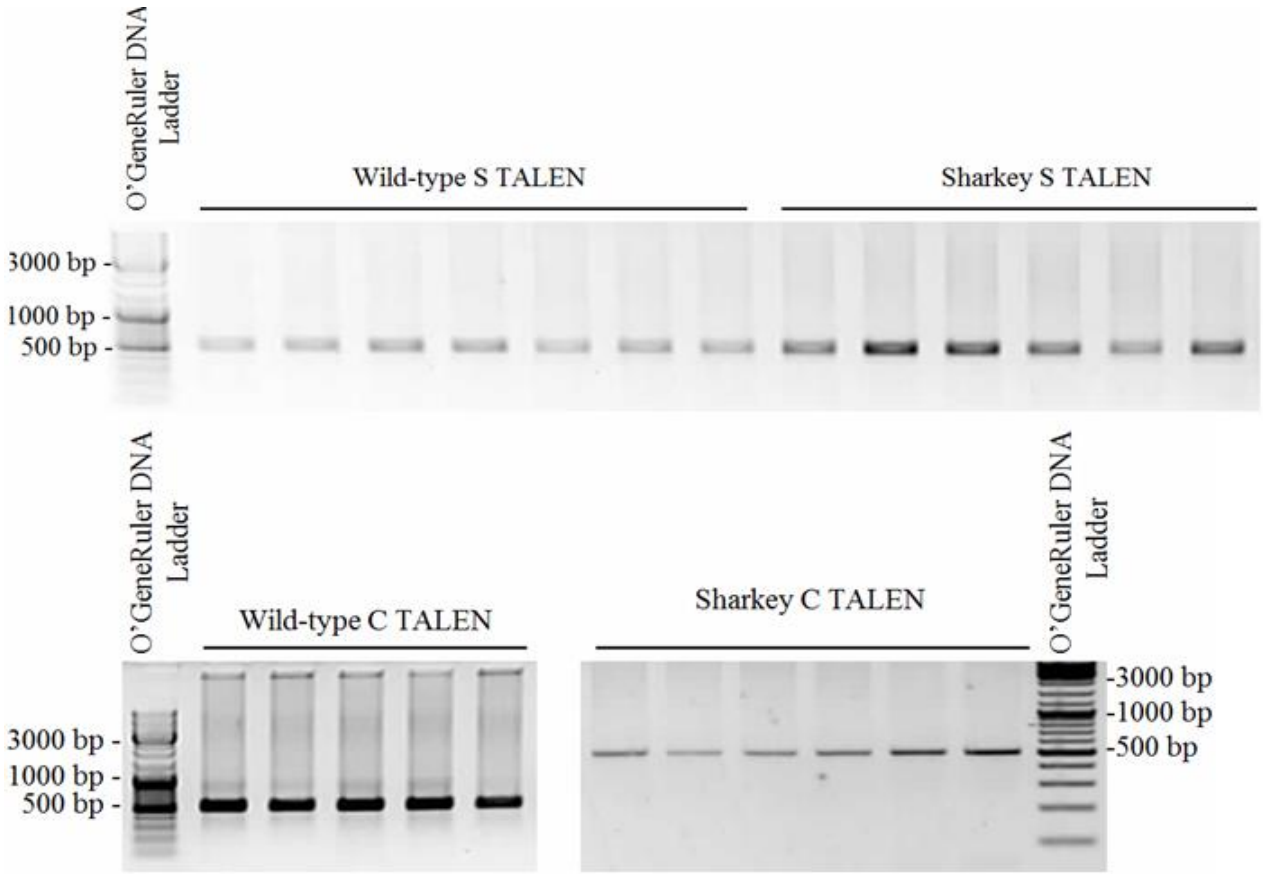

Figure 5.19: PCR amplification of S and C TALEN target site from experimental mice.

Total DNA from mouse livers treated with Sharkey and wild-type TALENs were extracted and S and C TALEN target sites amplified. PCR produced the expected band of ~520 bp. Lane 1: O'GeneRuler DNA ladder.

Chapter 6

6. References

ABRAMOFF, M., MAGALHAES, P. & RAM, S. 2004. Image processing with ImageJ. Biophotonics Int. 11: 36–42. *Google Scholar*.

ALLWEISS, L. & DANDRI, M. 2017. The role of cccDNA in HBV maintenance. *Viruses,* 9**,** 156.

AMITAI, G. & SOREK, R. 2016. CRISPR–Cas adaptation: insights into the mechanism of action. *Nature Reviews Microbiology,* 14**,** 67.

AUBERT, M., RYU, B. Y., BANKS, L., RAWLINGS, D. J., SCHARENBERG, A. M. & JEROME, K. R. 2011. Successful Targeting and Disruption of an Integrated Reporter Lentivirus Using the Engineered Homing Endonuclease Y2 I-Ani I. *PLoS One,* 6**,** e16825.

BECK, J. & NASSAL, M. 2007. Hepatitis B virus replication. *World journal of gastroenterology: WJG,* 13**,** 48.

BEERLI, R. R. & BARBAS, C. F. 2002. Engineering polydactyl zinc-finger transcription factors. *Nature biotechnology,* 20**,** 135-141.

BELFORT, M. & BONOCORA, R. P. 2014. Homing endonucleases: from genetic anomalies to programmable genomic clippers. *Homing Endonucleases.* Springer.

BESSESEN, M., IVES, D., CONDREAY, L., LAWRENCE, S. & SHERMAN, K. E. 1999. Chronic active hepatitis B exacerbations in human immunodeficiency virus-infected patients following development of resistance to or withdrawal of lamivudine. *Clinical infectious diseases,* 28**,** 1032-1035.

BETERAMS, G. & NASSAL, M. 2001. Significant interference with hepatitis B virus replication by a core-nuclease fusion protein. *Journal of Biological Chemistry,* 276**,** 8875-8883.

BIBIKOVA, M., CARROLL, D., SEGAL, D. J., TRAUTMAN, J. K., SMITH, J., KIM, Y.-G. & CHANDRASEGARAN, S. 2001. Stimulation of homologous recombination through targeted cleavage by chimeric nucleases. *Molecular and cellular biology,* 21**,** 289-297.

BITINAITE, J., WAH, D. A., AGGARWAL, A. K. & SCHILDKRAUT, I. 1998. FokI dimerization is required for DNA cleavage. *Proceedings of the national academy of sciences,* 95**,** 10570-10575.

BLOOM, K., ELY, A., MUSSOLINO, C., CATHOMEN, T. & ARBUTHNOT, P. 2013. Inactivation of hepatitis B virus replication in cultured cells and in vivo with engineered transcription activator-like effector nucleases. *Molecular Therapy,* 21**,** 1889-1897.

BLUM, H. E., GEROK, W. & VYAS, G. N. 1989. The molecular biology of hepatitis B virus. Elsevier.

BOCH, J., SCHOLZE, H., SCHORNACK, S., LANDGRAF, A., HAHN, S., KAY, S., LAHAYE, T., NICKSTADT, A. & BONAS, U. 2009. Breaking the code of DNA binding specificity of TAL-type III effectors. *Science,* 326**,** 1509-1512.

BOCK, C.-T., SCHRANZ, P., SCHRÖDER, C. H. & ZENTGRAF, H. 1994. Hepatitis B virus genome is organized into nucleosomes in the nucleus of the infected cell. *Virus genes,* 8**,** 215-229.

BOEKE, A., DOUMAS, P., REEVES, L., MCCLURG, K., BISCHOF, D., SEGO, L., AUBERRY, A., TATIKONDA, M. & CORNETTA, K. 2013. Vector production in an academic environment: a tool to assess production costs. *Human gene therapy methods,* 24**,** 49-57.

BOUARD, D., ALAZARD-DANY, N. & COSSET, F. L. 2009. Viral vectors: from virology to transgene expression. *British journal of pharmacology,* 157**,** 153-165.

BURGER, C., GORBATYUK, O. S., VELARDO, M. J., PEDEN, C. S., WILLIAMS, P., ZOLOTUKHIN, S., REIER, P. J., MANDEL, R. J. & MUZYCZKA, N. 2004. Recombinant AAV viral vectors pseudotyped with viral capsids from serotypes 1, 2, and 5 display differential efficiency and cell tropism after delivery to different regions of the central nervous system. *Molecular Therapy,* 10**,** 302-317.

CENCIC, R., MIURA, H., MALINA, A., ROBERT, F., ETHIER, S., SCHMEING, T. M., DOSTIE, J. & PELLETIER, J. 2014. Protospacer adjacent motif (PAM)-distal sequences engage CRISPR Cas9 DNA target cleavage. *PloS one,* 9**,** e109213.

CERMAK, T., DOYLE, E. L., CHRISTIAN, M., WANG, L., ZHANG, Y., SCHMIDT, C., BALLER, J. A., SOMIA, N. V., BOGDANOVE, A. J. & VOYTAS, D. F. 2011. Efficient design and assembly of custom TALEN and other TAL effector-based constructs for DNA targeting. *Nucleic acids research,* 39**,** e82-e82.

CHANDRASEGARAN, S. & CARROLL, D. 2016. Origins of programmable nucleases for genome engineering. *Journal of molecular biology,* 428**,** 963-989.

CHEN, J., ZHANG, W., LIN, J., WANG, F., WU, M., CHEN, C., ZHENG, Y., PENG, X., LI, J. & YUAN, Z. 2014. An efficient antiviral strategy for targeting hepatitis B virus

genome using transcription activator-like effector nucleases. *Molecular Therapy,* 22**,** 303-311.

CHENG, X., GUAN, W., SUN, S., LI, B., LI, H., KANG, F., KANG, J., YANG, D., NASSAL, M. & SUN, D. 2015. Stable Human Hepatoma Cell Lines for Efficient Regulated Expression of Nucleoside/Nucleotide Analog Resistant and Vaccine Escape Hepatitis B Virus Variants and Woolly Monkey Hepatitis B Virus. *PloS one,* 10**,** e0145746.

CHEVALIER, B. S., MONNAT JR, R. J. & STODDARD, B. L. 2001. The homing endonuclease I-CreI uses three metals, one of which is shared between the two active sites. *Nature Structural and Molecular Biology,* 8**,** 312.

CHO, S. W., KIM, S., KIM, Y., KWEON, J., KIM, H. S., BAE, S. & KIM, J.-S. 2014. Analysis of off-target effects of CRISPR/Cas-derived RNA-guided endonucleases and nickases. *Genome research,* 24**,** 132-141.

CHRISTIAN, M. L., DEMOREST, Z. L., STARKER, C. G., OSBORN, M. J., NYQUIST, M. D., ZHANG, Y., CARLSON, D. F., BRADLEY, P., BOGDANOVE, A. J. & VOYTAS, D. F. 2012. Targeting G with TAL effectors: a comparison of activities of TALENs constructed with NN and NK repeat variable di-residues. *PloS one,* 7**,** e45383.

CONG, L., ZHOU, R., KUO, Y.-C., CUNNIFF, M. & ZHANG, F. 2012. Comprehensive interrogation of natural TALE DNA-binding modules and transcriptional repressor domains. *Nature communications,* 3**,** 968.

CRADICK, T. J., KECK, K., BRADSHAW, S., JAMIESON, A. C. & MCCAFFREY, A. P. 2010. Zinc-finger nucleases as a novel therapeutic strategy for targeting hepatitis B virus DNAs. *Molecular Therapy,* 18**,** 947-954.

DANDRI, M. & PETERSEN, J. 2016. Mechanism of hepatitis B virus persistence in hepatocytes and its carcinogenic potential. *Clinical Infectious Diseases,* 62**,** S281-S288.

DAVIS, H. L., MCCLUSKIE, M. J., GERIN, J. L. & PURCELL, R. H. 1996. *DNA vaccine for hepatitis B: evidence for immunogenicity in chimpanzees and comparison with other vaccines* [Online]. [Accessed 14 93].

DE FRANCHIS, R., MEUCCI, G., VECCHI, M., TATARELLA, M., COLOMBO, M., DEL NINNO, E., RUMI, M. G., DONATO, M. F. & RONCHI, G. 1993. The natural history of asymptomatic hepatitis B surface antigen carriers. *Annals of internal medicine,* 118**,** 191-194.

DELAVAL, K. & FEIL, R. 2004. Epigenetic regulation of mammalian genomic imprinting. *Current opinion in genetics & development,* 14**,** 188-195.

DIGIUSTO, D. L., CANNON, P. M., HOLMES, M. C., LI, L., RAO, A., WANG, J., LEE, G., GREGORY, P. D., KIM, K. A. & HAYWARD, S. B. 2016. Preclinical development and qualification of ZFN-mediated CCR5 disruption in human hematopoietic stem/progenitor cells. *Molecular Therapy-Methods & Clinical Development,* 3.

DONG, C., QU, L., WANG, H., WEI, L., DONG, Y. & XIONG, S. 2015. Targeting hepatitis B virus cccDNA by CRISPR/Cas9 nuclease efficiently inhibits viral replication. *Antiviral research,* 118**,** 110-117.

DOYON, Y., VO, T. D., MENDEL, M. C., GREENBERG, S. G., WANG, J., XIA, D. F., MILLER, J. C., URNOV, F. D., GREGORY, P. D. & HOLMES, M. C. 2011. Enhancing zinc-finger-nuclease activity with improved obligate heterodimeric architectures. *Nature methods,* 8**,** 74-79.

DUDÁŠ, A. & CHOVANEC, M. 2004. DNA double-strand break repair by homologous recombination. *Mutation Research/Reviews in Mutation Research,* 566**,** 131-167.

DURAI, S., MANI, M., KANDAVELOU, K., WU, J., PORTEUS, M. H. & CHANDRASEGARAN, S. 2005. Zinc finger nucleases: custom-designed molecular scissors for genome engineering of plant and mammalian cells. *Nucleic acids research,* 33**,** 5978-5990.

DURANTEL, D. & ZOULIM, F. 2016. New antiviral targets for innovative treatment concepts for hepatitis B virus and hepatitis delta virus. *Journal of hepatology,* 64**,** S117-S131.

EHRKE-SCHULZ, E., BERGMANN, T., SCHIWON, M., DOERNER, J., SAYDAMINOVA, K., LIEBER, A. & EHRHARDT, A. 2016. Quantification of designer nuclease induced mutation rates: a direct comparison of different methods. *Molecular Therapy-Methods & Clinical Development,* 3.

ELIZALDE, M. M., SEVIC, I., LEDESMA, M. M. G. L., CAMPOS, R. H., BARBINI, L. & FLICHMAN, D. M. 2018. Human hepatocytes apoptosis induced by replication of hepatitis B virus subgenotypes F1b and F4: Role of basal core promoter and preCore mutations. *Virology,* 513**,** 160-167.

ELY, A. & ARBUTHNOT, P. 2010. Advances in the Use of RNAi to Treat Chronic Hepatitis B Virus Infection. *RNA Interference and Viruses: Current Innovations and Future Trends***,** 143.

FINE, E. J., CRADICK, T. J., ZHAO, C. L., LIN, Y. & BAO, G. 2013. An online bioinformatics tool predicts zinc finger and TALE nuclease off-target cleavage. *Nucleic acids research,* 42**,** e42-e42.

FU, Y., FODEN, J. A., KHAYTER, C., MAEDER, M. L., REYON, D., JOUNG, J. K. & SANDER, J. D. 2013. High-frequency off-target mutagenesis induced by CRISPR-Cas nucleases in human cells. *Nature biotechnology,* 31**,** 822.

FU, Y., SANDER, J. D., REYON, D., CASCIO, V. M. & JOUNG, J. K. 2014. Improving CRISPR-Cas nuclease specificity using truncated guide RNAs. *Nature biotechnology,* 32**,** 279.

GABRIEL, R., LOMBARDO, A., ARENS, A., MILLER, J. C., GENOVESE, P., KAEPPEL, C., NOWROUZI, A., BARTHOLOMAE, C. C., WANG, J. & FRIEDMAN, G. 2011. An unbiased genome-wide analysis of zinc-finger nuclease specificity. *Nature biotechnology,* 29**,** 816.

GAJ, T., GERSBACH, C. A. & BARBAS III, C. F. 2013. ZFN, TALEN, and CRISPR/Cas-based methods for genome engineering. *Trends in biotechnology,* 31**,** 397-405.

GLEBE, D. & URBAN, S. 2007. Viral and cellular determinants involved in hepadnaviral entry. *World journal of gastroenterology: WJG,* 13**,** 22.

GRAY, S. J., WOODARD, K. T. & SAMULSKI, R. J. 2010. Viral vectors and delivery strategies for CNS gene therapy. *Therapeutic delivery,* 1**,** 517-534.

GUILINGER, J. P., PATTANAYAK, V., REYON, D., TSAI, S. Q., SANDER, J. D., JOUNG, J. K. & LIU, D. R. 2014. Broad specificity profiling of TALENs results in engineered nucleases with improved DNA-cleavage specificity. *Nature methods,* 11**,** 429.

GUO, H., XU, C., ZHOU, T., BLOCK, T. M. & GUO, J.-T. 2012. Characterization of the host factors required for hepadnavirus covalently closed circular (ccc) DNA formation. *PloS one,* 7**,** e43270.

GUO, J., GAJ, T. & BARBAS, C. F. 2010. Directed evolution of an enhanced and highly efficient FokI cleavage domain for zinc finger nucleases. *Journal of molecular biology,* 400**,** 96-107.

GUSCHIN, D. Y., WAITE, A. J., KATIBAH, G. E., MILLER, J. C., HOLMES, M. C. & REBAR, E. J. 2010. A rapid and general assay for monitoring endogenous gene modification. *Engineered zinc finger proteins.* Springer.

HALFORD, S. E., CATTO, L. E., PERNSTICH, C., RUSLING, D. A. & SANDERS, K. L. 2011. The reaction mechanism of FokI excludes the possibility of targeting zinc finger nucleases to unique DNA sites. Portland Press Limited.

HELER, R., MARRAFFINI, L. A. & BIKARD, D. 2014. Adapting to new threats: the generation of memory by CRISPR-Cas immune systems. *Molecular microbiology,* 93**,** 1-9.

HESLOP, H. E., BRENNER, M. K., ROONEY, C., KRANCE, R. A., ROBERTS, W. M., ROCHESTER, R., SMITH, C. A., TURNER, V., SIXBEY, J. & MOEN, R. 1994. Administration of Neomycin Resistance Gene Marked EBV Specific Cytotoxic T Lymphocytes to Recipients of Mismatched-Related or Phenotypically Similar Unrelated Donor Marrow Grafts. St. Jude Children's Research Hospital, Memphis, Tennesse. *Human gene therapy,* 5**,** 381-397.

HILLE, F. & CHARPENTIER, E. 2016. CRISPR-Cas: biology, mechanisms and relevance. *Phil. Trans. R. Soc. B,* 371**,** 20150496.

HILLEGASS, J. M., SHUKLA, A., LATHROP, S. A., MACPHERSON, M. B., FUKAGAWA, N. K. & MOSSMAN, B. T. 2010. Assessing nanotoxicity in cells in vitro. *Wiley Interdisciplinary Reviews: Nanomedicine and Nanobiotechnology,* 2**,** 219-231.

HOEKSEMA, K. A. & TYRRELL, D. L. J. 2010. Inhibition of viral transcription using designed zinc finger proteins. *Engineered Zinc Finger Proteins.* Springer.

HOLKERS, M., CATHOMEN, T. & GONÇALVES, M. A. 2014. Construction and characterization of adenoviral vectors for the delivery of TALENs into human cells. *Methods,* 69**,** 179-187.

HOWARTH, J. L., LEE, Y. B. & UNEY, J. B. 2010. Using viral vectors as gene transfer tools (Cell Biology and Toxicology Special Issue: ETCS-UK 1 day meeting on genetic manipulation of cells). *Cell biology and toxicology,* 26**,** 1-20.

HSU, P. D., LANDER, E. S. & ZHANG, F. 2014. Development and applications of CRISPR-Cas9 for genome engineering. *Cell,* 157**,** 1262-1278.

HUY, T. T. T., NGOC, T. T. & ABE, K. 2008. New complex recombinant genotype of hepatitis B virus identified in Vietnam. *Journal of virology,* 82**,** 5657-5663.

HWANG, W. Y., FU, Y., REYON, D., MAEDER, M. L., TSAI, S. Q., SANDER, J. D., PETERSON, R. T., YEH, J. J. & JOUNG, J. K. 2013. Efficient genome editing in zebrafish using a CRISPR-Cas system. *Nature biotechnology,* 31**,** 227.

JACKSON, S. P. & BARTEK, J. 2009. The DNA-damage response in human biology and disease. *Nature,* 461**,** 1071.

JANKELE, R. & SVOBODA, P. 2014. TAL effectors: tools for DNA targeting. *Briefings in functional genomics,* 13**,** 409-419.

JASIN, M. & ROTHSTEIN, R. 2013. Repair of strand breaks by homologous recombination. *Cold Spring Harbor perspectives in biology,* 5**,** a012740.

JIANG, W., BIKARD, D., COX, D., ZHANG, F. & MARRAFFINI, L. A. 2013. RNA-guided editing of bacterial genomes using CRISPR-Cas systems. *Nature biotechnology,* 31**,** 233.

JINEK, M., CHYLINSKI, K., FONFARA, I., HAUER, M., DOUDNA, J. A. & CHARPENTIER, E. 2012. A programmable dual-RNA–guided DNA endonuclease in adaptive bacterial immunity. *science***,** 1225829.

KANDAVELOU, K., MANI, M., DURAI, S. & CHANDRASEGARAN, S. 2005. 'Magic'scissors for genome surgery. *Nature biotechnology,* 23**,** 686-687.

KARRAN, P. 2000. DNA double strand break repair in mammalian cells. *Current opinion in genetics & development,* 10**,** 144-150.

KHANNA, K. K. & JACKSON, S. P. 2001. DNA double-strand breaks: signaling, repair and the cancer connection. *Nature genetics,* 27**,** 247.

KIM, H. & KIM, J.-S. 2014. A guide to genome engineering with programmable nucleases. *Nature Reviews Genetics,* 15**,** 321-334.

KIM, Y.-G., CHA, J. & CHANDRASEGARAN, S. 1996. Hybrid restriction enzymes: zinc finger fusions to Fok I cleavage domain. *Proceedings of the National Academy of Sciences,* 93**,** 1156-1160.

KLUG, A. 2010. The discovery of zinc fingers and their applications in gene regulation and genome manipulation. *Annual review of biochemistry,* 79**,** 213-231.

KO, C., SHIN, Y.-C., PARK, W.-J., KIM, S., KIM, J. & RYU, W.-S. 2014. Residues Arg703, Asp777, and Arg781 of the RNase H domain of hepatitis B virus polymerase are critical for viral DNA synthesis. *Journal of virology,* 88**,** 154-163.

KÖCK, J., RÖSLER, C., ZHANG, J.-J., BLUM, H. E., NASSAL, M. & THOMA, C. 2010. Generation of covalently closed circular DNA of hepatitis B viruses via intracellular recycling is regulated in a virus specific manner. *PLoS pathogens,* 6**,** e1001082.

KÖNIGER, C., WINGERT, I., MARSMANN, M., RÖSLER, C., BECK, J. & NASSAL, M. 2014. Involvement of the host DNA-repair enzyme TDP2 in formation of the covalently closed circular DNA persistence reservoir of hepatitis B viruses. *Proceedings of the National Academy of Sciences,* 111**,** E4244-E4253.

KOO, T., LEE, J. & KIM, J.-S. 2015. Measuring and reducing off-target activities of programmable nucleases including CRISPR-Cas9. *Molecules and cells,* 38**,** 475.

KUHN, E. J. & GEYER, P. K. 2003. Genomic insulators: connecting properties to mechanism. *Current opinion in cell biology,* 15**,** 259-265.

KUMAR, S. & NUSSINOV, R. 2002. Close-range electrostatic interactions in proteins. *ChemBioChem,* 3**,** 604-617.

KUSCU, C., ARSLAN, S., SINGH, R., THORPE, J. & ADLI, M. 2014. Genome-wide analysis reveals characteristics of off-target sites bound by the Cas9 endonuclease. *Nature biotechnology,* 32**,** 677.

LAGO, B. V., MELLO, F. C., KRAMVIS, A., NIEL, C. & GOMES, S. A. 2014. Hepatitis B virus subgenotype A1: evolutionary relationships between Brazilian, African and Asian isolates. *PLoS One,* 9**,** e105317.

LAI, C.-L., WONG, D., IP, P., KOPANISZEN, M., SETO, W.-K., FUNG, J., HUANG, F.-Y., LEE, B. P., CULLARO, G. & WU, C. H. 2014. Profound reduction of HBV covalently closed circular DNA with long-term nucleoside/tide analogue therapy. *Hepatology*.

LEE, C. M., CRADICK, T. J., FINE, E. J. & BAO, G. 2016. Nuclease target site selection for maximizing on-target activity and minimizing off-target effects in genome editing. *Molecular Therapy,* 24**,** 475-487.

LEMOINE, M., NAYAGAM, S. & THURSZ, M. 2013. Viral hepatitis in resource-limited countries and access to antiviral therapies: current and future challenges. *Future virology,* 8**,** 371-380.

LI, J.-F., NORVILLE, J. E., AACH, J., MCCORMACK, M., ZHANG, D., BUSH, J., CHURCH, G. M. & SHEEN, J. 2013. Multiplex and homologous recombination–mediated genome editing in Arabidopsis and Nicotiana benthamiana using guide RNA and Cas9. *Nature biotechnology,* 31**,** 688.

LIANG, T. J. 2009. Hepatitis B: the virus and disease. *Hepatology,* 49.

LIEBER, M. R., MA, Y., PANNICKE, U. & SCHWARZ, K. 2003. Mechanism and regulation of human non-homologous DNA end-joining. *Nature reviews Molecular cell biology,* 4**,** 712.

LIN, S.-R., YANG, H.-C., KUO, Y.-T., LIU, C.-J., YANG, T.-Y., SUNG, K.-C., LIN, Y.-Y., WANG, H.-Y., WANG, C.-C. & SHEN, Y.-C. 2014. The CRISPR/Cas9 system facilitates clearance of the intrahepatic HBV templates in vivo. *Molecular Therapy-Nucleic Acids,* 3.

LIPPOW, S. M., AHA, P. M., PARKER, M. H., BLAKE, W. J., BAYNES, B. M. & LIPOVŠEK, D. 2009. Creation of a type IIS restriction endonuclease with a long recognition sequence. *Nucleic acids research,* 37**,** 3061-3073.

LOZANO, R., NAGHAVI, M., FOREMAN, K., LIM, S., SHIBUYA, K., ABOYANS, V., ABRAHAM, J., ADAIR, T., AGGARWAL, R. & AHN, S. Y. 2013. Global and

regional mortality from 235 causes of death for 20 age groups in 1990 and 2010: a systematic analysis for the Global Burden of Disease Study 2010. *The Lancet,* 380**,** 2095-2128.

MANICKAN, E., YU, Z., ROUSE, R. J., WIRE, W. S. & ROUSE, B. T. 1995. Induction of protective immunity against herpes simplex virus with DNA encoding the immediate early protein ICP 27. *Viral immunology,* 8**,** 53-61.

MARION, P. L. & ROBINSON, W. S. 1983. Hepadna viruses: hepatitis B and related viruses. *Current topics in microbiology and immunology.* Springer.

MCGLYNN, K. A., TSAO, L., HSING, A. W., DEVESA, S. S. & FRAUMENI, J. F. 2001. International trends and patterns of primary liver cancer. *International Journal of Cancer,* 94**,** 290-296.

MEKLER, V., MINAKHIN, L. & SEVERINOV, K. 2017. Mechanism of duplex DNA destabilization by RNA-guided Cas9 nuclease during target interrogation. *Proceedings of the National Academy of Sciences***,** 201619926.

MILLER, J. C., HOLMES, M. C., WANG, J., GUSCHIN, D. Y., LEE, Y.-L., RUPNIEWSKI, I., BEAUSEJOUR, C. M., WAITE, A. J., WANG, N. S. & KIM, K. A. 2007. An improved zinc-finger nuclease architecture for highly specific genome editing. *Nature biotechnology,* 25**,** 778-785.

MILLER, R. H. & ROBINSON, W. S. 1984. Hepatitis B virus DNA forms in nuclear and cytoplasmic fractions of infected human liver. *Virology,* 137**,** 390-399.

MOOLLA, N., KEW, M. & ARBUTHNOT, P. 2002. Regulatory elements of hepatitis B virus transcription. *Journal of viral hepatitis,* 9**,** 323-331.

MOSCOU, M. J. & BOGDANOVE, A. J. 2009. A simple cipher governs DNA recognition by TAL effectors. *Science,* 326**,** 1501-1501.

MUSSOLINO, C., MORBITZER, R., LÜTGE, F., DANNEMANN, N., LAHAYE, T. & CATHOMEN, T. 2011. A novel TALE nuclease scaffold enables high genome editing activity in combination with low toxicity. *Nucleic acids research,* 39**,** 9283-9293.

NASSAL, M. 2008. Hepatitis B viruses: reverse transcription a different way. *Virus research,* 134**,** 235-249.

NEWBOLD, J. E., XIN, H., TENCZA, M., SHERMAN, G., DEAN, J., BOWDEN, S. & LOCARNINI, S. 1995. The covalently closed duplex form of the hepadnavirus genome exists in situ as a heterogeneous population of viral minichromosomes. *Journal of virology,* 69**,** 3350-3357.

ORII, K. E., LEE, Y., KONDO, N. & MCKINNON, P. J. 2006. Selective utilization of nonhomologous end-joining and homologous recombination DNA repair pathways

during nervous system development. *Proceedings of the National Academy of Sciences,* 103**,** 10017-10022.

PABO, C. O., PEISACH, E. & GRANT, R. A. 2001. Design and selection of novel Cys2His2 zinc finger proteins. *Annual review of biochemistry,* 70**,** 313-340.

PARK, P. J. 2009. ChIP–seq: advantages and challenges of a maturing technology. *Nature Reviews Genetics,* 10**,** 669.

PASSMAN, M., WEINBERG, M., KEW, M. & ARBUTHNOT, P. 2000. In situ demonstration of inhibitory effects of hammerhead ribozymes that are targeted to the hepatitis Bx sequence in cultured cells. *Biochemical and biophysical research communications,* 268**,** 728-733.

PATTANAYAK, V., LIN, S., GUILINGER, J. P., MA, E., DOUDNA, J. A. & LIU, D. R. 2013. High-throughput profiling of off-target DNA cleavage reveals RNA-programmed Cas9 nuclease specificity. *Nature biotechnology,* 31**,** 839.

PATTANAYAK, V., RAMIREZ, C. L., JOUNG, J. K. & LIU, D. R. 2011. Revealing off-target cleavage specificities of zinc-finger nucleases by in vitro selection. *Nature methods,* 8**,** 765.

PEREZ, E. E., WANG, J., MILLER, J. C., JOUVENOT, Y., KIM, K. A., LIU, O., WANG, N., LEE, G., BARTSEVICH, V. V. & LEE, Y.-L. 2008. Establishment of HIV-1 resistance in CD4+ T cells by genome editing using zinc-finger nucleases. *Nature biotechnology,* 26**,** 808.

PILLAY, L. M., SELLAND, L. G., FLEISCH, V. C., LEIGHTON, P. L., CHENG, C. S., FAMULSKI, J. K., RITZEL, R. G., MARCH, L. D., WANG, H. & ALLISON, W. T. 2013. Evaluating the mutagenic activity of targeted endonucleases containing a Sharkey FokI cleavage domain variant in zebrafish. *zebrafish,* 10**,** 353-364.

PINGOUD, A. & JELTSCH, A. 2001. Structure and function of type II restriction endonucleases. *Nucleic acids research,* 29**,** 3705-3727.

PINGOUD, A. & SILVA, G. H. 2007. Precision genome surgery. *Nature biotechnology,* 25**,** 743.

POURKARIM, M. R., AMINI-BAVIL-OLYAEE, S., KURBANOV, F., VAN RANST, M. & TACKE, F. 2014. Molecular identification of hepatitis B virus genotypes/subgenotypes: revised classification hurdles and updated resolutions. *World journal of gastroenterology: WJG,* 20**,** 7152.

QASIM, W., ZHAN, H., SAMARASINGHE, S., ADAMS, S., AMROLIA, P., STAFFORD, S., BUTLER, K., RIVAT, C., WRIGHT, G. & SOMANA, K. 2017. Molecular

remission of infant B-ALL after infusion of universal TALEN gene-edited CAR T cells. *Science translational medicine,* 9**,** eaaj2013.

REARDON, S. 2016. First CRISPR clinical trial gets green light from US panel. *Nature News*.

REIK, A., ZHOU, Y., WAGNER, J., HAMLETT, A., MENDEL, M., LIU, P.-Q., LEE, G., PASCHON, D., REBAR, E. & ANDO, D. 2008. Zinc finger nucleases targeting the glucocorticoid receptor allow IL-13 zetakine transgenic CTLs to kill glioblastoma cells in vivo in the presence of immunosuppressing glucocorticoids. AACR.

REVILL, P. & LOCARNINI, S. 2016. Antiviral strategies to eliminate hepatitis B virus covalently closed circular DNA (cccDNA). *Current opinion in pharmacology,* 30**,** 144-150.

RITTIÉ, L. & PERBAL, B. 2008. Enzymes used in molecular biology: a useful guide. *Journal of cell communication and signaling,* 2**,** 25-45.

ROJO, F. 2001. Mechanisms of transcriptional repression. *Current opinion in microbiology,* 4**,** 145-151.

SANDER, J. D. & JOUNG, J. K. 2014. CRISPR-Cas systems for editing, regulating and targeting genomes. *Nature biotechnology,* 32**,** 347.

SCAGLIONI, P. P., MELEGARI, M. & WANDS, J. R. 1994. Characterization of hepatitis B virus core mutants that inhibit viral replication. *Virology,* 205**,** 112-120.

SCHIFFER, J. T., AUBERT, M., WEBER, N. D., MINTZER, E., STONE, D. & JEROME, K. R. 2012. Targeted DNA mutagenesis for the cure of chronic viral infections. *Journal of virology,* 86**,** 8920-8936.

SCHORNACK, S., MEYER, A., RÖMER, P., JORDAN, T. & LAHAYE, T. 2006. Gene-for-gene-mediated recognition of nuclear-targeted AvrBs3-like bacterial effector proteins. *Journal of plant physiology,* 163**,** 256-272.

SCHULZE, A., GRIPON, P. & URBAN, S. 2007. Hepatitis B virus infection initiates with a large surface protein–dependent binding to heparan sulfate proteoglycans. *Hepatology,* 46**,** 1759-1768.

SCOTT, J. N., KUPINSKI, A. P. & BOYES, J. 2014. Targeted genome regulation and modification using transcription activator-like effectors. *The FEBS journal,* 281**,** 4583-4597.

SEEGER, C. & MASON, W. S. 2015. Molecular biology of hepatitis B virus infection. *Virology,* 479**,** 672-686.

SEEGER, C. & SOHN, J. A. 2014. Targeting hepatitis B virus with CRISPR/Cas9. *Molecular Therapy-Nucleic Acids,* 3.

SELLS, M. A., CHEN, M. L. & ACS, G. 1987. Production of hepatitis B virus particles in Hep G2 cells transfected with cloned hepatitis B virus DNA. *Proceedings of the National Academy of Sciences,* 84**,** 1005-1009.

SELLS, M. A., ZELENT, A. Z., SHVARTSMAN, M. & ACS, G. 1988. Replicative intermediates of hepatitis B virus in HepG2 cells that produce infectious virions. *Journal of virology,* 62**,** 2836-2844.

SHLOMAI, A. & SHAUL, Y. 2003. Inhibition of hepatitis B virus expression and replication by RNA interference. *Hepatology,* 37**,** 764-770.

SILVA, G., POIROT, L., GALETTO, R., SMITH, J., MONTOYA, G., DUCHATEAU, P. & PÂQUES, F. 2011. Meganucleases and other tools for targeted genome engineering: perspectives and challenges for gene therapy. *Current gene therapy,* 11**,** 11-27.

SPEARMAN, C. & SONDERUP, M. W. 2014. Preventing hepatitis B and hepatocellular carcinoma in South Africa: The case for a birth-dose vaccine. *SAMJ: South African Medical Journal,* 104**,** 610-612.

STODDARD, B. L. 2011. Homing endonucleases: from microbial genetic invaders to reagents for targeted DNA modification. *Structure,* 19**,** 7-15.

STONE, D., NIYONZIMA, N. & JEROME, K. R. 2016. Genome editing and the next generation of antiviral therapy. *Human genetics,* 135**,** 1071-1082.

SUMMERS, J., O'CONNELL, A. & MILLMAN, I. 1975. Genome of hepatitis B virus: restriction enzyme cleavage and structure of DNA extracted from Dane particles. *Proceedings of the National Academy of Sciences,* 72**,** 4597-4601.

SZCZEPEK, M., BRONDANI, V., BÜCHEL, J., SERRANO, L., SEGAL, D. J. & CATHOMEN, T. 2007. Structure-based redesign of the dimerization interface reduces the toxicity of zinc-finger nucleases. *Nature biotechnology,* 25**,** 786.

TATEMATSU, K., TANAKA, Y., KURBANOV, F., SUGAUCHI, F., MANO, S., MAESHIRO, T., NAKAYOSHI, T., WAKUTA, M., MIYAKAWA, Y. & MIZOKAMI, M. 2009. A genetic variant of hepatitis B virus divergent from known human and ape genotypes isolated from a Japanese patient and provisionally assigned to new genotype J. *Journal of virology,* 83**,** 10538-10547.

TERASAKI, S. 1996. Latent multiple infections by herpes simplex virus type 1. *Kurume Med J,* 43**,** 127-36.

TRÉPO, C., CHAN, H. L. & LOK, A. 2014. Hepatitis B virus infection. *The Lancet,* 384**,** 2053-2063.

TSAI, S. Q., ZHENG, Z., NGUYEN, N. T., LIEBERS, M., TOPKAR, V. V., THAPAR, V., WYVEKENS, N., KHAYTER, C., IAFRATE, A. J. & LE, L. P. 2015. GUIDE-seq

enables genome-wide profiling of off-target cleavage by CRISPR-Cas nucleases. *Nature biotechnology,* 33**,** 187.

TUTTLEMAN, J. S., POURCEL, C. & SUMMERS, J. 1986. Formation of the pool of covalently closed circular viral DNA in hepadnavirus-infected cells. *Cell,* 47**,** 451-460.

VAN GENT, D. C., HOEIJMAKERS, J. H. & KANAAR, R. 2001. Chromosomal stability and the DNA double-stranded break connection. *Nature Reviews Genetics,* 2**,** 196.

VAN ZONNEVELD, M., HONKOOP, P., HANSEN, B. E., NIESTERS, H. G., MURAD, S. D., DE MAN, R. A., SCHALM, S. W. & JANSSEN, H. L. 2004. Long-term follow-up of alpha-interferon treatment of patients with chronic hepatitis B. *Hepatology,* 39**,** 804-810.

VERES, A., GOSIS, B. S., DING, Q., COLLINS, R., RAGAVENDRAN, A., BRAND, H., ERDIN, S., COWAN, C. A., TALKOWSKI, M. E. & MUSUNURU, K. 2014. Low incidence of off-target mutations in individual CRISPR-Cas9 and TALEN targeted human stem cell clones detected by whole-genome sequencing. *Cell stem cell,* 15**,** 27-30.

VINK, C. A., GASPAR, H. B., GABRIEL, R., SCHMIDT, M., MCIVOR, R. S., THRASHER, A. J. & QASIM, W. 2009. Sleeping beauty transposition from nonintegrating lentivirus. *Molecular Therapy,* 17**,** 1197-1204.

VIOLA, L., COLEMAN, J., FLUKER, J., BARRISON, I., PARADINAS, F., EVANS, B. & MURRAY-LYON, I. 1981. Natural history of liver disease in chronic hepatitis B surface antigen carriers: survey of 100 patients from Great Britain. *The Lancet,* 318**,** 1156-1159.

VON WEIZSÄCKER, F., BLUM, H. E. & WANDS, J. R. 1992. Cleavage of hepatitis B virus RNA by three ribozymes transcribed from a single DNA template. *Biochemical and biophysical research communications,* 189**,** 743-748.

WAH, D. A., HIRSCH, J. A., DORNER, L. F., SCHILDKRAUT, I. & AGGARWAL, A. K. 1997. Structure of the multimodular endonuclease FokI bound to DNA. *Nature,* 388**,** 97.

WANG, C.-S., CHANG, T.-T., YAO, W.-J., WANG, S.-T. & CHOU, P. 2012. Impact of increasing alanine aminotransferase levels within normal range on incident diabetes. *Journal of the Formosan Medical Association,* 111**,** 201-208.

WEBER, N. D., STONE, D., SEDLAK, R. H., FEELIXGE, H. S. D. S., ROYCHOUDHURY, P., SCHIFFER, J. T., AUBERT, M. & JEROME, K. R. 2014. AAV-mediated delivery of zinc finger nucleases targeting hepatitis B virus inhibits active replication. *PloS one,* 9**,** e97579.

WILSON, E. M., TANG, L. & KOTTILIL, S. 2016. Eradication strategies for chronic hepatitis B infection. *Clinical Infectious Diseases,* 62**,** S318-S325.

WONG, D., YUEN, M.-F., NGAI, V., FUNG, J. & LAI, C.-L. 2006. One-year entecavir or lamivudine therapy results in reduction of hepatitis B virus intrahepatic covalently closed circular DNA levels. *Antiviral therapy,* 11**,** 909.

WU, T.-T., COATES, L., ALDRICS, C. E., SUMMERS, J. & MASON, W. S. 1990. In hepatocytes infected with duck hepatitis B virus, the template for viral RNA synthesis is amplified by an intracellular pathway. *Virology,* 175**,** 255-261.

WURSTHORN, K., LUTGEHETMANN, M., DANDRI, M., VOLZ, T., BUGGISCH, P., ZOLLNER, B., LONGERICH, T., SCHIRMACHER, P., METZLER, F. & ZANKEL, M. 2006. Peginterferon alpha-2b plus adefovir induce strong cccDNA decline and HBsAg reduction in patients with chronic hepatitis B. *Hepatology,* 44**,** 675-684.

WYMAN, C. & KANAAR, R. 2006. DNA double-strand break repair: all's well that ends well. *Annu. Rev. Genet.,* 40**,** 363-383.

YAN, H., ZHONG, G., XU, G., HE, W., JING, Z., GAO, Z., HUANG, Y., QI, Y., PENG, B. & WANG, H. 2012. Sodium taurocholate cotransporting polypeptide is a functional receptor for human hepatitis B and D virus. *elife,* 1**,** e00049.

YANG, H.-C. & KAO, J.-H. 2014. Persistence of hepatitis B virus covalently closed circular DNA in hepatocytes: molecular mechanisms and clinical significance. *Emerging microbes & infections,* 3**,** e64.

YANG, L., GUELL, M., BYRNE, S., YANG, J. L., DE LOS ANGELES, A., MALI, P., AACH, J., KIM-KISELAK, C., BRIGGS, A. W. & RIOS, X. 2013. Optimization of scarless human stem cell genome editing. *Nucleic acids research,* 41**,** 9049-9061.

ZHANG, Z.-H., WU, C.-C., CHEN, X.-W., LI, X., LI, J. & LU, M.-J. 2016. Genetic variation of hepatitis B virus and its significance for pathogenesis. *World journal of gastroenterology,* 22**,** 126.

ZHANG, Z., VU, G.-P., GONG, H., XIA, C., CHEN, Y.-C., LIU, F., WU, J. & LU, S. 2013. Engineered external guide sequences are highly effective in inhibiting gene expression and replication of hepatitis B virus in cultured cells. *PloS one,* 8**,** e65268.

ZIMMERMAN, K. A., FISCHER, K. P., JOYCE, M. A. & TYRRELL, D. L. J. 2008. Zinc finger proteins designed to specifically target duck hepatitis B virus covalently closed circular DNA inhibit viral transcription in tissue culture. *Journal of virology,* 82**,** 8013-8021.

ZOULIM, F. & LOCARNINI, S. 2009. Hepatitis B virus resistance to nucleos (t) ide analogues. *Gastroenterology,* 137**,** 1593-1608. e2.

ZOULIM, F. & LOCARNINI, S. 2013. Optimal management of chronic hepatitis B patients with treatment failure and antiviral drug resistance. *Liver International,* 33**,** 116-124.

ZOULIM, F. & PERRILLO, R. 2008. Hepatitis B: reflections on the current approach to antiviral therapy. *Journal of hepatology,* 48**,** S2-S19.